Chapter 1:

Introduction

Introduction

1.1 Telomeres, immortalisation and cancer

One property upon which most cancers are dependent is the ability of their cells to replicate an unlimited number of times[7,8]. Normal somatic cells have a finite replicative capacity, and eventually undergo growth arrest accompanied by a complex series of biochemical and morphological changes referred to as senescence[9]. Escape from the normal proliferation limit and acquisition of an unlimited replicative capacity, termed immortalisation, has been demonstrated *in vitro* and *in vivo* in tumours[8,10]. Immortalisation appears to be a necessary step in the development of most cancers, in which the occurrence of intratumoral death and the need for clonal evolution usually mean that many more cell divisions are required for the cancer to become clinically significant than are allowed by the proliferative capacity of its normal tissue counterpart[8]. The genetic changes associated with immortalisation are also the most common genetic changes in cancer, and many carcinogens are able to immortalise human cells in culture[8,10]. It has been shown in many combined *in vitro/in vivo* experimental systems that immortalisation appears to be a prerequisite for the induction of tumours. Immortalisation usually depends on recessive mutations[11] and importantly for oncology, reversal of immortality can abrogate tumorigenicity[8,10,12].

Telomere maintenance appears to be the critical determinant of immortalisation. Human telomeres consist of 4-15 kb of the repetitive DNA sequence 5′-TTAGGG-3′ and undergo progressive shortening during proliferation of normal human somatic cells[13]. The reason that cell division induces telomeric shortening appears to be at

least in part due to the DNA replication machinery's inability to replicate the extreme ends of linear DNA molecules[14]. Telomere shortening eventually triggers senescence, thus acting as a barrier to unlimited cellular proliferation[15] and tumorigenesis[16-19].

The mechanism whereby cells sense short telomeres and trigger senescence involves loss of function of the specialised telomeric chromatin so that it can no longer evade DNA damage surveillance and/or suppress a DNA damage response[6,20]. An important function of telomeric chromatin is to avoid detection as a double strand break. The specialised telomere protein complex that is responsible for this has been termed Shelterin[6]. Tin2 is the lynchpin of the Shelterin complex, linking together the two double stranded telomeric binding proteins, TRF1 and TRF2[21] and the single stranded telomeric DNA binding protein POT1 that attaches to TIN2 via TPP1[22]. Rap1 is also a Shelterin component and binds to TRF2[23]. Some Shelterin complexes appear to contain only one type of double stranded telomere binding protein, either TRF1 or TRF2[24]. Other proteins (including MRE11/RAD50/Nbs1 complex, ERCC1/XPF, WRN helicase, BLM helicase, DNA-PK, PARP-2, Tankyrases and RAD51D) are necessary for proper telomeric chromatin function but, unlike Shelterin components, do not have predominantly telomeric roles (reviewed in de Lange[6]).

When telomeres become too short, it is the reduction in the number of bound Shelterin complexes that is thought to cause both the failure to evade recognition by DNA repair proteins and the failure to suppress the activity of these proteins at the telomere. Foci of 53BP1, phosphorylated H2AX, the MRE11 complex, Rip1 and ATM form at the telomeres[25,26]. A telomere dysfunction signal is generated that involves ATM and possibly ATR activation of the p53 pathway leading to cell cycle

arrest and senescence. However, ectoderm and mesenchyme derived cell types may respond differently to p53 activation with the mesenchyme derived cells usually undergoing senescence and ectoderm derived cells more likely to undergo apoptosis[27]. Deficiencies in the Shelterin components TRF2, TIN2 or POT1 can have the same effect as telomere shortening[27-29]. Work with TRF2 inhibition suggests that the p16/Rb pathway may also be activated by short telomeres, but in contrast to activation of the p53 pathway, it has a slow onset[30] and effects an irreversible cell cycle arrest involving extensive chromatin remodelling[31].

Shelterin's ability to protect the telomere from recognition by the DNA damage response may depend on enough Shelterin being present to fold the telomere into a T-loop[32,33] which masks the chromosome end (Fig 1.3A in Section 1.5). The T-loop is a conserved telomere structure[34] in which the terminal 3′ overhang invades the duplex telomere repeats, causing a displacement (D)-loop that is 75 to 200 nucleotides long[32]. Shelterin controls the creation, maintenance and elongation of the 3′ overhang[29,35-39] and is probably involved in folding the telomere to facilitate its invasion of the proximal duplex DNA[6].

Loss of normal function of the p53 and p16/Rb tumour suppressor pathways allows continued proliferation and telomere shortening beyond the length at which normal cells become senescent[40-42]. As the telomeres become extremely short the cell population stops proliferating, entering a state termed crisis[43,44]. Immortalisation of cells (and thus escape from crisis) requires additional genetic changes that always involve the activation of a telomere maintenance mechanism[45].

1.2 Telomerase and immortalisation

In cells of the germ line, telomere shortening is prevented by telomerase[46], an enzyme complex that contains a number of subunits including an RNA template molecule hTR (human Telomerase RNA) and a catalytic subunit, hTERT (human TElomerase Reverse Transcriptase). Telomerase adds TTAGGG repeats to telomeres by reverse transcribing the RNA template and thus compensates for the loss of telomeric DNA associated with normal cell division[47]. In normal tissues telomerase is either undetectable or present at very low levels that do not appear to be able to prevent telomere shortening[48-54].

Experiments involving the exogenous expression of telomerase *in vitro* suggest that, in some cell types, the maintenance of telomeres is the only change necessary for immortalisation[55-57]. However, it is possible that loss of the p53 and Rb pathways is necessary for re-expressing endogenous hTERT[8]. Furthermore, in other cell types hTERT expression does not affect proliferative life span unless the Rb pathway is inactivated[58-61].

A causal association between telomere maintenance and immortalisation is supported by studies of several unicellular organisms that normally exhibit telomerase activity and have an unlimited replicative capacity. Removal of telomerase activity by gene "knockout" technology resulted in progressive telomeric shortening followed by senescence[62-64]. Further, excessive telomere shortening in cells of late generation telomerase-null mice resulted in a state resembling crisis[65]. It is also possible that the mechanisms used for telomere maintenance have a more complicated role in immortalisation than just maintaining telomere length. Telomerase may have a role in

cell proliferation, differentiation and DNA damage response via interactions with other proteins (such as p53) or by influencing gene expression[66,67].

1.3 Evidence for Alternative Lengthening of Telomeres

Some mammalian cells without any telomerase activity are able to maintain the length of their telomeres for many population doublings (PDs)[68-71], thus indicating the existence of one or more telomerase independent mechanisms for telomere maintenance that have collectively been termed Alternative Lengthening of Telomeres (ALT)[72]. To date, clear evidence for ALT activity has only been found in abnormal situations, including human tumours, immortalised human cell lines (Table 1.1), and in telomerase-null mouse cell lines[69-71,73,74]. There is also evidence suggesting *in vivo* ALT activity in the tissues of late generation telomerase-null mice[70,75]. Although the molecular details of ALT are only just starting to be elucidated, there does not appear to be any protein whose predominant role is the ALT mechanism. However, there are a number of characteristics that are hallmarks for the presence of ALT activity.

1.4 Hallmarks of ALT cells

1.4.1 Long and heterogeneous telomere length distribution in ALT cells

ALT cells have a characteristic long and heterogeneous telomere length distribution. Telomeres are normally maintained in the human germ line at average lengths of 15 kb[76,77], as measured by terminal restriction fragment (TRF) Southern analysis. TRFs

include up to 5 kb of non-telomere repeat sequence[78] that is resistant to restriction, possibly due to base modification[79]. For normal somatic cells *in vitro*, the average

Table 1.1: Examples of human ALT cell lines

Cell Line	Cell type	Transformation	References
GM847	Fibroblast, skin	SV40	[69]
GM0637 (NSV)	Fibroblast, skin	SV40	[80]
LM217, KB319	Fibroblast, skin	SV40	[81]
HSF E-2B	Fibroblast, foreskin	SV40	[82]
JFCF-6/T.1R and 1J series	Fibroblast, jejunal	SV40	[83]
WI38-VA13/2RA	Fibroblast, lung	SV40	[69]
SW26-I	Fibroblast, lung	SV40	[78]
SV/HF-5/39	Fibroblast, bone marrow	SV40	[84]
MRC5-V2	Fibroblast, lung	SV40	Huschtscha unpub.
WHE-7 E7 Cl 1,2,3,4	Fibroblast, embryo	HPV E7	[85]
WHE-7 E6/E7 Cl 3	Fibroblast, embryo	HPV E6 and E7	[85]
82-cycA2	Fibroblast, foreskin	Cyclin A2	[86]
82-cdk1	Fibroblast, foreskin	CDK1	[86]
KMST-6	Fibroblast, embryo	Gamma irradiation	[87]
OUMS-24F	Fibroblast, embryo	Chemical	[88]
SUSM-1	Fibroblast, liver	Chemical	[69]
AT1BR44 neo	Fibroblast, skin; AT[a]	SV40	[89]
AT13LA(SV)	Fibroblast, skin; AT	SV40	[89]
AT18LA(SV)	Fibroblast, skin; AT	SV40	[89]
IIICF/a2, /b4, /b5, /c, .2/A1	Fibroblast, breast; LFS[b]	Spontaneous	[68,69,83]
IIICF-T series	Fibroblast, breast; LFS	SV40	[69]
IIICF-E series	Fibroblast, breast; LFS	HPV E6 +/- E7	[69]
HMS50-E7	Fibroblast, breast; LFS	HPV E7	[90]
MDAH087 series	Fibroblast, skin; LFS	Spontaneous	[91,92]
LCS-AF.1-2, .1-3, .3-1	Fibroblast, skin; LFS	Aflatoxin B1	[91,93]
LCS-4X2	Fibroblast, skin; LFS	X-Irradiation	[91,94]
W-V	Fibroblast, WS[c]	SV40	[95]
MeT-4A	Mesothelial	SV40	[69]
Saos-2	Osteosarcoma	Tumour	[73]
G-292	Osteosarcoma	Tumour	[73]
U-2 OS	Osteosarcoma	Tumour	[73]
ZK-58	Osteosarcoma	Tumour	[96]
SK-LU-1	Adenocarcinoma, lung	Tumour	[73]
DOS16	Leiomyosarcoma	Tumour	Gupta/Henson unpub.
BET-3M	Epithelial, bronchial	SV40	[69]

HIO107, 117 and 118	Epithelial, ovarian surface	SV40	[97]
OKF6-D1/Δp53	Keratinocyte, oral	Cyclin D1, p53	[98]

[a]AT, Ataxia Telangiectasia. [b]LFS, Li-Fraumeni syndrome. [c]WS, Werner syndrome.

TRF length progressively declines at a rate of 40 - 200 base pairs (bp) per cell division to 4 - 8 kb at senescence[99-102]. In most telomerase[+] human cancers or immortal cell lines, TRF lengths are relatively homogeneous with the mean length usually less than 10 kb[69,103,104]. In contrast, all of the human ALT[+] cell lines and cancers analysed so far have a longer mean TRF length with a very wide length distribution (Fig 1.1): the mean is around 20 kb, and TRF lengths range from less than 3 kb to over 50 kb[69,73,81,97,98]. Consequently, pulsed field rather than conventional gel electrophoresis is preferable for analysing TRFs of ALT cells. In cells that become immortalised and activate ALT during culturing *in vitro*, there is a good temporal correlation between the immortalisation event and the occurrence of the characteristic ALT telomere length phenotype[83].

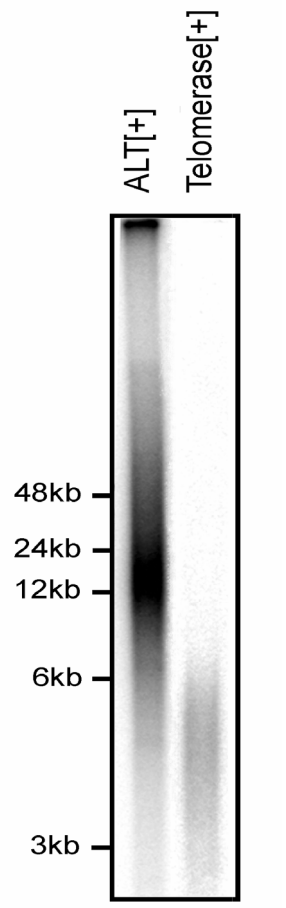

Figure 1.1: Telomere length distribution in ALT cells. Southern analysis of the telomeres from typical ALT[+] (GM847) and telomerase[+] (HeLa) cell lines, showing the more heterogeneous and on average, longer telomere length distribution in ALT cells. Southern analysis of telomeres was performed by digesting genomic DNA with restriction enzymes that do not recognise the telomeric sequence, TTAGGG, separating it by pulse field gel electrophoresis, and then hybridising the dried gel with a radioactively labelled probe complementary to the $(TTAGGG)_n$ sequence.

1.4.2 Intracellular telomere length heterogeneity

Visualisation of telomeres by fluorescence *in situ* hybridisation (FISH) shows that the telomere length heterogeneity characteristic of ALT cell populations reflects the heterogeneity that exists within individual cells. Some chromosome ends have no detectable telomeric sequence while others within the same cell have very strong telomere signals[105,106]. The same pattern of intracellular telomere length heterogeneity can be seen by immunostaining for the telomere specific binding proteins, TRF1 and TRF2[2,83].

1.4.3 Increased telomere length fluctuation in ALT cells

The telomere length distribution in ALT cells is dynamic, with fluctuations in length occurring on individual telomeres during cellular proliferation. In a key study, Murnane and colleagues observed the length dynamics of a tagged telomere in a telomerase[-] human cell line[81]. Telomeres underwent gradual shortening at a rate of 30 - 50 bp per cell division, which is similar to cells without a telomere maintenance mechanism[101]. In some cells, this erosion continued until there were less than 200 bp of telomeric repeats left before a rapid and heterogeneous increase in length, sometimes of > 23 kb, occurred. In other cells, rapid increases in telomere length occurred in telomeres that did not appear to be critically short. Rapid deletion events occurred occasionally in telomeres of any length. The frequency of these changes varied greatly between different subclones. The frequency of chromosomal fusion events seemed to be proportional to the frequency of rapid length changes.

Fluctuation of telomere length within ALT cells has also been found in a subsequent study. In an ALT cell line that contained a single Y chromosome, it was shown that the Y p- and q-arm telomere length ratios varied by more than 100-fold within the cell population, in contrast to a comparable telomerase[+] cell line where the ratio varied by less than two-fold[106]. In a clonal cell population in which one of the chromosomes can be identified, the variation in its p- and q-arm telomere length ratios can be used to assess the amount of telomere length fluctuation and hence is a measure of ALT activity[2].

1.4.4 Circular and linear extra-chromosomal telomeric repeats

Abundant extra-chromosomal telomeric repeats (ECTR) have been found in ALT cells that consist of both linear[107] (T Yeager *et al*., unpublished data) and circular[108,109] molecules. The presence of circular ECTR has been used as an assay for ALT activity[95,110]. In general, large amounts of ECTR are not detectable in telomerase[+] immortalised cells or in normal human cells[107]. However, ECTR have been reported in mortal EBV-transformed B lymphoblastoid cell lines[111]. They may also be present in otherwise normal fibroblasts from individuals with ataxia telangiectasia[112], a condition associated with accelerated telomere shortening *in vitro*[113].

The ECTR in ALT cells may be formed by a similar process to telomeric rapid deletion (TRD) that has been described in yeast[114]. TRD reduces longer telomeres to the length of the majority of the telomeres in a single cell division and requires the yeast *Mre11/Rad50* complex[114] in a mechanism that may involve recombination of a t-loop structure[115]. Rapid reduction of telomere length is known to occur in ALT cells (Section 1.4.3) and the circular ECTR in ALT cells is of similar size to the loop region in their t-loops[108]. T-loops are at risk of forming a Holliday junction by base pairing of the 5′ end of the telomere with the displacement loop. Branch migration of the Holliday junction (HJ) towards the centromere could generate a double HJ[6]. Resolution of these single or double HJ could delete the whole loop as nicked or intact circular DNA or linear DNA and leave a drastically shortened telomere at the chromosomal end (Section 1.5). All these products of intratelomeric recombination are seen in greater abundance in ALT cells. Nicked circular telomeric DNA and drastically shortened telomeres can be induced in non-ALT cells by expressing a

TRF2 mutant. As might be expected this was dependent on the MRE11 complex and XRCC3 but, for less obvious reasons, the telomere shortening was only detectable after replication and on the leading strand[109].

1.4.5 Increased intertelomeric recombination

The first evidence for intertelomeric recombination events in human ALT cells was obtained by targeting a DNA tag into telomeres[3]. FISH analysis of clonal cultures showed a progressive increase in the number of tagged telomeres with increasing PDs. At PD 23 the tag was found in two or three telomeres. By PD 63 it was found on up to five telomeres in any one cell and, within the clonal population, ten different chromosomes were tagged. This phenomenon was not seen when the tag was located immediately centromeric to the telomere in ALT cells, and was not seen in telomerase[+] cells. Furthermore, chromosome specific subtelomeric probes showed that the increased telomeric recombination in the ALT cell line did not extend into the subtelomeric region[4]. This intertelomeric recombination could also be indirect via recombination with ECTR. Microcell mediated chromosome transfer has been used to introduce a tagged telomere into a cell line to test for ALT activity[95].

1.4.6 Increased postreplicative telomeric exchanges

Intertelomeric recombination that involves post-replicative exchange from a leading to lagging strand (or vice versa) can be readily assayed in cell lines by chromosome orientation (CO) -FISH[116]. In this technique, newly synthesised DNA in each metaphase chromatid is degraded and the G-strand and C-strand regions on the remaining template strands are identified by hybridisation with their complementary

sequence. A G-strand (or C-strand) region on the template strand on the same arm of both sister chromatids indicates intertelomeric exchange has occurred. This could be due to telomeric sister chromatid exchanges (SCEs) or post replicative exchanges/insertions from other telomeres or ECTR. Telomeric exchanges were one to two orders of magnitude higher in ALT cells than the highest levels seen in non-ALT cells, including non-ALT cells with long telomeres or mutations that generally increased SCEs. No increase in the rate of non-telomeric SCE was seen in ALT cells[117-119]. This may be the most sensitive but least specific of the commonly used hallmarks of telomerase independent telomere maintenance. It was the only hallmark of ALT remaining (of five tested) in an atypical ALT cell line clone[110]. Increased telomere exchanges were also the only ALT characteristic seen in a clone of a mortal cell strain in which a small fraction of cells (1/3000 and 1/200) were able to escape two telomere shortening induced crises[118]. The mechanism behind this was not elucidated, but perhaps as previously proposed[119], asymmetric post-replicative telomere SCE allowed a small fraction of cells in the population to maintain their telomeres at the expense of a faster demise of their siblings. It was also postulated that telomeric exchanges could also be increased in mortal cells during repair of damaged telomeres[120].

1.4.7 Increased instability of specific minisatellite repeats

ALT cell lines have increased instability at some minisatellite loci. A large increase in instability at the MS32 (D1S8) minisatellite locus was found in ALT[+] cell lines[121]. The amount of instability varied greatly between 15 ALT[+] cell lines tested, but was on average 55 fold greater than in ALT[-] cell lines. The MS32 minisatellite contains

10-1000 tandem arrays of a 29 bp repeat unit that is 62% GC rich and has a moderate segregation of G and C onto opposite strands. The MS32 locus is commonly unstable due to crossover or conversion events during meiosis in the germline. However, the changes seen in ALT[+] instability involved a variety of different types of mutations over the entire length of the array, which suggests an ALT specific mechanism. No instability was seen in five other minisatellite sequences tested[121]. Minisatellite instability has also been reported for ALT[+] cell lines at loci hybridising to the 33.6 and 33.15 minisatellite probes[122]. These minisatellite arrays also contain a segregation of G and C onto opposite strands and are known to mispair to form intrahelical pseudoknots and interhelical associations *in vitro*[123]. In contrast, no increase in microsatellite instability was seen[122].

1.4.8 ALT-associated PML bodies

Another characteristic of ALT cell lines is the presence of nuclear structures referred to as ALT-associated PML bodies (APBs), i.e. PML (promyelocytic leukaemia protein) nuclear bodies with ALT-specific contents. PML nuclear bodies are aggregates of PML and other proteins, that are usually bound to the nuclear matrix[124-129]. PML nuclear bodies are present in many but not all tissues. They are dynamic structures with PML and other proteins continually being incorporated and released. Their number, size, morphology, constituents and function may be influenced by the expression, alternative splicing and post-translational modification of PML and may vary with the cell cycle, state of the cell and external influences. Some other proteins are also important for the formation of PML nuclear bodies, but many components may only be present in specific cellular contexts and only in a subset of PML nuclear

bodies. Sp100, a common constituant of PML nuclear bodies is also present in nuclear bodies that do not contain PML[130]. The processes in which PML nuclear bodies are claimed to be involved include tumour suppression, cell cycle regulation, senescence, apoptosis, immune and inflammatory responses, antigen presentation, protein refolding and degradation and differentiation. PML and other common constituents of PML nuclear bodies may regulate transcription and modify chromatin. PML nuclear bodies are closely associated with replication domains and the interaction of viral DNA with PML nuclear bodies may be necessary for optimal viral replication. It has been proposed that PML nuclear bodies facilitate this vast array of functions by sequestering and releasing proteins, localising proteins to sites of action and facilitating interactions between proteins including those that result in post-translational modifications.

APBs are distinguished from other PML nuclear bodies by their telomeric contents, including telomeric DNA[83]. Not surprisingly, APBs have also been found to contain the specific telomeric binding proteins, TRF1, TRF2[83] and hRap1[131] and non-specific telomere binding proteins MRE11/RAD50/NBS1 complex[132,133], ERCC1/XPF[37], WRN[134], BLM[135,136], PARP2[137], RAD51D[138] and hnRNPA2[139]. APBs have also been found to contain proteins not known to reside at telomeres, that have roles in homologous recombination (HR) and DNA repair, including RAD51, RAD52, RPA[83], BRCA1[131], 9-1-1 complex (including hRad17), phosphorylated H2AX[140]and RIF1[141] (Table 1.2). Like their normal counterparts, APBs have the appearance of disc or ring shaped structures in two dimensions, often with PML detected in the outer rim (Fig 1.2). In view of the postulated functions for PML nuclear bodies, it is possible that APBs may focus, colocalise, or modify proteins required for the ALT mechanism. It

is also possible that APBs are involved in removing by-products of the ALT process, as there is some evidence that PML nuclear bodies could be sites of intranuclear proteolysis[142]. APBs are seen in only about 5% of interphase cells within an exponentially dividing ALT[+] population[83], possibly indicating that their formation may be cell cycle related. Most cells with APBs are in the late S/G2/M phase of the cell cycle[97,132].

Prior to the observation that telomeric DNA is present in APBs[83], DNA had not been found in PML nuclear bodies. It has since been shown that PML may localise in nuclear foci with BLM, RPA and RAD51 in response to DNA damage[143]. Although the relationship between PML nuclear bodies and RAD51 foci is not clear, it seems possible that the function of APBs is to repair telomeric DNA that is recognised by the cell as being damaged. The telomeric DNA in APBs may be a subset of the total extrachromosomal telomeric repeat (ECTR) DNA that is abundant in ALT cells[107,144].

Table 1.2: Proteins found in ALT-associated PML bodies (APBs)

Protein	Comments	References
TRF1 and TRF2	Telomeric specific double stranded DNA binding protein components of the Shelterin complex that regulate telomere structure and length. Also important for localising DNA repair and replication proteins to the telomere and regulating their functions. May be involved in attaching the telomere to the nuclear matrix. TRF1 negatively regulates telomere lengthening by telomerase and is down regulated in some telomerase positive cancers. TRF1 also is important in regulating entry and exit from mitosis. TRF2 is important for maintaining t-loop structure and telomere integrity, at least partly by inhibiting non-homologous end joining (NHEJ) and HR at the telomere and possibly at non-telomeric sites. Double strand breaks (DSB) cause rapid phosphorylation of TRF2 which is transiently present at the site of DNA damage suggesting TRF2 is generally involved in coordinating management of DNA damage. TRF2 also	6,34,83,109,145-156

	influences base-excision repair. Phosphorylated TRF2 is present in APBs and at telomere damage induced foci in non-ALT cells.	
Rap1	Binds TRF2 and negatively regulates telomere length.	131,157
MRE11/ RAD50/ NBS1 complex (MRN)	Integral to DSB recognition and response, including S phase cell cycle arrest and DNA repair by HR. Its ability to act as a molecular bridge between two DNA helices appears important for HR and also facilitates telomere maintenance by telomerase. Also has nuclease activities. Associates with Shelterin and may regulate t-loop formation or resolution. Is required for t-loop HR mediated by TRF2 deficiency. Sequestration of MRN by SP100 overexpression inhibits ALT activity. NBS1 is required for phosphorylation and activation of the complex and is usually only present with the complex in S phase. Localisation of NBS1 to APBs coincides with active DNA synthesis in APBs. In *S. cerevisiae*, *Rad50* is required for type II but not type I telomerase-null survivors. An MRN homologue is required for recombination mediated replication in T4 phage.	2,6,131-133,149,158-165
WRN and BLM	RecQ helicases that resolve alternative DNA structures and intermediates of HR and replication and coordinate replication with HR. Activities are modified by Shelterin. Can complement *sgs1*, the *S. cerevisiae* RecQ helicase that is required for *S. cerevisiae* type II telomerase-null survivors. BLM may influence telomeric DNA synthesis in ALT and regulates t-loop formation/resolution and interacts with top3α. WRN is needed for telomeric lagging strand synthesis and may also resolve t-loops and degrade the 3′ telomeric overhang.	134,136,166-173
PARP2	Binds and negatively regulates TRF2 telomere binding. PARP2 is involved in maintaining telomere integrity and general DNA integrity via regulating topoisomerase I.	137,174
ERCC1/XPF	3′ flap endonuclease for nucleotide excision repair and the resection of the telomere 3′ overhang after TRF2 loss. ERCC1/XPF associates with Shelterin and may be necessary to avoid inappropriate telomeric HR.	6,37,175
RAD52	Binds double stranded DNA ends and assists RAD51 activity. Colocalises with RAD51 foci and RAD50/MRE11 foci that form during DSB repair. In *S. cerevisiae Rad52* is required for HR, both telomerase-null survival pathways, and production of ribosomal DNA mini-circles.	83,159,176-179
RAD51	RecA-like DNA strand transfer protein involved in single and DSB repair by HR. Associates with proteins including RPA, BLM and PML that form foci at sites of DNA breaks or unscheduled DNA synthesis. In yeast the Rad51p complex is needed for gene conversion in which donor DNA is transcriptionally repressed. *Rad51* is required for type I but not type II survival pathway in telomerase-null yeast.	83,159,177,180,181
RAD51D	RAD51 paralog involved in early steps of HR and Holliday junction processing. RAD51D knockout causes telomere shortening and dysfunction and cell death in ALT and non-ALT cells.	5,138,182,183

RPA	A single stranded DNA-binding protein that facilitates DNA unwinding and modulates activity of other enzymes. Plays an essential and possibly a coordinating role in DNA replication, recombination and repair. RPA-deficient yeast have reduced telomere length.	83,184-186
BRCA1	Tumour suppressor involved in regulating HR, NHEJ and nucleotide excision repair (NER). BRCA1 deficiency results in telomere uncapping and shortening, BRCA1 interacts with MRN complex.	131,187-191
9-1-1 complex and RAD17	9-1-1 clamp (hRad9, hRad1 and hHUS1) is loaded onto DNA damage by RAD17 and is important for DNA damage induced HR in S and G2 phases of cell cycle and is also required for telomere stability. 9-1-1 complex member, hRad9, interacts with TRF2 and RAD51 and is important for phosphorylated H2AX focus regulation.	140,192
Phosphorylated H2AX	One of the earliest responses to DSB is phosphorylation of H2AX on a large region of chromatin surrounding the break. Phosphorylated H2AX recruits DNA damage response proteins to the area surrounding the break and removal of phosphorylated H2AX allows resumption of the cell cycle. H2AX is also important for meiotic telomere clustering.	140,193,194
Rif1	Part of the 53BP1/ATM DNA damage response including DNA replication arrest.	141
hnRNPA2	Role in controlling cellular proliferation and mRNA processing. Binds single stranded telomeric G-strand and hTR and may function as an adaptor at the telomere.	139,195-197

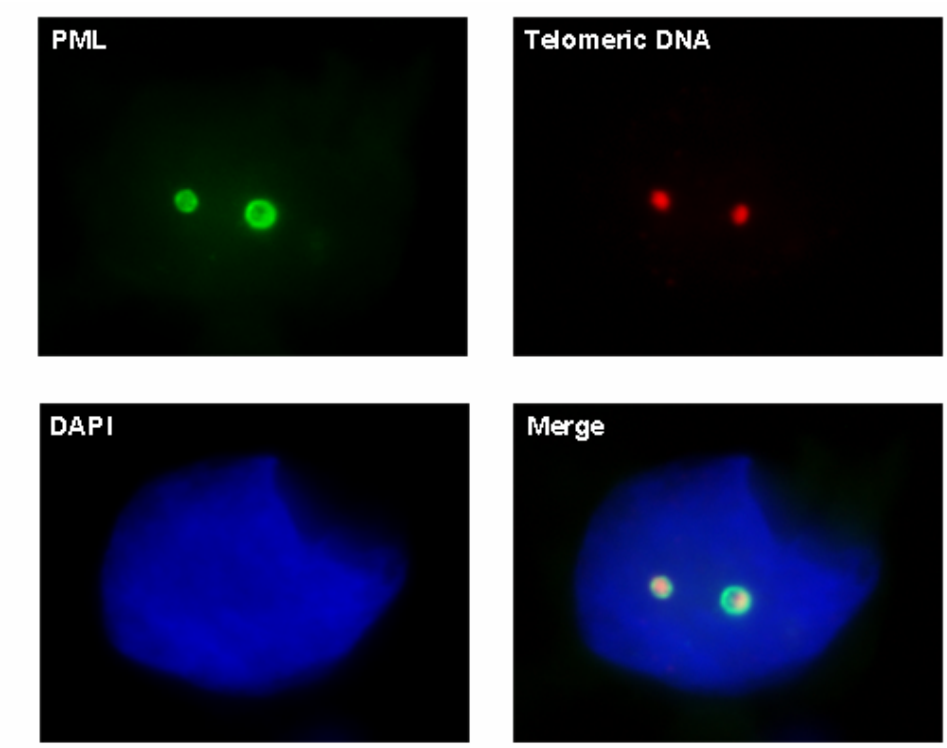

Fig 1.2: ALT-associated PML Bodies (APBs) in an ALT[+] human tumour. APBs are PML nuclear bodies that contain *telomeric DNA*. While PML nuclear bodies are ubiquitous, APBs are a hallmark of ALT. *PML* has been detected by indirect immunofluorescence (FITC label) and is often concentrated in the outer rim of PML nuclear bodies. *Telomeric DNA* has been detected with telomere fluorescence *in situ* hybridisation using a Cy3 conjugated peptide nucleic acid probe. The nucleus of this ALT[+] human osteosarcoma cell was counterstained with 4',6-diamidino-2-phenylindole (*DAPI*) and analysed with an 100x objective. The foci of telomeric DNA that colocalise with PML in the *merge*d image represent APBs. Telomeres are not bright enough relative to the telomeric DNA in APBs to be visible with the exposure time used.

There seems to be a tight correlation between the presence of APBs within a cell line and the presence of ALT, as manifested by the characteristic telomere length pattern. At the time this study commenced, APBs had been reported in 15/15 ALT[+] and 0/7 telomerase[+] cell lines, and in 0/5 mortal cell strains[83,95,97]. APBs had been detected in ALT[+] tumours[83], although the number examined was small. A temporal correlation has been found between the immortalisation event and the occurrence of

also repressed[106]. APBs were also shown to be the sites of DNA synthesis[132,140] supporting a possible functional link with the ALT mechanism. The investigations of this study into the association between APBs and ALT are described in Chapter 3.

1.5 ALT mechanism involves recombination mediated replication

There is strong evidence that recombination is involved in the ALT mechanism. The most direct evidence is the dependence of ALT on the MRE11/RAD50/NBS1 complex[2] and possibly the RAD51D protein[138], both of which are involved in HR. DNA synthesis in APBs is also inhibited by caffeine, suggesting that it is initiated by ATM and/or ATR[140] and supporting the presence of recombination mediated replication in ALT. Furthermore, HR is specifically increased at the telomeres in ALT cells[198] and this includes intertelomeric recombination-mediated replication of telomeric tags[3], postreplicative telomeric exchanges[117-119] and intratelomeric recombination-mediated telomeric deletions[108,109]. The proximal telomeric hypervariable region appears to be included in the increased levels of telomeric recombination in ALT[199]. ALT cells display large length fluctuations in individual telomeres that do not appear synchronised with other telomeres in the cell or with other cells[81,105,106], which is consistent with telomeric recombination. It has been proposed that ALT cells are defective in suppressing HR at the telomere[6]. Since HR is not increased elsewhere in ALT cells[117,198] except possibly at certain minisatellites[121,122], it would seem probable that the alteration is in a telomere specific protein such as a Shelterin component or an unknown telomere and/or minisatellite binding factor[200,201]. A TRF2 mutant is known to increase intratelomeric HR when expressed in non ALT cells[109]. However, there are other potential causes of the

telomere-specific recombination increase, such as the telomeric susceptibility to DNA damaging agents[202].

Data from other organisms also suggest that telomeres may under some circumstances be maintained by a recombinational process. Recombination is the primary mechanism of telomere maintenance in the mosquito malarial vector, *Anopheles gambiae*[203], and possibly for the telomeres of linear mitochondrial DNA in some species of yeast[204]. Recombination is also used by some species of yeast as a back up mechanism for telomere maintenance. In the yeast *Saccharomyces cerevisiae*, inactivation of telomerase leads to loss of telomeric repeats with cell division, and eventually death of most of the cells; survivors are dependent on the *Rad52* gene which encodes a protein required for recombination[176]. There are two categories of such survivors: in type I there is amplification of a subtelomeric tract repeat element with a short terminal telomeric repeat and in type II there is elongation of telomeric repeats[177,180,205]. The telomere length phenotypes of the Type II telomerase-null survivors in *S. cerevisiae* and also the *Rad52*-dependent telomerase-null survivors in *Kluveromyces lactis* resemble those of ALT[+] human cells[205,206]. Recent studies suggest that for both telomerase-null survivors in *K. lactis* and the mitochondria of *Candida parapsilosis*, small circular ECTR is involved in the elongation mechanism[207,208].

On the basis of some of these considerations, a telomere maintenance mechanism (TMM) involving inter-telomeric recombination was proposed for mammalian ALT cells[209] (Fig 1.3A). This was the simplest explanation for the replication of a telomeric tag onto different telomeres[3]. The same mechanism could conceivably elongate the

telomere using other telomeric templates: linear ECTR, circular ECTR (rolling circle replication) or the same telomere (T-loop replication; Fig 1.3). Recombination mediated replication could also occur indirectly by recombinant mediated replication events occurring between the ECTR concentrated in APBs and then recombining the replicated linear or circular ECTR into the telomeres.

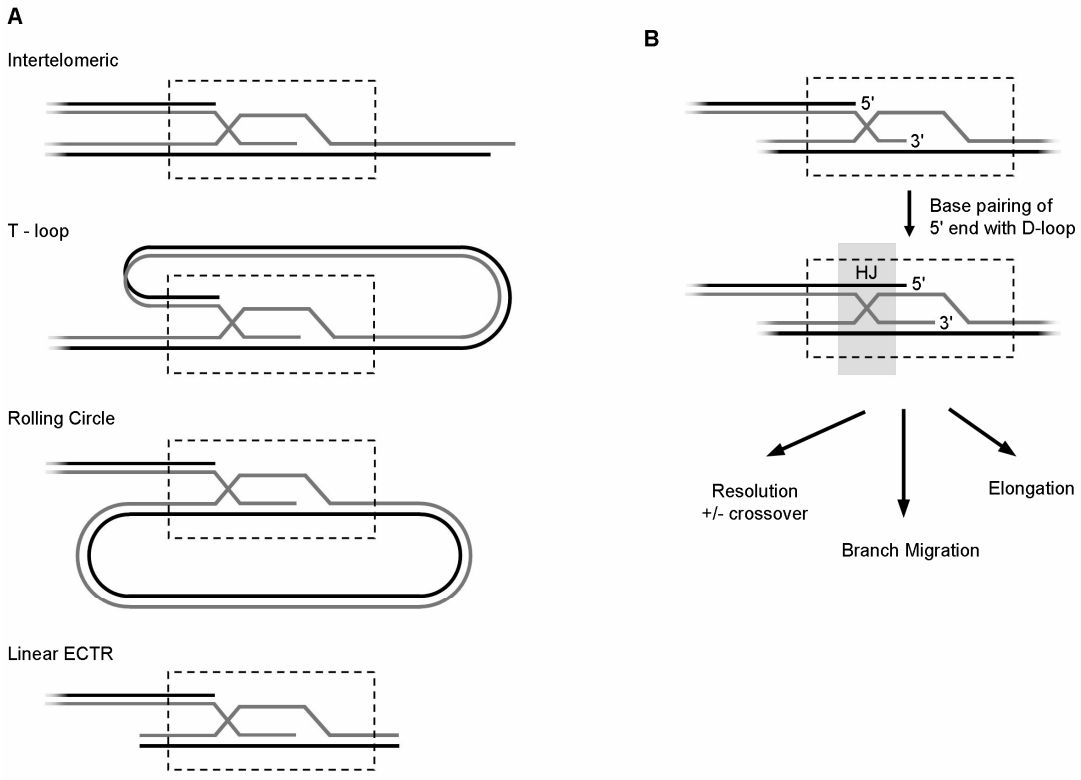

Figure 1.3: Proposed model for homologous recombination dependent elongation of telomeres. **A:** Regardless of template type, the local topology (dashed box) of the 3′ invasion is the same. The template telomeric DNA could be another telomere, the same telomere or circular/linear ECTR. **B:** The 3′ telomere end invades a telomeric duplex creating a D-loop. If the 5′ end base pairs with the D-loop, a Holliday junction (HJ) will be formed. This may then be recognised by recombination proteins for branch migration, elongation or resolution with or without crossover events[3-6].

1.5.1 T-loop replication

T-loops have been postulated to be a mechanism for hiding the telomere ends from various proteins, but also provide a structure that could result in elongation or shortening of the telomere. The strand invasion by the 3′ overhang in t-loops is equivalent locally to the structure used in recombination-dependent replication. It has been suggested that replication is normally inhibited by the telomeric DNA end binding protein, POT1[210]. If replication does occur on the invading strand, formation of a HJ (by base pairing of the 5′ end with the D-loop) and branch migration together with lagging strand synthesis may allow the t-loop to roll with replication continuing indefinitely (Fig 1.3B). Interestingly, the average loop to tail ratio for T-loops in ALT cells appear lower than non ALT cells[108]. This may be consistent with recent t-loop replication events in ALT telomeres. However, there are other explanations such as the possibility that a large part of the proximal telomeric repeats in ALT cells may not be functioning properly as a telomere.

1.5.2 Rolling circle replication

Another possible recombination-mediated mechanism of telomere lengthening involves a rolling circle of replication in which the 3′ single stranded telomeric overhang invades a circle of ECTR (Fig 1.3A). HJ formation and branch migration of the 3′ overhang may then allow rolling of the circle and essentially unlimited elongation. Artificial circular DNA containing telomeric repeats has been shown to be utilised by *K. lactis* to greatly extend its telomeres[211]. In *C. parapsilosis* and other yeast species with linear mitochondrial DNA, rolling circles may be used for maintaining the mitochrondrial DNA termini[208,212].

The circular ECTR in ALT cells may also be a by-product of ALT activity rather than being used in the ALT mechanism. Circular ECTR are not unique to ALT cells: small amounts of telomere repeat circles have been found in human tumours and non-ALT cell lines[109,213]. Other types of small circular DNA found in human cells are considered to be a marker of genomic instability[214,215]. In yeast mutations in the RecQ helicase *sgs1*, increases the formation of rDNA circles and possibly subtelomeric repeat circles[216].

1.5.3 Linear ECTR DNA and the ALT mechanism

Linear ECTR[107] could be used to elongate telomeres by end-joining reactions or by HR and copy templating. The small size of much of the linear ECTR makes it unlikely that this could account for rapid, large increases in telomere length in ALT cells.

ECTR may also be indirectly involved in ALT by titrating out telomere binding proteins. Although it is entirely possible that the ECTR within APBs is only a subset of the total ECTR in ALT cells, the colocalisation within APBs of ECTR and proteins involved in recombination suggests either that they are involved in the ALT mechanism or are its by-products. APBs appear in the late S/G2/M compartment of the cell cycle[97,132], when HR is most active[217].

1.6 Telomerase components in ALT cell lines

The absence of telomerase activity from ALT cells correlates with lack of expression of hTERT and sometimes hTR[218,219]. In ALT cells that express the gene encoding

hTR, hTERC, the sequence is wild-type and expression of exogenous hTR in hTR negative ALT cells does not result in telomerase activity[219]. This is consistent with the finding that ALT cells have undetectable levels of the full-length hTERT transcript[218]. Lack of hTERT and hTR expression in ALT lines are both associated with ALT specific chromatin remodelling in their control regions, including promoter CpG island methylation[220,221], histone hypoacetylation and histone methylation changes. The latter includes Lys20 histone H4 methylation[222] which is associated with DNA damage recognition by 53BP1[223].

Expression of exogenous hTERT in hTR-expressing ALT cells induces telomerase activity, as detected by an *in vitro* assay[224], indicating that the other telomerase subunits are expressed at sufficient levels to support telomerase activity in these cells. For hTR-negative ALT cells, expression of both exogenous hTR and hTERT was required to induce telomerase activity[224].

1.7 Ability of ALT and telomerase activity to co-exist in human cells

Expression of exogenous telomerase in ALT cells is usually compatible with continued ALT activity, even though telomerase lengthens the shortest telomeres[106,225-227]. Subclones of late passage (> 100 PD) ALT cells expressing telomerase activity showed >100-fold reduction in the number of chromosome ends with telomere sequences that were undetectable by FISH[106]. The very long telomeres persisted however, and there was no significant change in the proportion of cells with APBs[106,225,226]. Telomere length heterogeneity was still being generated rapidly after more than 100 PDs with telomerase activity[106] and circular ECTR also persisted[108].

This means that the repression of ALT seen in some hybrids between ALT[+] and telomerase[+] cells is unlikely to be due to telomerase activity *per se*. It also suggests that ALT can act on telomeres that are not critically short, unlike the situation in yeast where telomeric recombination in telomerase-null survivors is repressed by re-expression of telomerase activity[205]. In one study, however, expression of telomerase in a human ALT cell line resulted in reduced evidence of ALT activity in two of nine clones[227]. One possible explanation might be that ALT may be switched off as a stochastic event in some cells (as has been demonstrated for telomerase in telomerase[+] cells[228]); these cells would lose proliferative capacity unless exogenous telomerase is present. Another explanation could be that ALT and telomerase may compete for common molecular components or access to the telomere. Thus ALT may be repressed under circumstances where a particularly high level of a telomerase subunit such as TERT is present. A further explanation might be that in some ALT cells the ALT mechanism only elongates critically short telomeres, which occur less frequently in the presence of exogenous telomerase.

1.8 ALT genetics and repression

Immortalisation usually depends on recessive mutations[11], and human cell lines have been assigned to at least four complementation groups for immortality[229]. Presumably, at least some of the genes corresponding to these complementation groups are repressors of a TMM: telomerase or ALT. However, some of these genes may act through other pathways because the mortal phenotype can be restored in somatic cell hybrids despite the presence of telomerase activity (as detected by an *in vitro* assay, which does not necessarily reflect continuing telomerase activity at the telomere)[69].

That ALT results from recessive mutation(s) was demonstrated by the observation that fusion of an ALT[+] immortal cell line with normal cells resulted in senescent hybrids that had lost the ALT telomere phenotype[230]. Further, some telomerase[+] immortalised cells appear to contain repressors of ALT activity: ALT was repressed in immortal hybrid cells formed by fusing an ALT[+] cell line from immortalisation complementation group A with either of two telomerase[+] cell lines from the same complementation group[106,230]. In contrast, fusion of ALT[+] and telomerase[+] cell lines from immortalisation complementation group D resulted in immortal hybrids with ALT active and telomerase repressed[231], indicating that ALT cells may contain a repressor of telomerase.

The observation that ALT cell lines have been assigned to at least two immortalisation complementation groups (A and D) suggests the possibility that there may be more than one gene that can repress ALT[232]. Introduction of chromosome 7 into ALT[+] cells suppressed both immortality and ALT[87,233]. The chromosome 7 gene(s) may not specifically repress ALT, however, because chromosome 7 also restored mortality to a group D telomerase[+] cell line[234]. In another ALT cell line introduction of chromosome 7 had no effect on immortality but introduction of chromosome 6 appeared to suppress immortality and ALT. Chromosome 6 monosomy has also been found in ALT cell lines derived from normal human fibroblasts by transformation with cell cycle genes[86]. Chromosome 8 has been suggested to harbour an ALT repressor based on findings that this chromosome had a high rate of loss of heterozygosity in 8/13 ALT cell lines. Understanding the mechanisms whereby ALT activity is repressed in normal cells may make it possible to design anti-cancer therapies that restore this repression.

1.9 Proteins that may be involved in the ALT mechanism or its regulation

Many of the proteins that have been identified in APBs may be involved in the ALT mechanism (Table 1.2). RAD52, RAD51, RAD51D, RPA, the MRE11/RAD50/NBS1 complex, and RecQ helicases have functions compatible with HR and recombination-dependent replication. All of these proteins are present in APBs. Another common component of PML nuclear bodies, SUMO-1, is a small ubiquitin-related modifier protein that can be covalently attached to other proteins, including PML, RAD51, RAD52 and PCNA[142,235-237]. Mutation of the *Schizosaccharomyces pombe* homologue of SUMO-1 causes rapid telomere elongation[236]. Thus it is possible that modification of proteins in APBs could alter their usual function.

Recent evidence suggests that the MRN complex and RAD51D, both of which are present in APBs, may be required for the ALT mechanism. Over-expression of SP100 inhibits ALT activity and this is dependent on its ability to sequester the MRN complex. All hallmarks of ALT activity tested (including telomere length fluctuations and APB formation) were lost when there was sequestration of the MRN complex but not when truncation mutants of SP100 unable to bind MRN were used[2]. This suggests that in addition to any role at the telomere in non-ALT cells[160,165], MRN is needed for the ALT mechanism. Furthermore, location to APBs of NBS1 (NBS1 is required for phosphorylation and activation of MRN[238]) coincides with active DNA synthesis in APBs[131,132,140]. RAD51D also appears necessary for ALT maintenance of telomeres as its knockdown caused telomeres to become shorter and less heterogeneous[138]. However, other hallmarks of ALT activity were not tested so it is not known if

RAD51D is inhibiting ALT activity specifically or having an overriding non-ALT specific effect on the telomeres.

The role of the RecQ helicases, including BLM, WRN and RECQL4, in disruption of alternative DNA structures, in the resolution of intermediates of HR and replication, and in acting as an interface between DNA replication and HR suggests they could be involved in the ALT mechanism, perhaps by directly facilitating HR-mediated copying of telomeric repeats that would be otherwise inefficient[169,173]. Indeed, over-expression of GFP-BLM has been found to cause an ALT specific increase in telomeric DNA[136]. The *S. cerevisiae* RecQ helicase, *sgs1,* is required for *S. cerevisiae* Type II telomerase-null survivors and is known to be complemented by BLM and WRN[134,166,167]. The telomere binding proteins, TRF1, TRF2 and POT1 are known to interact with both BLM and WRN and influence their activities[136,168,170,171,239,240]. WRN and BLM are found at telomeres in non-ALT cells[135,170,172]. BLM may function normally at the telomere to assist t-loop formation or resolution[136,168]. WRN's main role at the telomere in normal cells appears to be the resolution of G-quadruplex structures that form on the G-strand and block lagging strand replication of the telomere[172]. *In vitro* WRN can also resolve t-loops and degrade the 3′ overhang[168,171]. Not much is yet known about the role of RECQL4; however, recent data is suggests that similarly to BLM and WRN it may be present in APBs[241]. RECQL4 is required for initiation of replication in *Xenopus laevis*[242]. Mutations in BLM, WRN and RECQL4 cause the cancer predisposition syndromes Bloom syndrome (BS), Werner syndrome (WS) and Rothmund-Thomson syndrome (RTS), respectively. The cancer spectrum of BS is mainly haematological and gastrointestinal. In WS the majority of cancers are spread among soft tissue sarcomas, thyroid carcinomas, melanomas and

meningiomas. RTS is predominantly associated with osteosarcomas and non-melanoma skin cancers[243].

Epigenetic modification of telomeric chromatin is important for telomere length regulation and may also be important for allowing ALT activity. Telomeric chromatin has distinct nucleosomal spacing[244] and histone modifications which are similar to pericentric heterochromatin[245]. In mice, alteration of histone methyl and acetyl adducts by knockout of all three Rb family proteins or both Suv39h histone methyltransferases (HMTs) leads to greatly elongated and heterogeneous telomeres[246-248]. This is probably due to the telomeric chromatin becoming more open and accessible to telomerase that is constitutively expressed in mice. However, the regulation of telomere length may also be affected and the more accessible telomeres may facilitate HR. Activation of ALT by transformation of human fibroblasts with Human Papilloma Virus (HPV) oncogenes seems to require E7[85], which is responsible for the inactivation of Rb family proteins[249]. Thus opening up of the telomeric chromatin by Rb family deficiency may be necessary for ALT. Loss of the Suv39h HMT also abrogates Heterochromatin Protein 1 (HP1) family binding which probably contributes to the opening of the telomeric chromatin into a more accessible state[247]. HP1 mutation in yeast and flies enhances non-telomerase telomere maintenance[250-252]. In yeast, modification of histones can regulate recombination[253] and methylation of histone H4 lysine 20 is important for DNA damage recognition by yeast 53BP1[223]. At the hTERT and hTR promoters (humans), histone H4 lysine 20 is specifically methylated in ALT cells[222]. However, this may not be significant for the ALT mechanism as telomeric histone remodelling induced by loss of Rb family proteins includes decreased histone H4 lysine 20 tri-methylation[248].

The fact that the DNA damage response proteins phosphorylated-TRF2, phosphorylated-H2AX, 9-1-1 complex and Rif1 are present at telomeric DNA specifically in ALT cells[140,141] suggests that ALT telomeres may be eliciting a damage response. This may be due to actual damage or lack of suppression of a damage signal, i.e., lack of telomere capping. This could be either a cause or effect of the ALT mechanism. Short telomeres are a likely candidate for a damage signal, however, telomeres are also prone to DNA damage by oxygen radicals and alkylating agents[202]. Thus it is possible that increased creation or lack of removal of an endogenous DNA modifying agent occurs in ALT. This could stimulate ALT directly or indirectly by disruption of TRF2 binding[254].

It is possible that ALT is controlled by repressors of recombination; these may be specific for the telomere, or may also have a role elsewhere in the genome. One possible repressor is TRF2 which is known to be involved in suppressing non-homologous end joining (NHEJ)[146] and HR[109] at the telomere. Both HR (Section 1.5) and NHEJ[81,96] are increased at ALT telomeres.

The general immortalisation suppressor p53 could also inhibit ALT directly by its role in suppressing inappropriate HR[255]. Thus p53 could suppress both TMMs[256,257]. Razak *et al*.[258] showed that p53 binds telomeric DNA and inhibits DNA synthesis specifically in ALT cell lines. This did not require a functional transactivation domain but did require specific DNA binding ability and/or its ability to suppress HR. In particular, R175H, R248Q and R273H mutations abrogated the ability of transactivation incompetent p53 to inhibit DNA synthesis in ALT. Li Fraumeni

syndrome (LFS), which is associated with germ-line mutations that diminish the function of p53, appears to predispose to ALT. LFS is defined by an inherited increased risk of various cancers including sarcomas and brain cancers[259]. ALT is the TMM in 70% (26 of 37) LFS immortal cell lines and 2 of 2 LFS tumours[68,73,90,92,260,261] (Huschtscha, L, Reddel, R unpublished results). However, these cell lines and tumours are from just four LFS families, with a high prevalence of ALT in cell lines from an individual with a germline p53 codon R248Q (GC to AT transition)[92] and also in cell lines and a tumour from a family with a large germline p53 truncation mutation (intron 4 inclusion)[68,73,260]. In contrast, the cell lines from an individual with a p53 codon 133 mutation had a low prevalence of ALT[90,261]. Thus it appears that the predisposition to ALT in LFS may depend on the type of germline p53 mutation or genetic characteristics of each family. Different p53 mutations are known to have a different predisposition to cancer in different cellular contexts[262,263].

Other proteins that could conceivably be involved in ALT include poly(ADP-ribose) polymerase 1 (PARP1), which binds single and double stranded DNA breaks and poly ADP-ribosylates proteins including itself, causing it to shuttle on and off the DNA. It is known to interact with p53 and there is evidence that it is involved in DNA repair and suppressing recombination at DSB[264]. In mouse embryo fibroblasts loss of both PARP1 and p53 results in a telomere length phenotype that resembles ALT. The double null mutants had an increased prevalence of tumours compared to single mutants. However, when a tumour in a double null mouse was investigated, it had decreased telomere length[264]. Another candidate is Rif2p which may specifically inhibit recombination at the telomeric repeats in *S. cerevisiae*. Type II telomerase-null survivors are inhibited by Rif2p[180] and it is postulated that Rif2p may interfere with

the Rad50p complex. The mammalian homologue of Rif2p has not yet been identified. Finally, the mismatch repair (MMR) genes may suppress recombination more generally, especially homeologous recombination. It has recently been observed that defects in the MMR pathway provide a growth advantage to telomerase-null yeast cells as they approach senescence[265]. Defective MMR is an important cause of inherited and sporadic cancer, a diagnostic feature of which is microsatellite (tandem repeats of 1-4 nucleotide sequences) instability (MSI)[266]. However, as mentioned in Section 1.4.7, ALT cells have not been found to have increased MSI.

1.10 Telomeric recombination in normal cells

Although interest has so far centred on telomere maintenance by recombination in immortalised cells and cancers, there is some evidence in support of normal human cells using a recombination-mediated mechanism to maintain very short telomeres at the expense of longer telomeres. When telomeres on individual chromosome arms in a mass culture of normal human fibroblasts were examined, it was found that the shorter telomeres were maintained above 1 to 2 kb, while the longer telomeres experienced some rapid deletion events[101]. The proliferation capacity was found to correlate with the mean telomere length and not the lengths of the four shortest telomeres, supporting the notion that the mechanism is non-reciprocal recombination between long and short telomeres. The authors suggested that the limited reprieve from senescence provided by lengthening the shortest telomeres in this way could be influenced by mutations affecting the cell's predisposition to recombination.

There is some evidence that recombinational telomere lengthening may occur in some mouse cells *in vivo* under exceptional conditions. In mice that had lost telomerase activity due to a knockout mutation (mTERC-/-), the germinal centre lymphocytes lost 7 kb of telomere repeats after immunisation, consistent with proliferation in the absence of telomerase. In later generations of mTERC-/- mice there were only a few germinal centres, but the lymphocytes had elongated their telomeres by an average of 12 kb. One possible explanation is the utilisation of an ALT-like mechanism[75].

1.11 Significance of ALT in cancer

Cancers maintain the length of their telomeres with either telomerase[267,268] or ALT[73], with only a few having no known TMM[73,269-271]. Approximately 85% of all human tumours have telomerase activity[272], but the presence of ALT in tumours had not been examined extensively prior to this study. An early study of ALT in tumours[73] found that 7/57 (12%) of various tumour types were ALT[+]. The prevalence of the two TMMs appears to vary among different tumour types (Table 1.3). For example, only about 50% of sarcomas and

Table 1.3: Prevalence of telomerase[-] cancer

Cancer type	Telomerase[-] (%)	Total number	References
Cancers in general	15%	2015	272
Colorectal cancer	11%	619	268,273-284
Non-small cell lung carcinoma	27%	655	285-295
Soft tissue sarcoma	48%	333	96,296-305
Malignant fibrous histiocytoma	48%	50	296,297,299,301,303
Leiomyosarcoma	45%	33	296,297,299,303,304
Osteosarcoma	52%	126	96,271,299,301,305
Papillary carcinoma of the thyroid	51%	312	306-322

Follicular carcinoma of thyroid	70%	82	306-314,316,317,319,321,322
Anaplastic carcinoma of thyroid	62%	29	307-309,312,321,322

thyroid carcinomas are telomerase[+] (Table 1.3) and two recent studies have found ALT to be common in osteosarcomas (66% ALT[+])[271] and glioblastoma multiforme (GBM; 25% ALT[+])[270]. There is increasing evidence that some tumours contain a mixture of areas with and without telomerase activity[271,323-327], but intratumoral spatial heterogeneity had not previously been demonstrated for ALT.

It is likely that the study of ALT in cancer will be useful for clinical practice. In GBM the presence of ALT was found to correlate more strongly with long-term survival than the standard prognostic indicator, patient age[270]. In osteosarcomas, however, ALT[+] and telomerase[+] tumours appeared to be equally aggressive and longer survival correlated well with the absence of both TMMs[271]. ALT, like telomerase, may become an attractive drug target if it proves to be common in a number of tumour types, especially since repression of ALT in ALT[+] immortal cell lines results in senescence and cell death[87,230].

1.12 Project aims

The initial aim of this study was motivated by the need for a practical method of screening routinely archived tumours for ALT to facilitate the study of ALT in cancer. Detection of ALT in tumours has been dependent on extracting good quality genomic DNA to test for the characteristic heterogeneous telomere length distribution of ALT cells by Southern analysis. Because it is sometimes more convenient to study tumours archived as paraffin-embedded blocks, this study investigated whether another hallmark of ALT cells, the presence of APBs[83], could be utilised as an assay

for ALT. The results presented in Chapter 3 show that detection of APBs is a reliable method for detecting ALT in paraffin sections of human tumours.

Chapter 4 describes use of the APB assay to survey tumours of various types for the presence of ALT to determine if ALT is common in some types of cancer. This study focused on tumours which had been shown to have a relatively low prevalence of telomerase activity (Table 1.3). By analysing the clinical data with reference to ALT status, Chapter 4 also investigates the effect of ALT activity on patient survival and tumour aggressiveness.

Results obtained during this study supported there being a gene expression pattern associated with the activation of ALT in tumours. Chapter 5 describes the use of RNA microarray analysis to identify genes that may have altered expression in ALT. Even if not directly involved in the ALT mechanism, expression changes strongly correlated with the activation of ALT may help in designing treatment strategies for ALT[+] tumours. Studies described in Chapter 4 were also designed to improve our understanding of genes necessary for ALT by investigating if losses of tumour suppressors in cancer predisposition syndromes affect the prevalence of ALT.

Chapter Two:

Materials and Methods

Materials and Methods

2.1 Reagents

2.1.1 Chemicals and general reagents

The general reagents and chemicals commonly used in the experimental methods of this thesis are listed below (Table 2.1).

Table 2.1: Chemicals and general reagents

Reagent	Source
Acetone	BDH
Acrylamide (30% acryl/bis 29:1)	Biorad
Acrylamide (40% acryl/bis 19:1)	Amresco
Agarose, SeaKem® LE	Cambrex
4-(2-aminoethyl)-benzenesulphonyl fluoride hydrochloride (AEBSF)	ICN Biomedicals
Ammonium persulphate	Roche
Boric acid	BDH
Bovine serum albumin (BSA), Fraction V	Roche
Bromophenol blue	LKB Produkter AB
Calf thymus DNA (ultra pure)	Sigma
3-[(3-cholamidopropyl)-dimethylammonio]-1-propanesulphonate (CHAPS)	Pierce
Citric acid	BDH
Diethyl pyrocarbonate (DEPC)	BDH
1,4 Diazabicyclo(2.2.2)octane (DABCO)	Sigma
4',6-Diamidino-2-phenylindole dihydrochloride (DAPI)	Sigma
Disodium hydrogen orthophosphate	BDH
Dithiothreitol (DTT)	Sigma
Ethanol	BDH
Ethidium bromide	Sigma

Ethylenediaminetetraacetate (EDTA)	BDH
Ethylene glycol-bis(2-aminoethylether)-N,N,N',N'- tetraacetate (EGTA) (molecular biology grade)	Sigma
Ficoll-400	Amersham Biosciences
Formaldehyde	BDH
Formamide	BDH
Glucose	Sigma
Glycerol (analytical grade)	BDH
Glycogen (molecular biology grade)	Roche
Hydrochloric acid	BDH
β-mercaptoethanol (molecular biology grade)	Sigma
Magnesium chloride	BDH
Methanol	BDH
Methylene Blue	Sigma
Nonidet P-40 (NP-40)	BDH
PCR nucleotide mix (dNTPs)	Roche
Phosphate buffered saline (PBS) tablets (without calcium or magnesium)	ICN
Polyoxyethylene-sorbitan monolaurate (TWEEN-20) (molecular biology grade)	Sigma
Polyvinylpyrrolidone 40 (PVP-40)	Sigma
Pronase	Sigma
Sodium acetate	BDH
Sodium bicarbonate	BDH
Sodium chloride	BDH
Sodium dihydrogen orthophosphate	BDH
Sodium dodecyl sulphate (SDS)	Amresco
Sodium hydroxide	BDH
N,N,N',N'-tetramethylethylenediamine (TEMED)	Amresco
Sybr® Green I	Molecular Probes
Tetrasodium pyrophosphate	Sigma
Trichloroacetic acid	BDH
Tris(hydroxymethyl)aminomethane (Tris)	Roche
Trisodium citrate	BDH

Triton-X 100	BDH
Xylene cyanol	Ajax
Xylenes	Ajax

2.1.2 Cell culture reagents

Reagents used for the maintenance of cells in culture are listed in Table 2.2. Tissue culture-grade products were used for the production of buffers and growth media unless otherwise indicated. Analytical grade reagents were also used in the production of some tissue culture buffers.

Table 2.2: Source of cell culture reagents

Reagent	**Source**
Collagen solution, Type 1	Sigma
Dimethylsulphoxide (DMSO)	Sigma
Dulbecco's Modified Eagle Medium (DMEM)	Gibco
Ethanol (Spectrasol grade)	Ajax
Fibronectin, bovine; lyophilised powder	Sigma
Fetal bovine serum (FBS)	Gibco
LHC-BM	Biofluids Inc
LHC-MM and LHC-9	Biosource
Phenol Red	Sigma
Roswell Park Memorial Institute (RPMI) 1640	Gibco
Soy Bean Trypsin Inhibitor (SBTI)	Gibco
Trypsin-EDTA	Gibco

2.1.3 Buffers and solutions

The buffers and solutions commonly used in the experimental methods of this thesis are listed below (Table 2.3).

Table 2.3: Buffers and Solutions

Solution	Composition of reagents	Preparation and storage
50X Denhardt's solution	1%(w/v) Ficoll-400, 1%(w/v) PVP, 1%(w/v) BSA (fraction V)	Store at -20°C
Diethyl pyrocarbonate (DEPC) water	0.01% (w/v) DEPC, H_2O	Prepare in glass bottles and fume hood. Shake well, leave overnight, autoclave
1 M dithiothreitol (DTT)	0.155 mg/ml dithiothreitol 0.01 M sodium acetate, pH 5.2	Store at -20°C
DNA gel loading dye (6X)	0.25% (w/v) bromophenol blue, 0.25% (w/v) xylene cyanol, 30% (v/v) glycerol	Aliquot and store at RT
10X 3-(N-morpholino) propane-sulphonic acid (MOPS) buffer	0.2 M (MOPS), 80 mM sodium acetate, 10 mM EDTA	made with DEPC water pH 7.0
RNA Loading Dye	50% (v/v) glycerol, 1mM EDTA pH 8.0, 0.25% (w/v) bromophenol blue, 0.2% (w/v) xylene cyanol	Store at RT
20X Sodium chloride-trisodium citrate buffer (SSC)	3 M NaCl 0.3 M tri-sodium citrate	pH to 7.0
10X Tris-borate-EDTA buffer (TBE)	0.9 M Tris 0.9 M borate acid 20 mM EDTA	pH to 8.0
Tris-EDTA buffer (TE)	10 mM Tris-Cl pH 8.0 1 mM EDTA	Sterilise by autoclaving
10X Tris-sodium chloride-EDTA buffer (TNE)	0.1 M Tris 10 mM EDTA 1 M NaCl	pH to 7.4 Filter sterilised

2.2 Cell culture

2.2.1 Cell lines and cell strains

Various human mortal cell strains and immortal cell lines were used in this study. Table 2.4 lists the *in vitro* immortalised cell lines and includes the media used for their culture. The tumour derived cell lines (Table 2.5) and mortal cell strains (Table 2.6) were grown in DMEM with 10% FBS except for DOS15, DOS16 and IIICF which were grown in RPMI 1640 medium with 10% FBS.

Table 2.4: *In vitro* immortalised human cell lines used in this study

Cell Line	Lineage	Method of immortalisation	Source and reference	Growth Media
293	Kidney, embryonal	Adenovirus 5	ATCC[328]	DMEM (10% FBS)
AT1BR44neo	Fibroblast; AT	SV40	J. Murnane[329]	DMEM (10% FBS)
AT22IJE-T	Fibroblast; AT	SV40	J. Murnane[330]	DMEM (10% FBS)
BET-3K	Epithelial, bronchial	SV40	Reddel Lab[331]	LHC-9
BET-3M	Epithelial, bronchial	SV40	Reddel Lab[331]	LHC-9
BFT-3K	Fibroblast, bronchial	SV40	Reddel Lab[331]	LHC-9
F80-TERT/K1-1	Fibroblast, mammary	hTERT, SV40	Reddel Lab, C. Toouli unpub.	DMEM (10% FBS)
GM0637	Fibroblast, skin	SV40	NIGMS[80]	DMEM (10% FBS)
GM639	Fibroblast, skin; galactosaemia	SV40	NIGMS[332]	DMEM (10% FBS)
GM847DM (GM847)	Fibroblast, skin; LNS	SV40	O. Pereira-Smith[11]	DMEM (10% FBS)
IIICF/c	Stromal fibroblast breast carcinoma; LFS	Spontaneous	Reddel Lab[68]	RPMI (10% FBS)
IIICF/c-EJ-*ras*	Stromal fibroblast breast carcinoma; LFS	Spontaneous, Ras	Reddel Lab[83]	RPMI (10% FBS)
JFCF-6/hTERT/1	Fibroblast, jejunal; CF	hTERT	Reddel Lab, Z H Zhong unpub.	DMEM (10% FBS)
JFCF-6/T.1J/1-3C	Fibroblast, jejunal; CF	SV40	Reddel Lab, P Bonnefin unpub.	DMEM (10% FBS)
JFCF-6/T.1J/1-4D	Fibroblast, jejunal; CF	SV40	Reddel Lab, P Bonnefin unpub.	DMEM (10% FBS)
JFCF-6/T.1J/1D	Fibroblast, jejunal; CF	SV40	Reddel Lab, P Bonnefin unpub.	DMEM (10% FBS)
JFCF-6/T.1J/4D	Fibroblast, jejunal; CF	SV40	Reddel Lab, P Bonnefin unpub.	DMEM (10% FBS)
JFCF-6/T.1J/5H	Fibroblast, jejunal; CF	SV40	Reddel Lab, P Bonnefin unpub.	DMEM (10% FBS)
JFCF-6/T.1J/6B	Fibroblast, jejunal; CF	SV40	Reddel Lab, P Bonnefin unpub.	DMEM (10% FBS)
JFCF-6/T.1J/6G	Fibroblast, jejunal; CF	SV40	Reddel Lab, P Bonnefin unpub.	DMEM (10% FBS)

JFCF-6/T.1J/9E	Fibroblast, jejunal; CF	SV40	Reddel Lab, P Bonnefin unpub.	DMEM (10% FBS)
JFCF-6/T.1J/11C	Fibroblast, jejunal; CF	SV40	Reddel Lab, P Bonnefin unpub.	DMEM (10% FBS)
JFCF-6/T.1J/11E	Fibroblast, jejunal; CF	SV40	Reddel Lab, P Bonnefin unpub.	DMEM (10% FBS)
JFCF-6/T.1P	Fibroblast, jejunal; CF	SV40	Reddel Lab, P Bonnefin unpub.	DMEM (10% FBS)
JFCF-6/T.1R	Fibroblast, jejunal; CF	SV40	Reddel Lab[83]	DMEM (10% FBS)
KMST-6	Fibroblast, embryonal	γ - irradiation	A Cuthbert[87]	DMEM (10% FBS)
MeT-4A	Mesothelial	SV40	C Harris Lab,[333]	LHC-MM,3%FCS
MeT-5A	Mesothelial	SV40	C Harris Lab[334]	LHC-MM,3%FCS
MeT-5A/6TGR-B	Mesothelial	SV40	Reddel Lab, N Whitaker unpub.	LHC-MM,3%FCS
MRC5-V1	Fibroblast, lung (embryonal)	SV40	L Huschtscha[335]	DMEM (10% FBS)
MRC5-V2	Fibroblast, lung (embryonal)	SV40	L Huschtscha[335]	DMEM (10% FBS)
SHB-PE6	Epithelial, mammary	HPV-E6	Reddel Lab, L Huschtscha unpub.	RPMI (10% FBS)
SUSM-1	Fibroblast, liver	4-nitroquinoline treatment	M Namba[336]	DMEM (10% FBS)
WI38-VA13/2RA	Fibroblast, lung (foetal)	SV40	ATCC[337]	DMEM (10% FBS)
W-V	Fibroblast	SV40	L Huschtscha[338]	DMEM (10% FBS)

AT: Ataxia Telangiectasia, LNS: Lesch-Nyhan syndrome, LFS: Li Fraumeni Syndrome, CF: cystic fibrosis, ATCC: American Type Culture Collection, NIGMS: National Institute of General Medical Sciences Human Genetic Cell Repository.

Table 2.5: Tumour derived human cell lines used in this study

Cell Line	Lineage	Source
A2182	Adenocarcinoma, lung	LHC
A549	Adenocarcinoma, lung	ATCC
DOS16	Leiomyosarcoma	R D Gupta, Prince of Wales Hospital, Sydney, NSW, Australia; unpublished
G-292	Osteosarcoma	ATCC
HeLa	Cervical carcinoma	ATCC
HT1080	Fibrosarcoma	ATCC
LOX-IMVI	Melanoma	NCI-Frederick
MG-63	Osteosarcoma	Rebecca Mason, University of Sydney, Sydney, NSW, Australia[339]
Saos-2	Osteosarcoma	ATCC
SK-LU-1	Adenocarcinoma, lung	ATCC
SKOV-3	Adenocarcinoma, ovary	ATCC
SJSA-1	Osteosarcoma	ATCC
TE-85	Osteosarcoma	ATCC
U-2 OS	Osteosarcoma	ATCC
WM1175	Melanoma	G. Mann, Westmead Millennium Institute, Sydney, NSW, Australia[83]

ATCC: American Type Culture Collection, LHC: Laboratory of Human Carcinogenesis, NCI-Frederick: National Cancer Institute at Frederick Division of Cancer Treatment Tumor Repository.

Table 2.6: Mortal human cell strains used in this study

Cell Type	Lineage	Source
BF10	Fibroblast, bronchial	Reddel Lab, R Reddel unpub.
DOS15	Gastrointestinal Stromal Tumour	R D Gupta Prince of Wales Hospital, Sydney, NSW, Australia; unpub.
HFF5	Fibroblast, foreskin	Ralph Böhmer, Ludwig Institute of Cancer Research, Melbourne, Vic, Australia[69]
IIICF	Fibroblast, stromal - breast carcinoma; LFS	Reddel Lab[68]
JFCF-6	Fibroblast, jejunal; CF	Reddel Lab, P Bonnefin unpub.
MRC-5	Fibroblast, lung (embryonal)	CSL[335]
WI-38	Fibroblast, lung (foetal)	CSL[268]

LFS: Li Fraumeni Syndrome, CF: cystic fibrosis, CSL: Commonwealth Serum Laboratories.

2.2.2 Growth of cell cultures

All cells were grown as monolayer cultures in disposable plastic cell culture vessels (Falcon®, Becton Dickinson) in 5.0% carbon dioxide (CO_2) (3.0% for epithelial and mesothelial cell lines), humidified air and water-jacketed CO_2 incubators at 37°C. The growth medium (described in Section 2.2.1) was replenished twice weekly. Epithelial and mesothelial cells were grown in flasks coated with a matrix of collagen and fibronectin (see Section 2.2.5.3). All solutions added to cell cultures were pre-warmed to 37°C. All manipulations were performed aseptically in biohazard hoods using sterile equipment.

2.2.3 Harvesting and passaging of cell cultures

Cells were detached from the plastic substratum of the cell culture vessel by trypsinisation[340]. Medium was removed from the flask and the cellular monolayer was washed once with PBS. Trypsin-EDTA (at half strength for epithelial cells) was added (1 ml/75 cm^2 flask) and the flask was incubated at 37^oC for approximately 5

min. After detachment of the cells, the trypsin was neutralised with 8 ml of either media with 10% (v/v) FBS (fibroblast and mesothelial cell cultures) or 5 ml SBTI (10 mg/ml; epithelial cell cultures) and the cell suspension was transferred to a 15 ml centrifuge tube (Falcon®, Becton Dickinson). Cells were centrifuged at RT for 5 min at 200 x g. If being passaged, the cell pellet was resuspended in 8 ml of growth medium and an appropriate fraction transferred to a new flask containing growth medium.

2.2.4 Cryopreservation and thawing of cell cultures

To cryopreserve cultured cells a harvested pellet was resuspended in 1.0 ml of 10% DMSO in FBS. The cells were transferred to a cryogenic vial (Corning Inc) and immediately placed in a -80°C freezer overnight before transfer to -195°C liquid nitrogen for long term storage. Vials removed from liquid nitrogen were thawed rapidly in a 37°C water bath and cells were immediately rinsed in growth medium to remove the freezing medium.

2.2.5 Preparation of cell culture solutions

All cell culture media were prepared with ultra-filtered (Milli-Q) water.

Dulbecco's Modified Eagle's Medium (DMEM)

To prepare DME medium, 133.7 g of DME powder and 12 g of sodium bicarbonate were dissolved in 8 L of water, the pH was adjusted to 7.4 with 1 M HCl or 1 M NaOH, and the volume was then made up to 10 L. The final medium was filter sterilised through a positive pressure 0.2 μm filter unit (MediaKap-10), and stored in 500 ml aliquots at 4°C in glass bottles in the dark. Before use, 55 ml of FBS was added to the medium.

2.2.5.1 HEPES-Buffered Saline (HBS)

HEPES (4.76 g), NaCl (7.07 g), KCl (0.20 g), glucose (1.70 g), and disodium hydrogen orthophosphate (Na_2HPO_4) (1.022g) were dissolved in 900 ml of distilled water. 0.25 ml of 0.05% phenol red was added, the pH adjusted to 7.5, and the final volume adjusted to 1L. The solution was filter sterilised (0.2 μm; Corning Inc) and stored at room temperature (RT).

2.2.5.2 Collagen/Fibronectin Coating Buffer

Fibronectin (5 mg) was dissolved in 20 ml of LHC-BM by heating to 37°C for 2 h. To this was added 50 ml of bovine serum albumin (BSA; 1 mg/ml in HBS), 20 ml Type 1 Collagen solution (1 mg/ml), and LHC-BM (470 ml). The solution was filter sterilised (0.2 μm; Corning Inc) and stored at 4°C in dark. At least 2 h before using flasks, 1.5 ml of the coating buffer/75 cm^2 was spread over the entire growth surface and incubated at 37°C. Immediately prior to use the excess coating buffer was removed.

2.2.5.3 Laboratory of Human Carcinogenesis-Basal Medium (LHC-BM)

LHC-BM containing stocks 4, 11, calcium and glutamine[340] (154.3 g), was dissolved in 8 L of water, 10 g of $NaHCO_3$ was added, the pH adjusted to 7.4 with 1M HCl or 1M NaOH, and the final volume was adjusted to 10 L. The medium was filter sterilised (0.2 μm) and 500 ml aliquots were stored at 4°C in glass bottles in the dark.

2.2.6 Mycoplasma testing

Routine laboratory mycoplasma testing was performed on all cell lines and strains used in this study using the Mycoplasma PCR Elisa kit (Roche) according to the manufacturer's instructions. Two cell lines KMST-6 and MRC5-V2 had mycoplasma infections. Repeated testing on all other cell lines and strains showed that mycoplasma infection had not spread to any other cell line or strain during this study.

Testing of various cryopreserved aliquots of the two infected cell lines indicated that the infection had been present throughout this study.

2.3 Tumour specimens

2.3.1 Human tumour specimens

Tumour specimens were acquired with approval of the Children's Hospital at Westmead Human Ethics Committee (Westmead, NSW, Australia) and approval from the Ethics Committees or Institutional Review Boards of the source institutions. Jonathan A Hannay, Dihua Yu and Raphael E Pollock provided frozen specimens and paraffin sections of the adult soft tissue sarcomas (STS) that were from 68 patients of the MD Anderson Cancer Center, Houston, Texas, USA. The 65 STS patients for whom survival data were available were all treated surgically at the MD Anderson Cancer Center between 1992 and 1999. Jinyoung Yoo and Robert A Robinson provided paraffin sections of the sixteen telomerase negative adult STS that were from the University of Iowa, Iowa City, Iowa and their telomerase status has been reported[297]. Anthony Henwood and Susan M Arbuckle provided paraffin sections of 33 paediatric STS that were from patients of the Children's Hospital at Westmead, NSW, Australia. Paraffin embedded specimens of osteosarcomas were from 58 patients of pathology departments in Sydney, NSW, Australia and were provided by Stanley W McCarthy, Royal Prince Alfred Hospital, Susan M Arbuckle, Children's Hospital Westmead and S Fiona Bonar, Douglass Hanly Moir Pathology. The subset of 39 osteosarcoma patients used for survival analysis were all treated by one surgeon, Paul D Stalley, and were diagnosed between 1997 and 2002 with operable non-metastatic osteosarcoma, and received similar preoperative chemotherapy. Janice A Royds, Stephen B Wharton and David A Jellinek provided paraffin sections of astrocytomas that were from 50 patients of the Royal Hallamshire Hospital, Sheffield,

UK and the University of Otago, Dunedin, New Zealand. The 32 GBM patients used for survival analysis were a subset of the patients described by Hakin-Smith *et al*.[270], for whom paraffin sections were available. Bruce G Robinson and Dianna L Learoyd provided paraffin embedded samples of papillary carcinomas of the thyroid that were from 17 patients of the Royal North Shore Hospital, St Leonards, NSW, Australia. The papillary carcinoma specimens were from three tumours > 4 cm (in maximum diameter), eleven tumours 1 - 4 cm, two tumours < 1 cm and one tumour specimen was taken from a lymph node. Paraffin sections of non small cell lung carcinomas from 291 patients of hospitals in the Baltimore metropolitan area were provided by Elise D Bowman and Curtis C Harris of the National Cancer Institute Maryland, USA. Emma Quinn and Robyn L Ward provided paraffin sections of colorectal carcinomas that were from 31 patients of St Vincent's Hospital, Darlinghurst, NSW, Australia. Rosalind A Eeles provided paraffin sections of the 14 tumour specimens that were from 12 patients with LFS (three lung adenocarcinomas were three separate but synchronous primary tumours in the same patient) who attended the Royal Marsden Hospital, Surrey, UK. Paraffin sections of three tumour specimens from two patients with WS were from Makoto Goto, Tokyo Metropolitan Otsuka Hospital, Tokyo, Japan. Lisa L Wang provided paraffin sections of the tumour specimens from two patients with RTS that were from the Texas Children's Cancer Center, Houston, Texas USA.

2.3.2 Tumorigenesis in nude mice

Tumour samples from the ALT[+] cell line IIICF/c-EJ-*ras* and the telomerase[+] cell line WM1175 were grown in nude mice and used as positive and negative controls (respectively) for the APB assay. For each cell line, ten Balb/c nu/nu mice (Animal Resources Centre, Murdoch, WA, Australia) at ten weeks old were injected

subcutaneously with $5x10^6$ cells in the interscapular region. Mice were assessed weekly for tumour development and size and when the tumour was more than 10 mm in diameter the mouse was euthanased, necropsied, and the tumour resected. In all mice no abnormalities were seen on visual inspection of heart, lungs, liver, spleen or kidneys. Resected tumours were either flash frozen in liquid nitrogen for storage at -80°C or fixed in 4% formaldehyde and paraffin embedded.

2.4 Immunostaining and fluorescence *in situ* hybridisation (FISH)

2.4.1 Detection of APBs and their constituents in cell culture monolayers

Cells grown in four-well or two-well chamber slides were rinsed with PBS, fixed for 15 min in 2% paraformaldehyde at room temperature and then permeated with methanol at -20°C for 12 min followed by acetone at -20°C for 30 sec. Cells were rehydrated in PBS and incubated with primary antibodies either for 1 h at room temperature or overnight at 4°C and then incubated with fluorescently conjugated secondary antibodies at room temperature for 30 to 60 min. To visualise DNA, slides were incubated for 3 min in PBS with 20μg/ml of 4, 6 diamidino-2-phenylindole (DAPI). Washes after each staining step were carried out by agitating in PBS with 0.1% Tween-20. Finally, the preparations were mounted in 90% glycerol (buffered with 20mM Tris-HCl pH 8.0) containing 2.33% antifade compound 1,4-Diazabicyclo[2.2.2]octane (DABCO). Images were captured on a Leica DMLB epifluorescence microscope using a cooled charge-coupled device camera (SPOT2; Diagnostic Instruments) and processed using Adobe Photoshop software.

Primary antibodies used preferentially for detection of APBs in monolayers were anti-TRF2 mouse antibody (1:200 dilution; Upstate Biotechnology) and anti-PML rabbit antibody (1:500 dilution; Chemicon). Other primary antibodies used for detecting

APBs or their constituents were anti-TRF1 rabbit antibody (1:400 dilution; polyclonal anti-TRF1 rabbit serum raised against a TRF1 peptide, residues 13 to 35), anti-PML mouse antibody (1:200 dilution; Santa Cruz) and anti-MLH1 mouse antibody (1:50 dilution; BD Biosciences). The secondary antibodies used were Texas Red or fluorescein isothiocyanate (FITC) conjugated goat anti-mouse and goat anti-rabbit antibodies (Jackson ImmunoResearch).

2.4.2 Detection of APBs in tumour specimens

Frozen sections were cut 5 - 7 microns thick and fixed in 1:1 methanol:acetone at -20°C for 12 min. After air drying, slides were rehydrated in PBS and stained immediately. Paraffin-embedded specimens were cut into 8 μm thick sections by the Histopathology Department, Children's Hospital at Westmead. Paraffin sections were then baked on Superfrost® Plus microscope slides (Menzel-Glaser) at 65 ^{o}C for 20 min and dewaxed in xylene for 5 min. Surface decalcification was needed for some osteosarcoma paraffin sections, in which case the paraffin-embedded specimen was pretreated with RDO Rapid Decalcifier according to manufacturer's instructions (Apex Engineering Products Corporation) . Slides were rehydrated and prepared for immunofluorescence and FISH by microwave heating to 120 ^{o}C in 90% glycerol (1 mM EDTA) buffered with 10mM Tris at pH 10.5, and maintained at 110-120 ^{o}C for 15 min. The slides were cooled and rinsed in PBS. All subsequent treatment of frozen and paraffin sections was identical. Immunofluorescence was performed with anti-PML rabbit antibody (Chemicon) and anti-rabbit FITC goat antibody (Sigma); the antigen retrieval technique was also suitable for TRF1/TRF2 immunofluorescence. Sections were then cross-linked with 4% formaldehyde for 10 min and dehydrated with increasing concentrations of ethanol for telomere FISH with a 5'-labelled Cy3-(5'-CCCTAA-3')$_3$ PNA probe (Applied Biosystems). A hybridisation mixture

containing 1 μg/ml probe, 70% formamide (deionised), 0.25% Blocking Reagent (Roche), 10 mM Tris, pH 7.5 and 5% $MgCl_2$ buffer (82 mM Na_2HPO_4, 9 mM citric acid and 25 mM $MgCl_2$) was applied to the slides which were then denatured at 80^{o}C for 3 min. After a 3 h hybridisation in the dark at room temperature, slides were washed in 70% formamide (0.01 M Tris pH 7.2), counterstained with 4'6-Diamidino-2-phenylindole (DAPI) in 0.05 M Tris pH 7.5, 0.15 M NaCl, 0.05% Tween-20 and mounted in 90% glycerol (buffered with 20 mM Tris-HCl pH 8.0) containing 2.33% antifade compound 1,4-Diazabicyclo[2.2.2]octane (DABCO). Images were captured on a Leica DMLB epifluorescence microscope using a cooled charge-coupled device camera (SPOT2; Diagnostic Instruments) and processed using Adobe Photoshop software.

A set of criteria was used to determine the APB status of tumour sections (Fig 2.1). Briefly, an APB was considered to be present if a focus of telomeric DNA was localised within (not adjacent or overlapping) a PML focus in the nucleus. To avoid false positives, it was also required that the telomeric DNA component of the APB to have a more intense fluorescence than that of the telomeres on that slide (for practical purposes, the working criterion used with the Cy3 conjugated telomeric probe was to require that with the appropriate camera exposure for the telomeric DNA component of the APB, the telomeres were not visible). The section was scored as positive for APBs if they were detected in 10 or more nuclei and in 0.5% or more of the cells in the section. To avoid artefacts, a cell was not considered to contain APBs if more than 25% of the co-localised foci occurred outside nuclei (correcting for ratio of nuclear area to non-nuclear area). Slides were not scored as negative unless >2000 tumour cell nuclei were examined. If a section fulfilled every criterion to be APB[+] except for the requirement for 0.5% or more of cells to have PML/telomeric DNA co-localisations, but had at least four telomeric DNA foci inside an outer ring of PML (as

illustrated in Fig 4.1) then it was scored as APB[+], but was noted as having a low frequency of APBs.

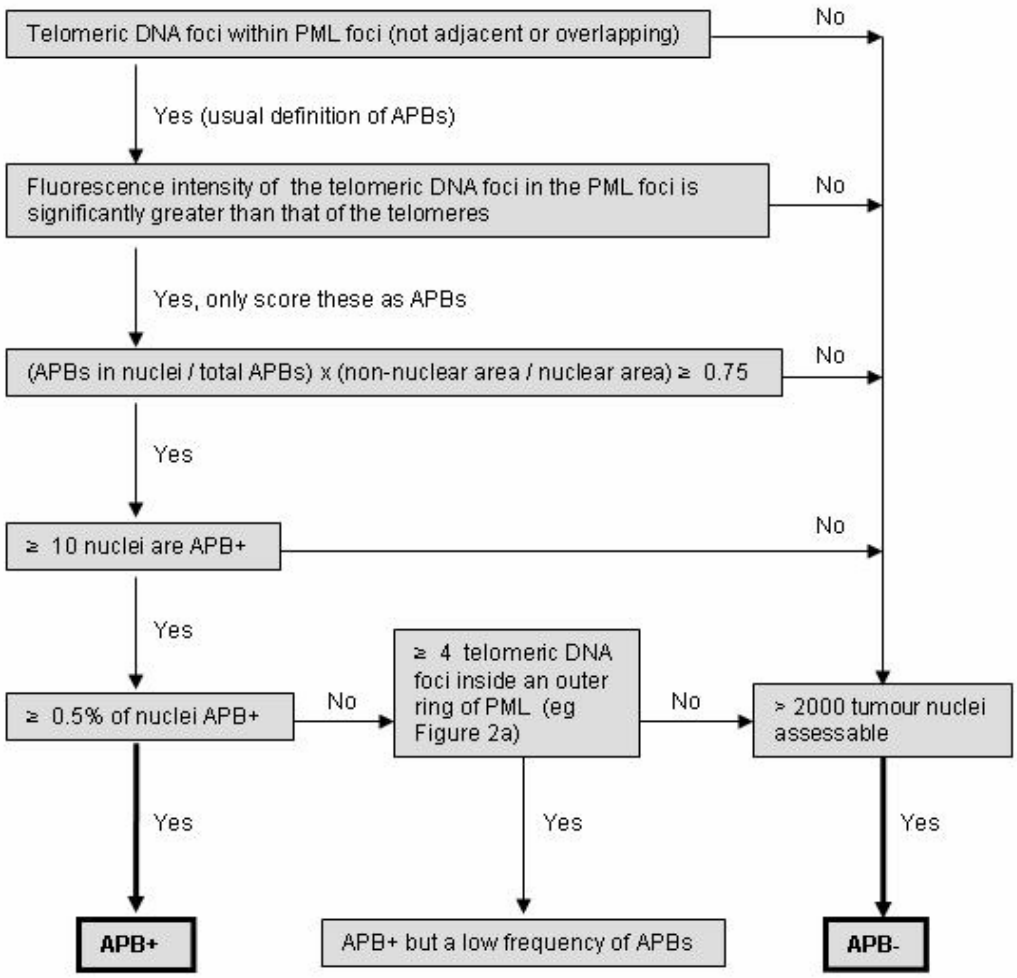

Figure 2.1: Flow chart for determining the APB status of tumour sections. The scoring criteria are designed to avoid staining artefacts and false positive colocalisations. These criteria should be applied to a contiguous and histologically homogeneous area.

2.4.3 Detection of APBs in fine needle aspiration biopsies (FNAB)

Cells were aspirated from resected tumour specimens (grown in nude mice, section 2.3.2) with a 25 gauge needle, placed on a Superfrost® plus microscope slide (Menzel-Glaser) and spread with a second slide. The slides were then fixed and permeated by air drying with a hair dryer and incubating in methanol at -20°C for 10

min followed by 95% ethanol at RT for 5 min and 100% ethanol for 2 min. Slides were then hybridised with the telomere FISH probe as described in section 2.4.2.

2.4.4 Native telomere FISH

To detect single stranded C-rich and G-rich telomeric repeats telomere FISH was carried out under non-denaturing conditions with a 3'-labelled (5'-TTAGGG-3')$_8$– FITC and (5'-CCCTAA-3')$_8$– biotin single stranded DNA probes (Sigma Genosys), respectively. Cells grown in four-well or two-well chamber slides were rinsed with PBS, fixed for 15 min in 2% paraformaldehyde at room temperature and then permeated with methanol at -20°C for 12 min followed by acetone at -20°C for 30 sec. After air drying, a hybridisation mixture containing 0.4 µg/ml probe, 30% formamide (deionised) in 2xSSC was applied to the slides and hybridisation was carried out without denaturing at room temperature, overnight in the dark. Slides were washed gently in 2xSSC then twice in PBS for 2 min each. Only if simultaneous detection of both C-rich and G-rich single stranded telomeric repeats was required, slides were crosslinked with 4% formaldehyde for 10 min and dehydrated by with increasing ethanol concentrations, and hybridisation was repeated with the complementary probe. PML immunostaining was carried out as described in section 2.4.1 at this stage if required. The native telomere FISH hybridisation signal was amplified by incubating for 30 min to 60 min with Alexa-Fluor® 598 anti-biotin mouse antibody (1:200 dilution, red fluorescence; Molecular Probes) or Alexa-Fluor® 488 anti-FITC goat antibody (1:400, green fluorescence; Molecular Probes). Slides were stained with DAPI, mounted and imaged as described in section 2.4.1.

2.5 Telomere length and telomerase analysis

2.5.1 DNA and protein isolation

For tumour samples, approximately 100 mg of frozen tissue was homogenised at 4 ^{o}C in 200 µl of 3-[(3-cholamidopropyl)-dimethylammonio]-1-propanesulphonate (CHAPS) lysis buffer (10 mM Tris-HCl, pH 7.5, 1 mM $MgCl_2$, 1 mM EGTA, 0.5% (v/v) CHAPS, 10% (v/v) glycerol, 5 mM β-mercaptoethanol, 0.1 mM AEBSF)[268], incubated on ice for 20 min and centrifuged at 18 000xg at 4 ^{o}C for 20 min before collecting 160 µl of supernatant for the telomerase assay. Genomic DNA was extracted from the remaining supernatant and pellet by homogenising lightly in 5.5 ml of lysis solution containing 50 mM Tris-HCl pH 8, 20 mM EDTA, 2% sodium dodecylsulphate and 100 µg/ml Pronase protease (Sigma) and incubating for 16 h with occasional gentle inversion. For cultured cells, protein and DNA were isolated from separate cell pellets, as described for tumour samples, except that the homogenisation steps were replaced by gentle mixing by pipetting. Protein extracts were flash-frozen in liquid nitrogen and stored at -80^{o}C. Lysates for genomic DNA extraction from tumour and cell culture samples were cooled on ice for 5 min, 2 ml of saturated NaCl was added and the mixture was incubated at 4^{o}C for 8 to 16 h. The precipitate was removed by repeated centrifugation (2000 x g at 4°C for 15 min) and the supernatant was transferred to a clean 15 ml centrifuge tube. The DNA was precipitated by adding 2.5 volumes of 100% ethanol and storing at -20 ^{o}C for at least 12 h. When the genomic DNA was required for further analyses, the sample was centrifuged at 2000 x g, 4°C for 15 min, washed with 70% ethanol, resuspended in 50 µl of TE and stored at 4°C.

2.5.2 Telomere restriction fragment (TRF) analysis

Terminal Restriction Fragments (TRFs) were generated from genomic DNA by digesting for 12-16 h with 4 U/μg each of HinfI and RsaI restriction enzymes (Roche; other restriction enzymes used only where stated and at same concentration) and 25 ng/μg RNAse (DNAse free; Roche), then heat inactivating at 80°C for 20 min and storing at 4°C. The digested DNA was quantitated by fluorometry: 2 μl of sample per 500 μl of Hœchst 33258 (0.1 μg/ml in TNE; Polysciences Inc), was analysed in a fluorescence spectrophotometer (Perkin-Elmer) with an excitation wavelength of 365 nm and an emission wavelength of 460 nm. Standards used were calf thymus DNA in TNE at concentrations of 0, 10, 20, 50, 100 and 200 and 250 μg/ml.

The digested genomic DNA samples (1.5 μg/well) were loaded onto a 1% agarose gel in 0.5X TBE buffer and TRFs separated by pulsed-field gel electrophoresis using a CHEF-DR II apparatus (BioRad), in recirculating 0.5X TBE buffer at 14^{o}C and with a ramped pulse speed of 1-6 s at 200 V for 14 h. A high and low DNA molecular weight marker, λ DNA restricted with cIind1ts857Sam7 (Invitrogen) and SPP-1 Phage DNA restricted with Eco RI (GeneWorks), respectively, were included in each gel. The gel was then stained in 0.5 μg/ml ethidium bromide and photographed on a UV transilluminator to confirm equal loading and record marker positions. The gel was dried under a vacuum at 55 ^{o}C until it was approximately 0.5 mm thick and had just turned translucent, washed in denaturing solution (0.5 M NaOH, 1.5 M NaCl) for 45 min, then washed in neutralising solution (1 M Tris-Cl pH 8.0, 1.5 M NaCl) for 45 min. The gel was pre-hybridised in 30 ml containing 5X SSC, 5X Denhardt's solution, 0.5 mM tetrasodium pyrophosphate and 10 mM disodium hydrogen orthophosphate at 37^{o}C for 2-6 h. An oligonucleotide $(TTAGGG)_3$ probe (150 ng; Sigma) was 5' end-labelled with 50μCi of [γ^{32}P]-dATP (3000Ci/mmol; New England

Nuclear, Dupont) and 10U T4 kinase (Promega) in a volume of 10 µl at 37°C for 30 min. The probe was purified by ethanol precipitation and resuspended in 30 µl of TE. $3x10^6$ counts per minute (cpm) of probe was added directly to the prehybridising gel, and incubated at 37°C overnight in a rotating oven (Hybaid). The gel was then washed three times in 0.1X SSC for 7 min at 37°C, exposed to a phosphor screen and scanned with a STORM 860 optical scanner with ImageQuant software (Molecular Dynamics). Molecular weights of telomeric bands were determined by constructing a standard curve from the DNA markers run on the same gel.

2.5.3 Determining the telomere length distribution from the TRF analysis

The telomere length distribution was determined using Telometric[341], with TRF smears from all tumours analysed together. This was done by scale transforming the TRF gel images with Adobe Photoshop so the markers from each gel were superimposed and combining all gels in the one image. The cell lines GM847 (ALT[+]) and HeLa (telomerase[+]) were run on each individual gel to confirm consistency. To avoid background noise affecting the results, all signal below 3kb was removed (Fig 2.2) and when selecting the TRF smear to be analysed by the Telemetric software, the box was drawn entirely within the smears. All signals above approximately 100 kb, at the nadir in the ALT like TRFs (Fig 2.2), was also ignored as these were assumed to reflect secondary structure more than size[108]. Any large smudge that was obviously artefact was also removed to avoid biasing the telomere length distribution. The method of determining ALT status from the telomere length distribution is developed in the results section 3.4.1.

Figure 2.2: Regions from tumour TRF gel image used for determining telomere distribution statistics. A: Boxed areas are the regions used for analysis by the Telometric[341] computer program. **B:** Two telomere length distributions are shown for each STS and control cell lines; on the left is the distribution that was actually used for analysis and only included telomeres above 3 kb, and on the right is shown the entire distribution. The reason for only using the telomeres above 3 kb for analysis is seen in the entire distribution. In all samples there is a dramatic peak in the frequency of telomeres as the length drops below 3 kb and this is completely separate from the main peak. This could be artefactual; the background noise may be amplified by the program when it calculates the frequency from the intensity on the gel. This is because Telometric gives extra weight to shorter telomeres that bind fewer probes than longer telomeres. Regardless of the cause, the resolution of ALT telomere length median, variance and range from non-ALT was improved by only analysing the main peak. All signals above approximately 100 kb, at the nadir in the ALT-like TRF length smears, were also ignored as these were assumed to reflect secondary structure more than size[108].

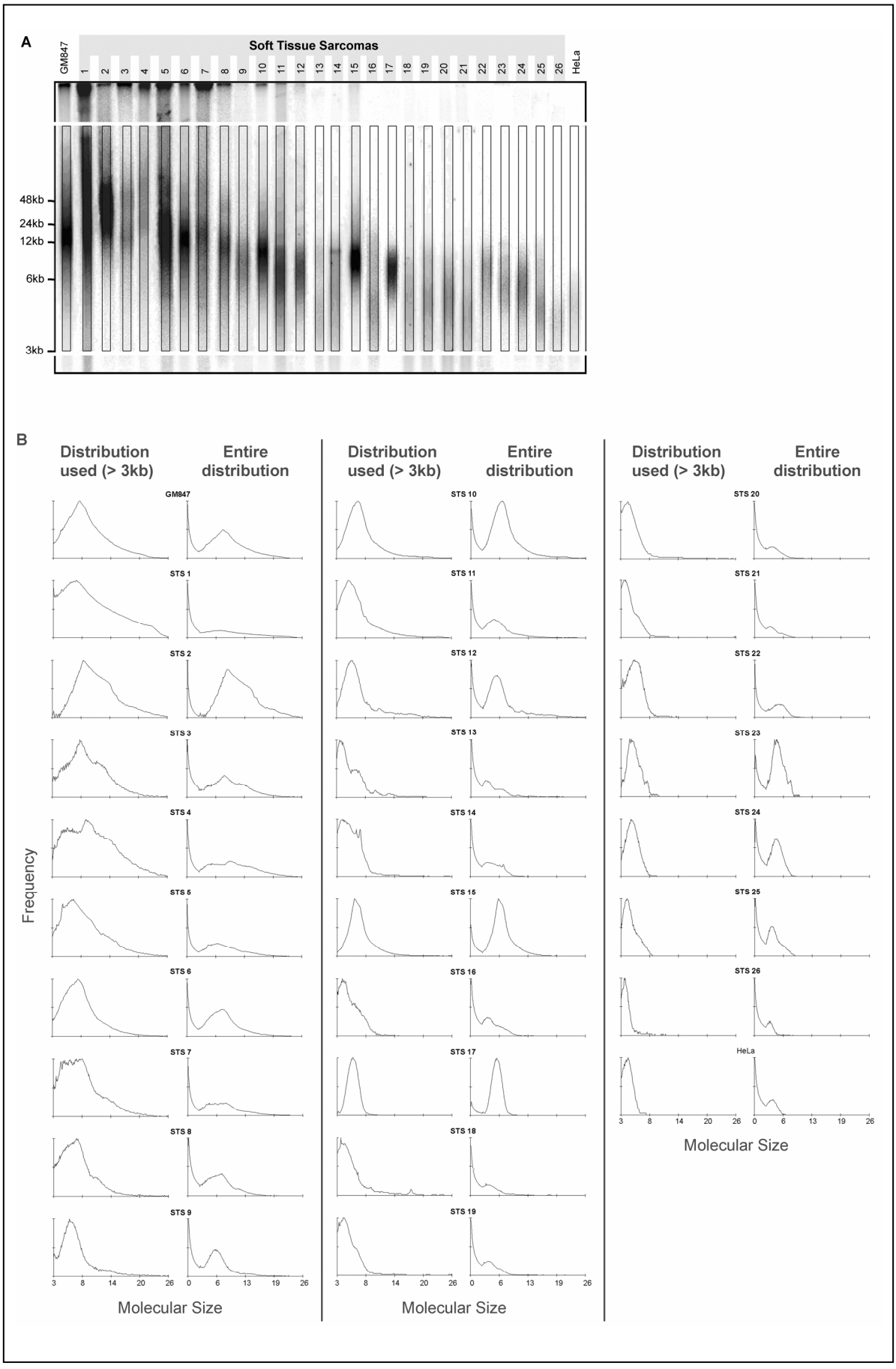
A
Soft Tissue Sarcomas
GM847
1
2
3
4
5
6
7
8
9
10
11
12
13
14
15
16
17
18
19
20
21
22
23
24
25
26
HeLa
48kb
24kb
12kb
6kb
3kb
B
Distribution used (> 3kb)
Entire distribution
Frequency
Molecular Size
GM847
STS 1
STS 2
STS 3
STS 4
STS 5
STS 6
STS 7
STS 8
STS 9
STS 10
STS 11
STS 12
STS 13
STS 14
STS 15
STS 16
STS 17
STS 18
STS 19
STS 20
STS 21
STS 22
STS 23
STS 24
STS 25
STS 26
HeLa

2.5.4 Native TRF analysis and modification of single stranded DNA

Native (non-denaturing) TRF analysis was performed as described in section 2.5.2, except that the denaturation and neutralisation of the DNA in the agarose gel was omitted. Also for all experiments investigating single stranded DNA, extracted genomic DNA was not stored at 4^{o}C for more than 48 h, and the restriction enzymes for creating TRFs were not deactivated at 80^{o}C. Mung Bean Nuclease digestion to remove single stranded DNA was performed after creation of TRFs by the restriction enzymes. Digested genomic DNA was ethanol precipitated and resuspended in Mung Bean Nuclease buffer (New England Biolabs) and incubated for 30 min at 30^{o}C with 2U Mung Bean Nuclease (New England Biolabs) per μg of genomic DNA. To create single stranded telomeric 5'-overhang, the single stranded telomeric 3'-overhang was first removed. Unrestricted genomic DNA resuspended in NEBuffer 2 (10 mM Tris-HCl, 10 mM $MgCl_2$, 50 mM NaCl, 1 mM DTT, ph 7.9; New England Biolabs) was incubated with 5U Exonuclease I (New England Biolabs) and 0.5 μg of RNAse (DNAse free; Roche) per μg of genomic DNA for 16 h at 37^{o}C. Single stranded telomeric 5'-overhang was then created by adding 1U Exonuclease III (New England Biolabs) per μg of genomic DNA for 2.5 hours at 37^{o}C. The nucleases were then heat deactivated by incubating for 20 min at 80 ^{o}C. TRFs were then created by the addition of HinfI and RsaI restriction enzymes as described in section 2.5.2 and analysed by native TRF analysis.

2.5.5 Telomere Repeat Amplification Protocol (TRAP)

Telomerase activity was assayed using the Telomere Repeat Amplification Protocol (TRAP)[268] with modifications previously described[106]. Protein concentration in extracts was measured using the with the Bradford Assay kit (Bio-Rad) and a 300 Bio UV-Vis spectrophotometer (Cary), according to the manufacturers' instructions.

Extracts were diluted to 1 µg/µl of protein with CHAPS lysis buffer and 2 µl added to a reaction mix containing 20 mM Tris-HCl (pH 8.3), 1.5 mM $MgCl_2$, 68 mM KCl, 0.05% Tween-20 and 1 mM EGTA with 50 µM dNTPs, 2 ng of telomerase substrate/primer 5'-AAT CCG TCG AGC AGA GTT-3'(Genset Pacific), 2 ng of reverse PCR primer 5'- CCC TTA CCC TTA CCC TTA CCC TAA-3' (Genset Pacific), 0.1 attograms of internal PCR control DNA and 2U of Taq Polymerase (Roche) in a 0.2 ml thin walled PCR tube, on ice. Each tube was placed in a thermal cycler (Hybaid) and allowed to incubate at 25°C for 30 min to allow extension by telomerase, followed by 94°C for 2 min, and then cycled according to the following program: 30 cycles of 94°C for 10 sec, 50°C for 25 sec, 72°C for 30 sec; and 1 cycle of 94°C for 15 sec, 50°C for 25 sec, and 72°C for 1 min. Of each TRAP reaction, 25 µl was mixed with 5 µl of TRAP loading dye (0.25% (w/v) Ficoll-400, 50 mM EDTA, 0.25% (w/v) bromophenol blue, 0.25% (w/v) methylene blue) and loaded onto a 10% acrylamide vertical gel (12.5 ml 40% acrylamide/bis 19:1, 2.5 ml 10X TBE, 35 ml H_2O, 45 µl TEMED, 130 µl 20% (w/v) ammonium persulphate with dimensions 13.5 cm x 13.5 cm x 1.5 mm; Hoefer Scientific Instruments). The gel was electrophoresed at 180 V for 3 - 4 h. Gels were stained for 20 min in 200 ml of a 1:10 000 dilution of SybR® Green I followed by rinsing in distilled/deionised H_2O for 10 min. Bands were visualised on a STORM 860 imager in the blue fluorescence range and analysed utilising ImageQuant software (Molecular Dynamics).

Since telomerase is a ribonucleoprotein, precautions against contamination with RNases were always taken, as well as conventional precautions against contamination with PCR products. Filtered pipette tips and dedicated pipettors were used; equipment was UV irradiated; reactions were set up in a hood; disposable plasticware was used; and the products of the PCR reaction were handled in a room separate from that in which the reactions were set up. All water used in the assay was treated with

DEPC to destroy RNases. Primers used for the TRAP assay were HPLC purified by Genset Pacific.

Positive lysates were confirmed by either heat inactivation of telomerase at 85 ^{o}C for 10 min or incubation with 50 ng of RNase (DNase free; Roche) per µl of lysate for 20 min at 37 ^{o}C. Negative lysates were assayed at dilutions between 10 and 1000 fold dilutions to overcome the possibility of TRAP inhibitors, and checked by spiking the lysate with 1 µl HeLa lysate (1 µg/µl protein concentration) to determine whether this reduced the activity of the HeLa sample. The internal PCR control used in all reactions was laboratory stock, consisting of 150 bp of rat myogenin DNA flanked by the TRAP primer sequences, that had been produced by PCR amplification using primers that had the TRAP primer sequences joined to myogenin sequences.

2.6 RNA microarray

2.6.1 RNA extraction

RNA was isolated from 50-70% confluent cell monolayers that had been grown for at least 2 weeks and eight population doublings since thawing, using RNeasy® Mini Kit (Qiagen) according to the manufacturer's instructions. The lysis buffer was added directly to 75cm^2 flasks immediately after rinsing the flasks with 15 ml of PBS (pre-warmed to 37 ^{o}C). RNA was resuspended in 50 µl of RNase-free H_2O and stored at -80^{o}C. RNA was quantitated in H_2O on a 300 Bio UV-Vis spectrophotometer (Cary) and the RNA solution was adjusted to pH 7.5 by adding Tris buffer (10 mM final concentration) before measuring the A_{260}/A_{280} ratio. RNA purity was also confirmed by agarose gel electrophoresis. RNA electrophoresis was performed using dedicated apparatus and reagents and (Milli-Q) ultra-filtered water was treated with DEPC. 3.3 µg RNA was brought to a volume of 20 µl with RNA loading solution (final

concentration: 1.67% v/v formaldehyde and 3.33% v/v deionised formamide in 1x MOPS buffer). The RNA was incubated at 65 ^{o}C for 10 min and in ice for 3 min, and loaded onto the gel with 2 µl of 10x RNA loading dye. Gel tanks were wiped down with 0.1 M NaOH prior to set up. RNA was separated using an agarose minigel (1% w/v agarose and 16.7% formaldehyde v/v in 1x MOPS buffer) and run in 1x MOPS buffer. The gel was electrophoresed at 160 V for 1.5 h, stained for 20 min in a 1:20 000 dilution of ethidium bromide followed by rinsing in DEPC treated H_2O for 30 min. Bands were photographed on a FluorChem™ 5500 transilluminator (Alpha Innotech Corporation).

2.6.2 RNA microarray

Gene transcription levels were determined by Human Genetic Signatures (Macquarie Park NSW, Australia) using an Expression Array System (Applied Biosystems). 40 µg total genomic RNA was reversed transcribed to cDNA, and each sample was added without amplification to a separate Human Genome Survey Microarray (Applied Biosystems) and analysed on a 1700 Chemiluminescent Microarray Analyser (Applied Biosystems) according to the manufacturer's instructions. Genome wide median expression and internal controls were used to normalise each gene for comparison with other microarrays according to the manufacturer's instructions. Initial data analyses were carried out using GeneSpring 7.2 software (Agilent). This included identification of differentially expressed genes by the Mann-Whitney test and hierarchical clustering using Spearman correlation for the similarity measure.

2.7 Western blotting

2.7.1 Protein extraction

Cell pellets harvested from 75cm^2 flasks were resuspended in 100 µl of ice cold lysis buffer (100 mM NaF (Fluka), 0.5% NP-40, 120 mM NaCl, 50 mM Tris-HCl (pH 8.0), 200 µM Na_3VO4 (Fluka) with one Complete protease inhibitor tablet (Roche) and 100 µg leupeptin (Roche) added to 10 ml of lysis buffer immediately before use). Lysates were mixed by aspirating six times with a 21 gauge needle and incubated at 4 ^oC for 20 min, flash frozen in liquid nitrogen, and stored at -80 ^oC. Protein concentration was determined with the Bradford Assay kit (Bio-Rad) and a 300 Bio UV-Vis spectrophotometer (Cary), according to the manufacturers' instructions.

2.7.2 SDS-polyacrylamide gel electrophoresis (SDS-PAGE)

125-250 µl of protein extract (in < 24 µl) was brought to 32 µl with H_2O and mixed with 16 µl of 3xSDS loading buffer (6% SDS, 0.10% Bromophenol Blue, 200 mM Tris (pH 6.8), 6mM 0.5M EGTA and 28% glycerol with 137µl/ml β-mercaptoethanol added immediately before use). The sample was boiled for 5 min and cooled on ice before loading, together with10 - 20 µl of protein marker (All Blue, Precision Plus Protein™ Standards; Bio-Rad). 20 - 48 µl protein samples were electrophoresed in running buffer (24 mM Tris, 192 mM glycine and 0.1% SDS) at 15.6 Vcm^{-1} through 7.5% - 15% acrylamide gels (acrylamide:bis = 29:1, 0.1% SDS, 375 mM Tris (pH 8.8)) in an Xcell™ Mini-Cell (Novex) or a Protean® II xi Cell (Bio-Rad) gel electrophoresis chamber.

2.7.3 Western blotting

A Novex Transfer Module was used according to the manufacturer's instructions, for western blotting onto an Immobilon-P membrane (Millipore). Before use, the

Immobilon-P membrane was soaked in 100% methanol for 15 sec, rinsed in H_2O for 2 min, then soaked in transfer buffer (24 mM Tris and 192 mM glycine with 20% v/v methanol added immediately before use). The acrylamide gel was removed from its casing and soaked in transfer buffer for 10 min before transfer at 30 V for 2 h at 4^{o}C.

2.7.4 Protein detection

After transfer, the membrane was soaked in methanol for 10 sec then stained with Ponceau-S for 5 min to confirm equal loading and record markers and lane positions. All immunodetection solutions and washes used PBS with 0.1% Tween-20, which also contained 0.5% PVP-40 (Sigma) when used for dilution of antibodies. The membrane was blocked with 3% BSA, incubated with primary antibodies for 1-2 h at RT or 12-16 h at 4 ^{o}C and then incubated with HRP-conjugated secondary antibodies for 30 min at RT. Secondary antibodies were detected with Super-Signal chemiluminescent reagent (Pierce) according to the manufacturer's instructions and recorded with Biomax™ MR film (Kodak). If necessary, membranes were stripped by soaking in 0.2 M NaOH for 30 min.

Primary antibodies used for detection of protein were anti-DRG2 chicken antibody (1:2000 dilution; GenWay), anti-MGMT mouse antibody (1:200 dilution; NeoMarkers), anti-SATB1 mouse antibody (1: 250 dilution; BD Transduction Laboratories), anti-Fen1 mouse antibody (1:250 dilution; BD Transduction Laboratories) and anti-actin mouse antibody (1:250 dilution; Sigma). The secondary antibodies used were Horseradish Peroxidase (HRP) conjugated goat anti-chicken (GenWay), goat anti-mouse (DakoCytomation) and swine anti-rabbit antibodies (DakoCytomation).

To compare protein levels between gels, levels of actin were determined and the same protein lysate from one cell line, A2182, was included on both gels. For each cell line, the intensity of the protein bands was corrected for loading by dividing by the intensity of the corresponding actin band. Corrected values on both gels were compared by multiplying the corrected values from the second blot by (corrected level for A2182 lysate on gel 1/ corrected level for A2182 lysate on gel 2).

2.8 Data analysis

All analyses (APB detection, TRF analysis and TRAP assay) were blinded with respect to previous results, patient data and clinical outcome. The log-rank test was used to compare Kaplan-Meier estimates of overall survival time in different groups. Fisher's exact test was used to compare proportions including associations between ALT status and other factors. Binomial distribution was used to determine the probability that proportions were within a specified range. Mann-Whitney test was used to compare non-normal distributions between groups with different telomere maintenance mechanism status (pair-wise). Spearman's correlation was used to test for gene co-regulation and correlations between measures of gene expression. The Bonferroni method was used to adjust p-values of differentially expressed genes to take into account false positives, and the Benjamini and Hochberg method was used to estimate the false positive rate. Centroid linkage with Spearman correlation as the similarity measure was used for hierarchical clustering. Statistical analysis was performed with SPSS 11.0, GeneSpring 7.2 (Agilent) and Microsoft™ Office Excel (Microsoft Corporation).

Chapter Three:

Development of the APB Assay for ALT in Tumours

Development of the APB Assay for ALT in Tumours

3.1 Introduction

The research discussed in this chapter provides a reliable and validated alternative to the Southern analysis (Telomere Restriction Fragment (TRF) analysis) test for ALT in tumour specimens. In particular this assay allows testing for ALT in tumours archived only as paraffin embedded blocks which do not provide the unfragmented genomic DNA required for the Southern analysis technique[342]. This assay uses one of the known hallmarks of ALT: ALT-associated PML bodies (APBs). APBs, as reviewed in Section 1.4.8, are PML bodies that contain telomere-related materials, including DNA with the telomeric $(5'\text{-TTAGGG-}3')_n$ sequence and the telomere specific binding proteins, TRF1 and TRF2. Here, a practical and reliable technique was developed for testing tumour sections for the presence of ALT-associated PML bodies (APBs) and it was verified that APBs correlate with ALT activity in human tumours. The difficulties intratumoral heterogeneity poses for this assay were also investigated.

3.2 Correlation between APBs and ALT in cell lines

3.2.1 Survey of APBs in cell lines

APBs had already been shown to correspond to presence of ALT activity in cell lines[83,97](Table 3.1A). To strengthen this correlation, fourteen more ALT cell lines, 23 more telomerase cell lines and five more mortal cell strains were tested for APBs by PML and TRF2 immunostaining (Figs 3.1 and 3.2). Table 3.1B summarises these results. Combined with the pre-existing data, 29/31 ALT[+] cell lines, 3/31 telomerase[+] cell lines and 0/10 mortal cell strains contain APBs. As discussed in Section 6.1, both of the APB[-]/ALT[+] cell lines are the result of *in vitro* transformations; this situation may be unlikely to occur in tumours often enough to

affect the sensitivity of the APB assay. Both these cell lines would also be scored as ALT[-] by the current assay for ALT in tumours (TRF analysis; they are classified as ALT[+] because they have a telomerase[-] TMM). Furthermore, one of these cell lines, AG11395, does have a variant form of APBs even though it is classified as APB[-]. AG11395 has bright telomeric foci that colocalise with the recombination proteins that are usually found in APBs, but these aggregates are adjacent to PML bodies rather than inside them[95]. Thus if the same phenomenon was present in tumours, these foci probably would be obvious with the APB assay.

The three telomerase positive cell lines that contained APBs (Fig 3.2) only had a low frequency of APB[+] cells (<0.5%). It remains to be determined if this is a result of ALT being occasionally activated in all cells or the existence of a stable ALT[+] subpopulation. It is possible that APBs may occasionally form in the absence of full ALT-like recombination events and this may need to be taken into account in using APBs as an assay for ALT. APBs were not associated with telomerase[+] cell lines with long telomeres (T7 and T8 in Table 3.1A) indicating that APBs are associated with ALT rather than with long telomeres.

The various morphologies of APBs found in the ALT[+] cell lines are shown in Fig 3.1. In some cells APBs can be seen to be touching other APBs and possibly telomeric foci not in PML bodies. These non-random distributions of telomeric foci can assist in analysing tumour specimens for APBs by increasing the likelihood that foci seen are not artefactual. However, this was not incorporated into the criteria for scoring APBs (Section 2.4.2).

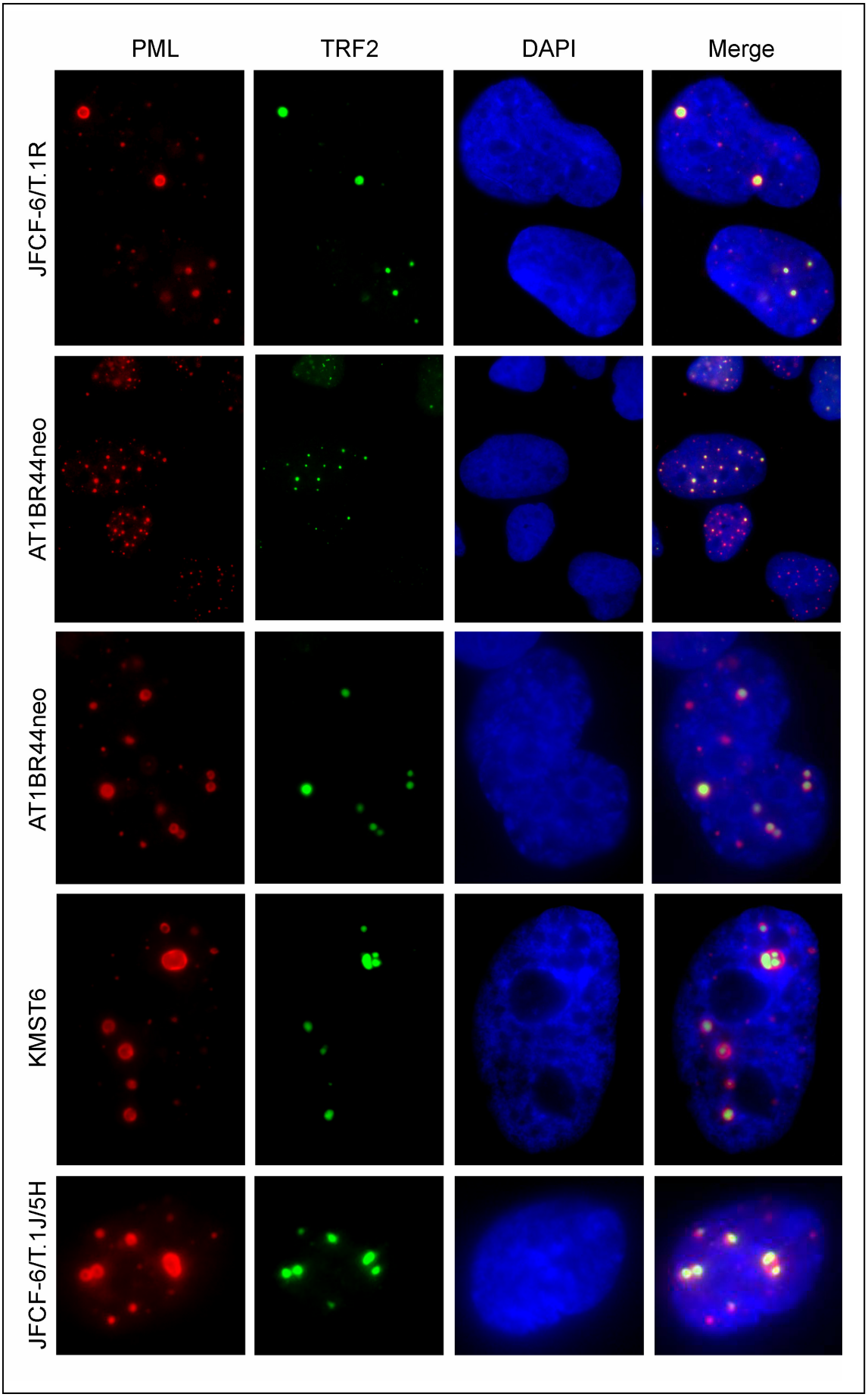
PML
TRF2
DAPI
Merge
JFCF-6/T.1R
AT1BR44neo
AT1BR44neo
KMST6
JFCF-6/T.1J/5H

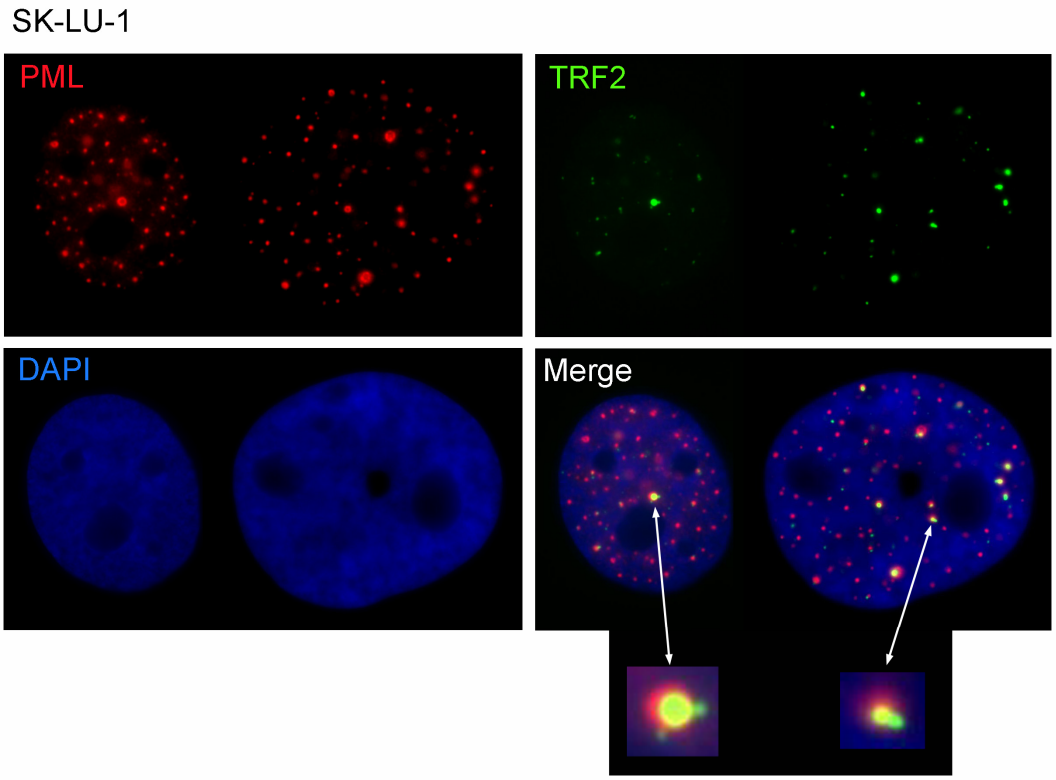

Figure 3.1: APBs in ALT[+] cell lines. Immunostaining for PML and TRF2 in cell culture monolayers analysed with a 100x objective. Indirect immunofluorescence with Texas Red and FITC (green) was used for PML and TRF2 respectively. Nuclei were counterstained with 4′,6-diamidino-2-phenylindole (*DAPI*). Foci of TRF2 that colocalise with PML (*Merge*) represent APBs. Telomeres are not bright enough relative to the telomeric DNA in APBs to be visible with the exposure time used. Like other PML bodies, APBs have the appearance of disc or ring shaped structures in two dimensions, with PML protein either detected in the outer rim (e.g. JFCF-6/T.1R, larger nucleus) or PML staining throughout the foci (e.g. JFCF-6/T.1R, smaller nucleus). APBs can be seen in the ALT[+] cell lines JFCF-6/T.1R, AT1BR44neo, KMST-6, JFCF-6/T.1J/5H and SK-LU-1. Associations between telomeric foci can sometimes be seen in ALT[+] cells: multiple foci of telomeric chromatin in one APB (KMST-6), APBs appearing to divide or fuse (AT1BR44neo and JFCF-6/T.1J/5H) or PML-negative telomeric foci adjacent to APBs (SK-LU-1, enlarged in insets).

Figure 3.2: APBs in ALT[-] cell lines. Immunostaining for PML and TRF2 in cell culture monolayers analysed with a 100x objective. Indirect immunofluorescence with Texas Red and FITC (green) was used for PML and TRF2, respectively. Nuclei were counterstained with *DAPI*. APBs could not be detected in the mortal cell strain JFCF-6 or telomerase[+] cell lines SHB-PE6 or MeT-5A/6TGR-B. A very low frequency of APB[+] nuclei (<0.5%) can be seen in the telomerase[+] cell lines MeT-5A and SKOV-3.

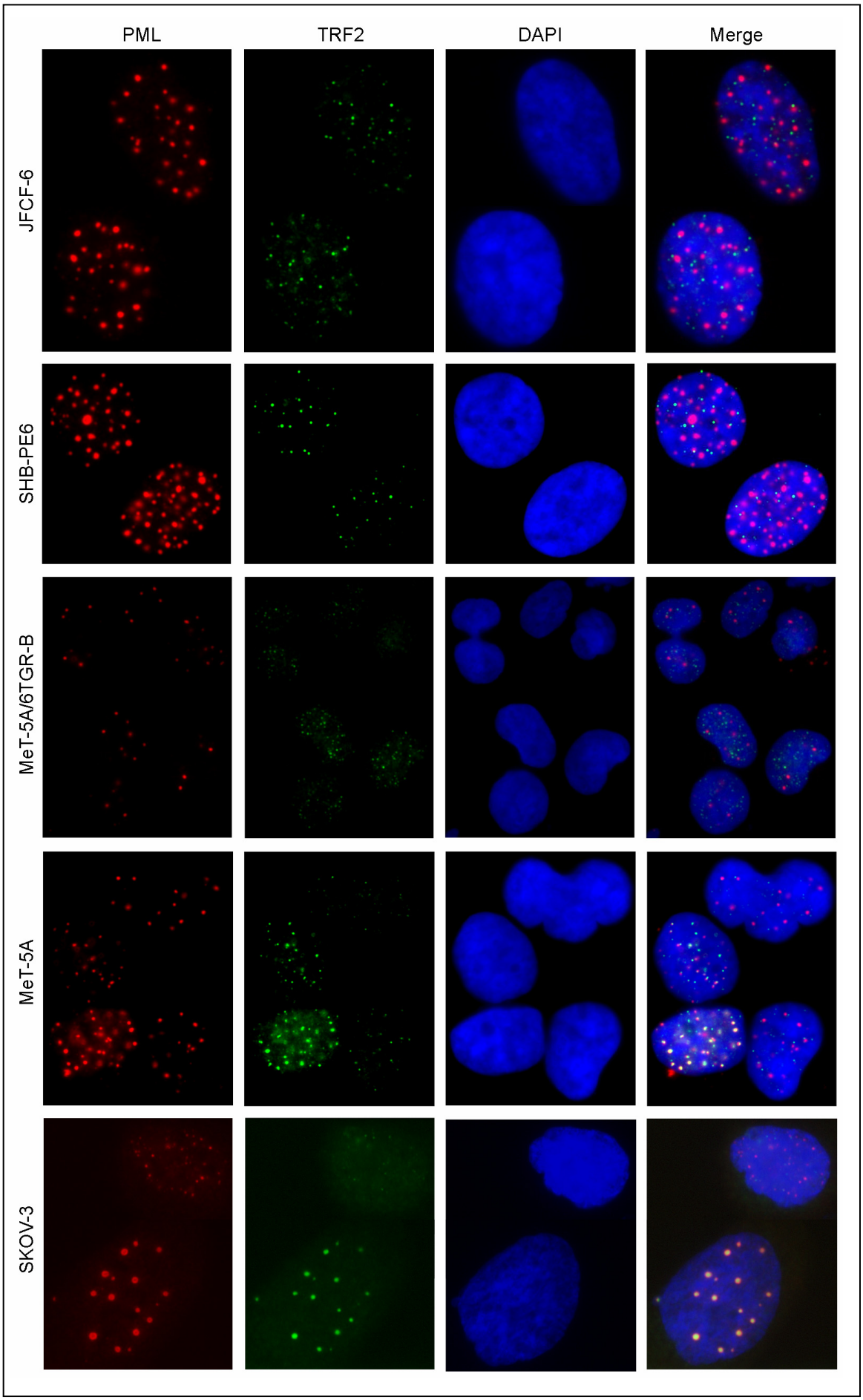
PML
TRF2
DAPI
Merge
JFCF-6
SHB-PE6
MeT-5A/6TGR-B
MeT-5A
SKOV-3

Table 3.1A: Relationship between APBs and TMM, previous data

	Cell Line/Strain	Cell Type (immortalizing agent)	TMM (reference)	APB (reference)
A1	GM847	Fibroblast (SV40)	ALT[69]	+[83]
A2	WI38-VA13/2RA	Fibroblast (SV40)	ALT[69]	+[83]
A3	IIICF-T/B1	Fibroblast (SV40)	ALT[69]	+[83]
A4	JFCF-6/T.1R	Fibroblast (SV40)	ALT[83]	+[83]
A5	SUSM-1	Fibroblast (chemical carcinogen)	ALT[69]	+[83]
A6	KMST-6	Fibroblast (γ-irradiation)	ALT[87]	+[83]
A7	IIICF/a2	Fibroblast (spontaneous)	ALT[83]	+[83]
A8	IIICF/b4	Fibroblast (spontaneous)	ALT[83]	+[83]
A9	IIICF/b5	Fibroblast (spontaneous)	ALT[83]	+[83]
A10	IIICF/c	Fibroblast (spontaneous)	ALT[69]	+[83]
A11	BET-3M	Epithelial (SV40)	ALT[69]	+[83]
A12	SAOS-2	Osteosarcoma	ALT[73]	+[83]
A13	HIO107	Ovarian epithelial (SV40)	ALT[97]	+[97]
A14	HIO117	Ovarian epithelial (SV40)	ALT[97]	+[97]
A15	HIO118	Ovarian epithelial (SV40)	ALT[97]	+[97]
A16	AG11395	Fibroblast (SV40)	ALT[95]	-[a, 95]
A17	C3-c16[b]	Fibroblast (SV40)	ALT[110]	-[110]
T1	BFT-3B	Fibroblast (SV40)	Tel[69]	-[83]
T2	JFCF-6/T.1C	Fibroblast (SV40)	Tel[83]	-[83]
T3	BET-3b	Epithelial (SV40)	Tel[69]	-[83]
T4	293	Epithelial (adenovirus)	Tel[69]	-[83]
T5	HeLa	Cervical carcinoma	Tel[232]	-[83]
T6	MCF-7	Breast adenocarcinoma	Tel[73]	-[83]
T7	JFCF-6/T.2H/2FL-6	Fibroblast (SV40)	Tel (L Colgin unpublished)	- (L Colgin unpublished)
T8	HT1080/hPOT1 (variant 1 clones)	Fibroblast (SV40)	Tel[36]	- (L Colgin unpublished)
M1	Bre-80	Breast epithelial strain	-[83]	-[83]
M2	MRC-5	Fibroblast strain	-[83]	-[83]
M3	HFF5	Fibroblast strain	-[69]	-[83]
M4	JFCF-6/T.1R	Fibroblast, preimmortal (SV40)	-[83]	-[83]
M5	IIICF/c	Fibroblast, preimmortal	-[83]	-[83]

[a]AG11395 is classified as APB[-] but could be considered to have a variant of APBs; telomeric foci and the recombination proteins normally found in APBs colocalise in AG11395, but these foci are adjacent to PML nuclear bodies and not inside them[95].
[b]Clone from a transformation of WI38-VA13/2RA with catalytically inactive telomerase.

Table 3.1B: Relationship between APBs and TMM, results of this study

	Cell Line/Strain	Cell Type (immortalizing agent)	TMM[a] (reference)	APB
A18	AT1BR44neo	Fibroblast (SV40)	ALT[89]	+
A19	MeT-4A	Mesothelial (SV40)	ALT[69]	+
A20	G-292	Osteosarcoma	ALT[73]	+
A21	MRC5-V2	Fibroblast (SV40)	ALT (L Huschtscha)	+
A22	GM0637 (NSV)	Fibroblast (SV40)	ALT[80]	+
A23	U-2 OS	Osteosarcoma	ALT[73]	+
A24	SK-LU-1	Adenocarcinoma	ALT[73]	+
A25	JFCF-6/T.1J/1-3C	Fibroblast (SV40)	ALT (A Englezou)	+
A26	JFCF-6/T.1J/1-4D	Fibroblast (SV40)		+
A27	JFCF-6/T.1J/11E	Fibroblast (SV40)		+
A28	JFCF-6/T.1J/1D	Fibroblast (SV40)		+
A29	JFCF-6/T.1J/5H	Fibroblast (SV40)		+
A30	W-V	Fibroblast (SV40)	ALT[95]	+
A31	DOS16	Leiomyosarcoma	ALT (this study)	+
T9	BFT-3K	Fibroblast (SV40)	Tel[69]	-
T10	AT22IJE-T	Fibroblast (SV40)	Tel[89]	-
T11	MeT-5A/6TGR-B	Mesothelial (SV40)	Tel (N Whitaker)	-
T12	SJSA-1	Osteosarcoma	Tel[73]	-
T13	BET-3K	Epithelial (SV40)	Tel[69]	-
T14	MRC5-V1	Fibroblast (SV40)	Tel (L Huschtscha)	-
T15	F80-hTERT/K1	Fibroblast (SV40/hTERT)	Tel (C Toouli)	-
T16	HT1080	Fibroblast (SV40)	Tel[232]	-
T17	A549	Adenocarcinoma	Tel[232]	-
T18	JFCF-6/T.1J/6G	Fibroblast (SV40)	Tel (A Englezou)	-
T19	JFCF-6/T.1J/6B	Fibroblast (SV40)		-
T20	JFCF-6/T.1J/11C	Fibroblast (SV40)		-
T21	JFCF-6/T.1J/9E	Fibroblast (SV40)		-
T22	JFCF-6/T.1J/4D	Fibroblast (SV40)		-
T23	JFCF-6/T.1P	Fibroblast (SV40)		-
T24	GM639	Fibroblast (SV40)	Tel[69]	-
T25	TE-85	Osteosarcoma	Tel[232]	-
T26	MG-63	Osteosarcoma	Tel[73]	-
T27	A2182	Adenocarcinoma	Tel[73]	-
T28	SHB-PE6	Breast epithelial (E6)	Tel (A Englezou)	-
T29	MeT-5A	Mesothelial (SV40)	Tel[69]	+[b]
T30	SKOV-3	Adenocarcinoma, ovary	Tel[268]	+[b,c]
T31	JFCF-6/hTERT/1	Fibroblast (hTERT)	Tel (Z Zhong)	+[b]
M6	WI-38	Fibroblast strain	-[268]	-
M7	JFCF6	Fibroblast strain	- (A Englezou)	-
M8	IIICF	Fibroblast strain	-[68]	-
M9	BF10	Fibroblast strain	- (R Reddel)	-
M10	DOS15	GIST	- (this study)	-

[a] *Tel*, denotes telomerase and -, denotes no TMM.
[b] Low percentage of APB positive nuclei (< 0.5%).
[c] SKOV3 also APB[+] with telomere FISH/PML immunostaining.

3.2.2 Evidence that APBs are associated with ALT activity

Clones of the ALT[+] IIICF/c cell line (Table 3.1A) have been derived[2] that have their APBs disrupted by overexpression of exogenous Sp100 (Fig 3.3A). This is possibly due to sequestration of the Mre11-RAD50-NBS1 complex away from PML bodies into aggregates formed by the exogenous SP100 protein[2]. At physiological levels SP100 is a constituent of PML bodies and other nuclear foci[130] and is known to bind NBS1[343].

To determine whether Sp100-induced suppression of APB formation was accompanied by inactivation of the ALT mechanism, terminal restriction fragment (TRF) analysis was performed on two clones expressing high levels of YFP-SP100 (Fig 3.3B, right two panels). The telomere lengths in these clones over a period of 70 to 90 population doublings (PDs) from the earliest time point possible (PD 28 or 29[2]) were compared to IIICF/c mass culture and clones with vector only, YFP, and low-level YFP-SP100 expression. Densitometric analysis of an invariant band (Fig 3.3B), which corresponds to interstitial $(TTAGGG)_n$ DNA sequences, confirmed equal sample loading. In each of the APB[+] clones (IIICF/c-vector, -YFP, -SP100low), faint higher-molecular-weight telomeric bands were visible at early PDs, which gradually reduced in size and then disappeared into the terminal restriction fragment smear pattern (Fig 3.3B). This effect in clonally derived populations of IIICF/c cells presumably results from the brief persistence of terminal restriction fragment bands corresponding to individual telomeres undergoing steady attrition as in other telomerase[-] cells, together with the stochastic lengthening and shortening events in cells within the ALT[+] population[81], that maintain the average telomere length.

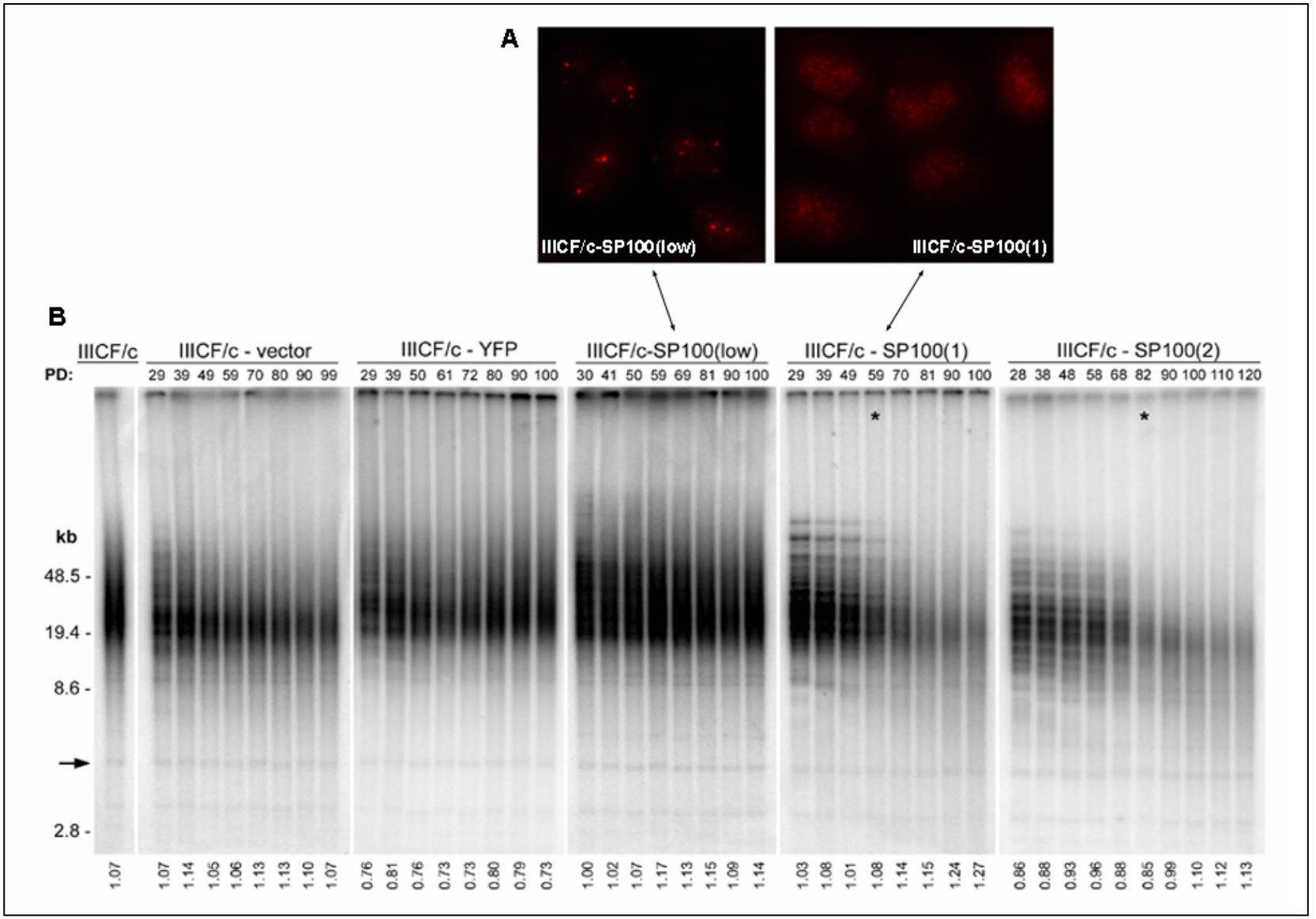
A
IIICF/c-SP100(low)
IIICF/c-SP100(1)
B
IIICF/c
IIICF/c - vector
IIICF/c - YFP
IIICF/c-SP100(low)
IIICF/c - SP100(1)
IIICF/c - SP100(2)
PD:
29 39 49 59 70 80 90 99
29 39 50 61 72 80 90 100
30 41 50 59 69 81 90 100
29 39 49 59 70 81 90 100
28 38 48 58 68 82 90 100 110 120
kb
48.5
19.4
8.6
2.8
1.07
1.07 1.14 1.05 1.06 1.13 1.13 1.10 1.07
0.76 0.81 0.76 0.73 0.73 0.80 0.79 0.73
1.00 1.02 1.07 1.17 1.13 1.15 1.09 1.14
1.03 1.08 1.01 1.08 1.14 1.15 1.24 1.27
0.86 0.88 0.93 0.96 0.88 0.85 0.99 1.10 1.12 1.13

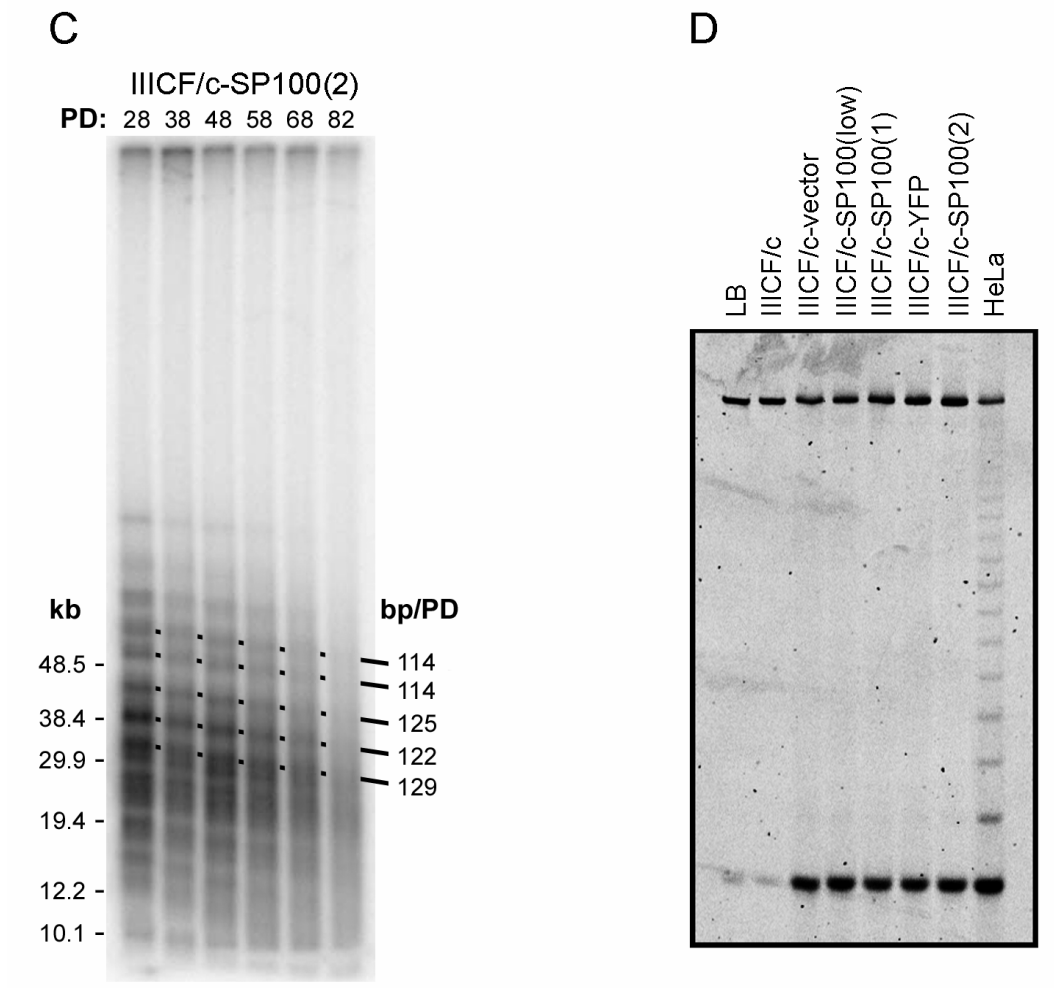

Figure 3.3: Suppression of APBs coincides with suppression of ALT activity. High levels of exogenous YFP-SP100 expression in the ALT cell line IIICF/c suppressed APBs[102]. This is shown here in ***A*:** Telomere FISH using a Cy3 conjugated telomeric peptide nucleic acid probe shows APBs still present in the clone expressing low amounts of YFP-SP100, *IIICF/c-SP100(low)*, but no APBs in a clone with high YFP-SP100 expression, *IIICF/c-SP100(1)*. The bright telomeric foci in *IIICF/c-SP100(low)* represent APBs which are significantly brighter than the telomeres that can barely be seen at this exposure. The exposure is longer for the *IIICF/c-SP100(1)* clone so the telomeres can be seen, however the bright telomeric foci denoting APBs are absent. This is described in detail by Jiang et al.[102]. ***B*:** Progressive telomere shortening in clones over-expressing YFP-SP100. Terminal length distributions determined by TRF analysis of genomic DNA from parental *IIICF/c* cells and *IIICF/c-vector,-YFP,-SP100(low),-SP100(1)* and *-SP100(2)* cells at the population doubling (*PD*) indicated. The asterisk indicates the PD levels at which small patches of revertant cells appeared within the cultures[102]. Densitometric analysis of an invariant band *(arrow)*, which corresponds to interstitial telomeric repeats, was performed to confirm equal sample loading and the intensity of this band for each sample is shown below its lane. Variation was <30% overall and <15% within each cell line. ***C*:** The rate of telomere shortening in an ALT suppressed clone. The rate was determined for *IIICF/c-SP100(2)* by measuring the lengths of the five indicated TRF bands from *PD* 28 to 68. The average shortening rate was 121 bp/PD. ***D*:** All clones (and lysis buffer *LB*) remained negative for telomerase activity as assessed by TRAP assay. The internal control was positive for all samples (upper bands) and the telomerase[+] (control) cell line, *HeLa*, gave a six base pair ladder indicating products from telomerase activity. The IIICF/c clones named *IIICF/c-vector,-YFP,-SP100(low),-SP100(1)* and *-SP100(2)* correspond to clones IIICF-4,-11,-9,-10 and -17 in Jiang et al.[102]

In contrast, clones IIICF-SP100(1) and -SP100(2), in which APBs were suppressed, had much more distinct higher molecular weight bands at early PDs that underwent progressive shortening with further cellular proliferation and remained visible until PDs 60 and 80, respectively. The rate of shortening of individual bands was calculated for IIICF-SP100(2) by reference to the molecular weight markers and was found to be very similar for each of the bands (Fig 3.3C). The mean rate of shortening was 121 base pairs per PD, which is within the range reported for normal human cells without an active TMM[157] and for somatic cell hybrids in which ALT has been repressed[106]. Telomerase remained inactive in all clones (Fig 3.3D).

The persistence for so many PDs of distinct, albeit shortening, terminal restriction fragment bands corresponding to individual telomeres in the clonally derived IIICF-SP100(1) and -SP100(2) cultures indicates that the stochastic telomere lengthening and shortening events characteristic of ALT were substantially reduced or abolished in these cells. The onset of blurring of the terminal restriction fragment bands (at PD 60 and 80 in IIICF-SP100(1) and IIICF-SP100(2), respectively; Fig 3.3B), coincided with a gradual decrease in YFP-SP100 protein levels and the gradual reappearance of APBs[2]. There was thus a close association between the presence of APBs and an active ALT mechanism.

3.3 Optimum technique for detecting APBs in tumours

APBs are the only PML bodies in which telomeric chromatin has been visualised. APBs are nuclear colocalisations of PML protein with telomeric chromatin, detected by probing for telomeric DNA or the telomeric binding proteins TRF1 or TRF2[83]. However, it has not been determined if the telomeric DNA needs to be of a minimum size or completely inside the PML body for APBs to remain ALT specific. Confocal microscopy has shown rare small colocalisations of telomeric and PML foci in

telomerase positive cell lines (Muntoni, A. personal communication) and telomeric foci were seen frequently to colocalise with the rim of the PML bodies in the melanoma cell line, LOX-IMVI, for which no APBs have yet been demonstrated (by the criteria described in methods; Fig 3.4). For scoring tumour sections for APBs stringent criteria were used to avoid false positive results. As described in Section 2.4.2, we required the telomeric foci to be an order of magnitude brighter in the APBs than the surrounding telomeres and that the telomeric foci are completely inside the PML foci.

For detecting APBs in cell lines it is more convenient technically to show telomeric chromatin inside PML bodies using PML immunostaining combined with TRF2 or TRF1 immunostaining rather than PML immunostaining combined with telomere FISH. However, telomere FISH is more direct as TRF2 has been found to bind non-telomeric DNA[154] and it could also be possible for TRF1 foci not to be bound to telomeres.

We compared telomere FISH/PML immunostaining to TRF2/PML immunostaining in 61 different paraffin embedded tumour specimens: 38 glioblastomas multiforme (GBM), 19 soft tissue sarcomas (STS), two osteosarcomas, one adrenal adenocarcinoma and one ureteric carcinoma. In 60 of the 61 tumour specimens both methods gave identical results, with 24 of these 60 tumour specimens being APB[+]. However one STS was APB[+] by telomere FISH/PML immunostaining (Fig 3.5) and APB[-] by TRF2/PML immunostaining (also APB[-] by TRF1/PML immunostaining). This paraffin embedded specimen had been stored at room temperature for nine years and for this and all other stored specimens, anti-TFR2 foci

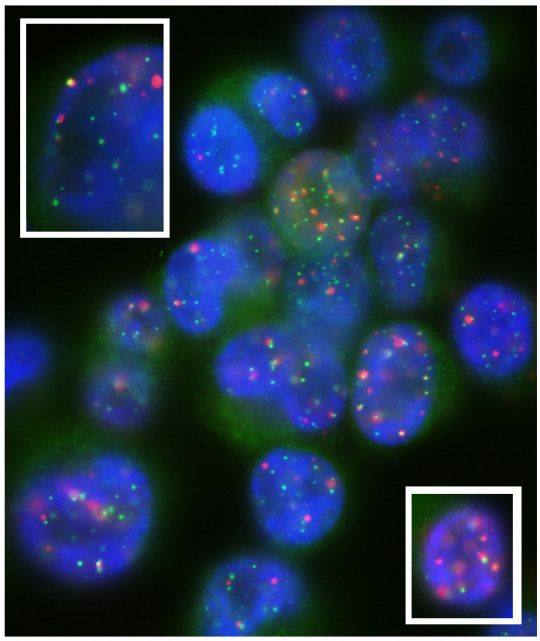

Figure 3.4: Example of telomere/PML associations not fulfilling criteria for APBs. Immunostaining for PML and TRF2 in the tumour cell line, LOX-IMVI. Indirect immunofluorescence, Texas Red (red) and FITC (green) labels, was used for the PML and TRF2 respectively. Nuclei were counterstained with 4′,6-diamidino-2-phenylindole (DAPI; blue). Insets show nuclei seen in other fields of view. Telomeric foci appear adjacent to PML nuclear bodies, but these telomeric foci are not an order of magnitude brighter than the telomeres and (due to their small size) cannot be judged to be completely inside the PML nuclear bodies. Thus, by the criteria used (Section 2.4.2), this specimen is negative for APBs.

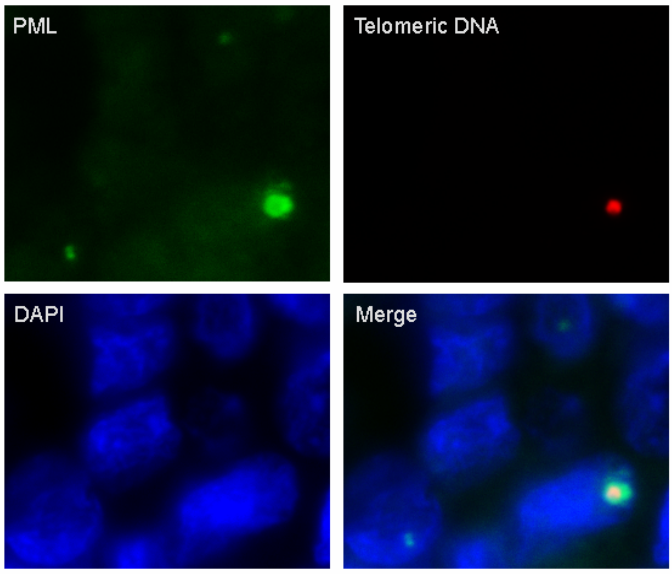

Figure 3.5: STS that was APB[+] by telomere FISH but APB[-] by TRF2 immunofluorescence. Combined PML immunofluorescence and telomere FISH in a STS paraffin section analysed with a 100x objective. Indirect immunofluorescence (FITC label) was used for the PML protein and telomere FISH was done with a Cy3 conjugated telomeric peptide nucleic acid probe. Nuclei were counterstained with DAPI. A bright focus of telomeric DNA can be seen inside a ring of PML representing one of the APBs seen in this section. Repeated immunofluorescence detection of TRF2 or TRF1 with immunofluorescence for PML failed to find APBs in this tumour specimen.

were less intense and less frequent than telomere FISH foci. In contrast, TRF2 immunostaining was not found to be less intense than telomere FISH in monolayers of cell lines. The poor staining of TRF2 in paraffin embedded tumour sections may have been due to inefficiency of antigen retrieval or degradation of TRF2, especially in older paraffin embedded specimens (up to 17 years old). For these reasons telomere-FISH with PML immunofluorescence was used for testing the APB status of tumour specimens.

For detecting APBs, paraffin sections eight microns thick were found to give the best compromise between minimising autofluorescence (Fig 3.6) and being able to find intact APBs. The antigen retrieval step during immunostaining provided equivalent access for the PNA probe to the telomeric DNA as the standard pepsin digestion (data not shown). Decalcification required for processing osteosarcomas before sectioning did not affect the APB status of two ALT[+] and two telomerase[+] tumour controls (Fig 3.7). A set of criteria for scoring APBs was devised (Section 2.4.2) and tested against the TRF analysis test for ALT in tumours.

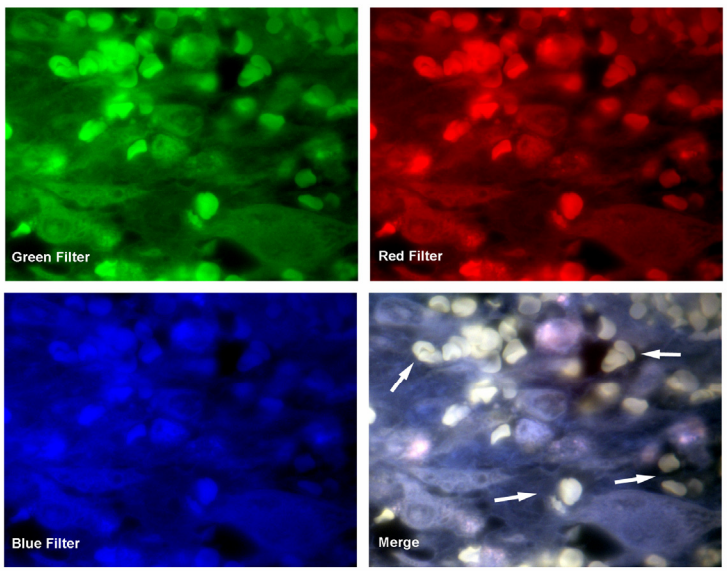

Figure 3.6: Autofluorescence in a STS. This paraffin section demonstrates autofluorescence in a paraffin section of a STS that has been treated as for combined immunofluorescence and telomere FISH except that no antibodies or probes were added. Autofluorescence can be seen across all channels and especially in red blood cells (*arrows*).

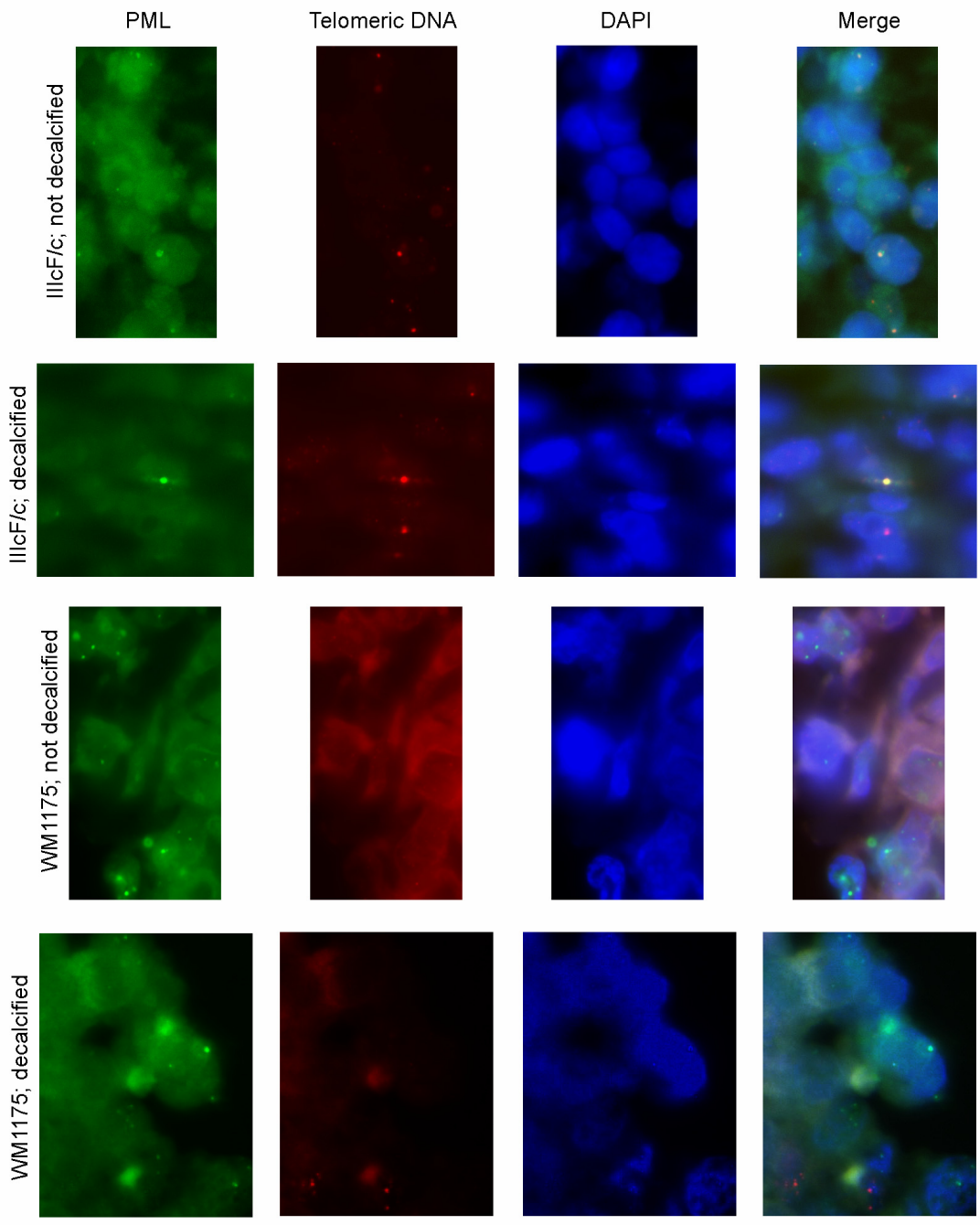

Figure 3.7: Decalcification did not affect APB assay. Combined PML immunofluorescence and telomere FISH in a paraffin section of an ALT[+] and an ALT[-] tumour grown in nude mice from *IIICF/c* and *WM1175* cell lines, respectively. Indirect immunofluorescence (FITC label) was used for the PML protein and telomere FISH was done with a Cy3 conjugated telomeric peptide nucleic acid probe. Nuclei were counterstained with DAPI. Whether the sections were *decalcified* or *not decalcified* did not alter the APB status.

3.4 APB presence corresponds to ALT in human tumours

The main purpose of this chapter is to investigate if the presence of APBs can be used to detect ALT in human tumour samples. It was not known whether the very good correlation between ALT[+] and APB[+] in cell lines extended to tumour specimens, and conversely whether some of the discrepancies seen in cell lines may be due to artificial situations arising from *in vitro* transformation and therefore occur to an insignificant extent in tumours. We determined this by comparing the APB assay with the current test for ALT in tumour specimens, TRF analysis. Two sets of tumour specimens were obtained for validating the APB assay: 26 frozen samples of STS on which we could perform the APB assay, TRF analysis and test for telomerase activity with the TRAP assay, and 40 paraffin-embedded samples of astrocytoma brain tumours for which TRF analysis and TRAP assay had already been independently performed[270].

3.4.1 APBs in frozen sections of soft tissue sarcomas

The 26 frozen STS sections used for APB analysis were taken immediately adjacent to the region used for TRF analysis and TRAP assays. The APB assay was performed blinded to the TRF results.

Results for the TRF analysis of all 26 STS are shown in Figure 3.8A. Currently, there is no established criterion that unambiguously defines whether ALT is present based on TRF analysis results. In cell lines the ALT positive group is generally clearly separate from the ALT[-] group in terms of the average telomere length and heterogeneity of length[69]. However Fig 3.8A shows that this is not the case for these tumour specimens. Intermediate telomere length distributions have been reported for STS[323] and the ALT[+] osteosarcoma cell line Saos-2[73,344]. Previously, tumours have

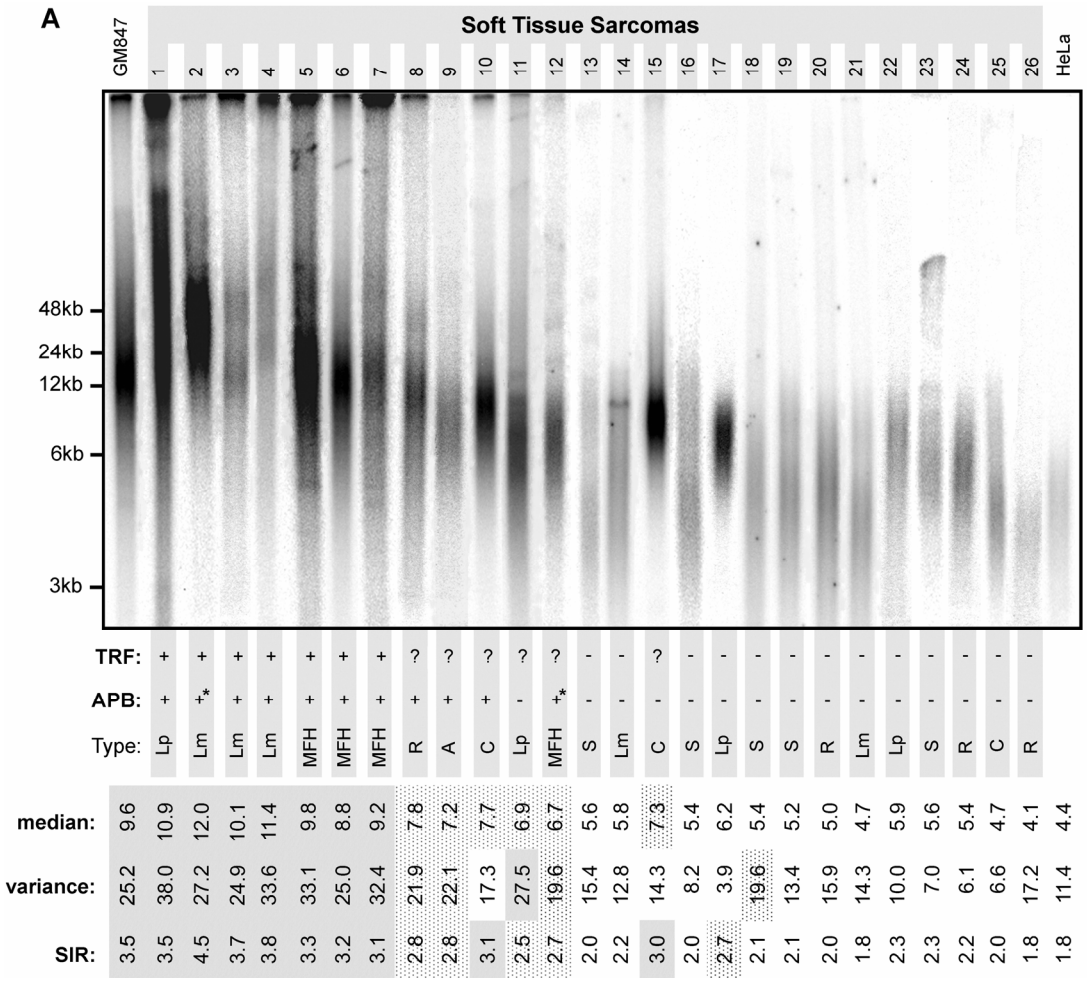

Figure 3.8: Agreement of the APB assay with the standard assay for ALT in tumours. ***A*:** terminal restriction fragment Southern analysis showing telomere length distributions of 26 STS and typical ALT[+] (GM847) and Telomerase[+] (HeLa) immortal cell lines. The lengths of telomeres in ALT[+] cells typically range from <3 to >50 kb. ALT[-] cells, including Telomerase[+] cells, typically have a more homogeneous distribution of telomere lengths and a shorter average length. ALT status for each STS determined by the TRF or APB assays: ALT[+] (+), ALT[-] (-) or equivocal (*?*). For the *APB* assay, * denotes APB[+] STS that had a low frequency (< 0.5%) of APB[+] nuclei. Telomere length distribution *median*, *variance* and semi-interquartile range (*SIR*) that were used to determine ALT status are shown for each sample and high values are *shaded*, intermediate values *stippled* and low values are *unshaded*. Type of STS: alveolar soft part sarcoma (*A*), chondrosarcoma (*C*), leiomyosarcoma (*Lm*), liposarcoma (*Lp*), malignant fibrous histiocytoma (*MFH)*, rhabdomyosarcoma (*R*), and synovial sarcoma (*S*). ***B*:** graph showing the frequency of the different TRF lengths calculated by Telometric software. Only TRFs over 3 kb were analysed (see Section 2.5.3). ***C*:** plot showing the distribution of values for *mean*, *median*, *mode*, *variance* and semi-interquartile range (*SIR*), of the telomere lengths of the STS (numbered *1* to *26*) and control cell lines GM847 (*closed diamond*) and HeLa (*open diamond*). Each distribution measure can be used to aggregate the STS into discrete clusters of high, intermediate and low value. The apparent intermediate range of values for each measure is *shaded*. ***D*:**, effect of a mixed sample on the TRF assay. TRF analysis of a mixture of genomic DNA from ALT[+] (GM847) and Telomerase[+] (HeLa) cell lines. Each lane was loaded with a total of 2 µg of combined genomic DNA from GM847 and HeLa cells. *% ALT*, the percentage of ALT[+] genomic DNA in each mixture. For the mixed samples the frequency of the different TRF lengths is shown in ***E*:** with each sample identified by the *percentage* of ALT[+] genomic DNA in the total mix. The change in each distribution measure as a function of percentage of ALT[+] genomic DNA in the total mix is plotted in ***F*:** with *shading* of the intermediate range determined for the STS in *C*.

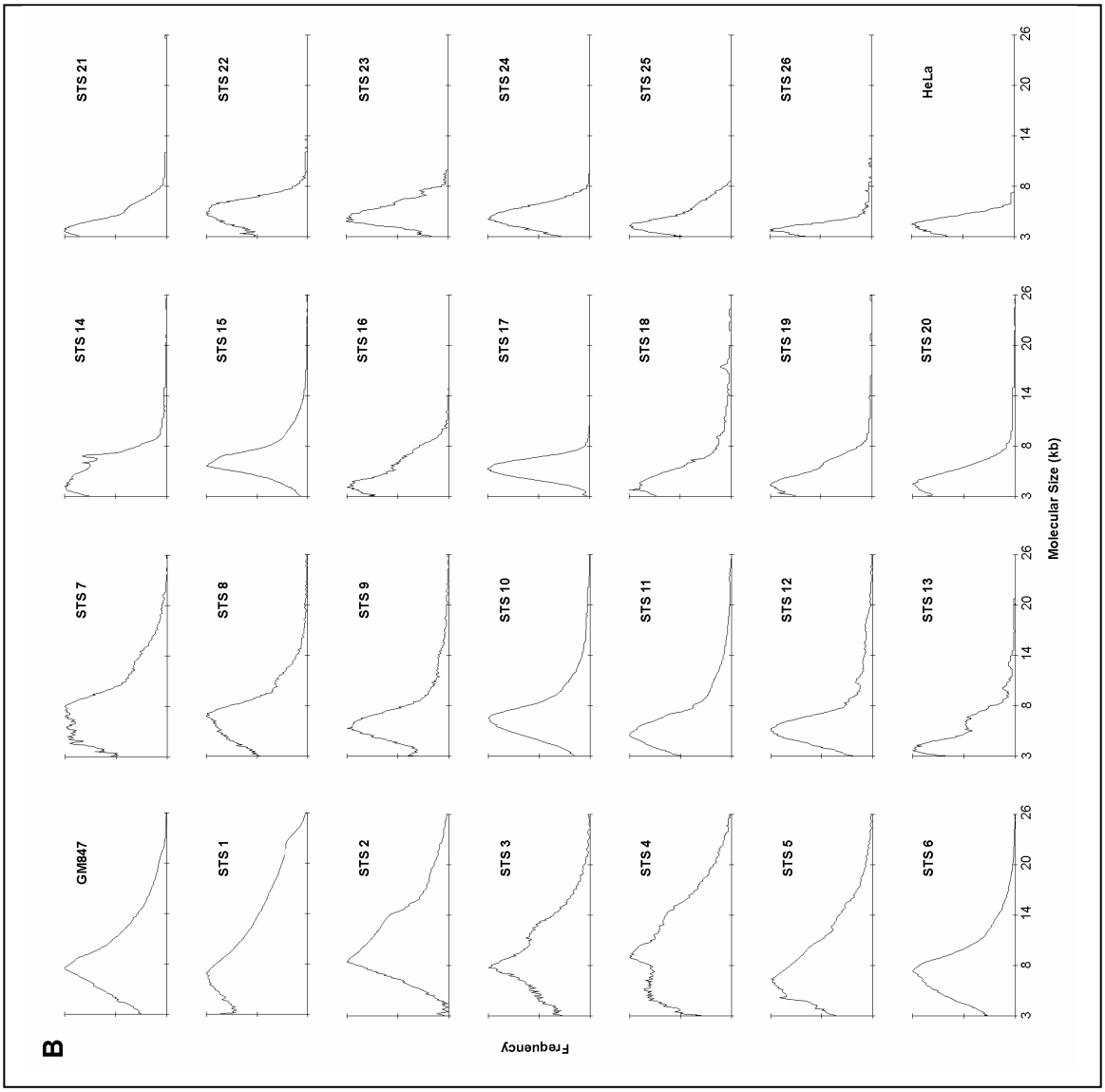
B
GM847
STS 7
STS 14
STS 21
STS 1
STS 8
STS 15
STS 22
STS 2
STS 9
STS 16
STS 23
STS 3
STS 10
STS 17
STS 24
STS 4
STS 11
STS 18
STS 25
STS 5
STS 12
STS 19
STS 26
STS 6
STS 13
STS 20
HeLa
Frequency
Molecular Size (kb)
3
8
14
20
26

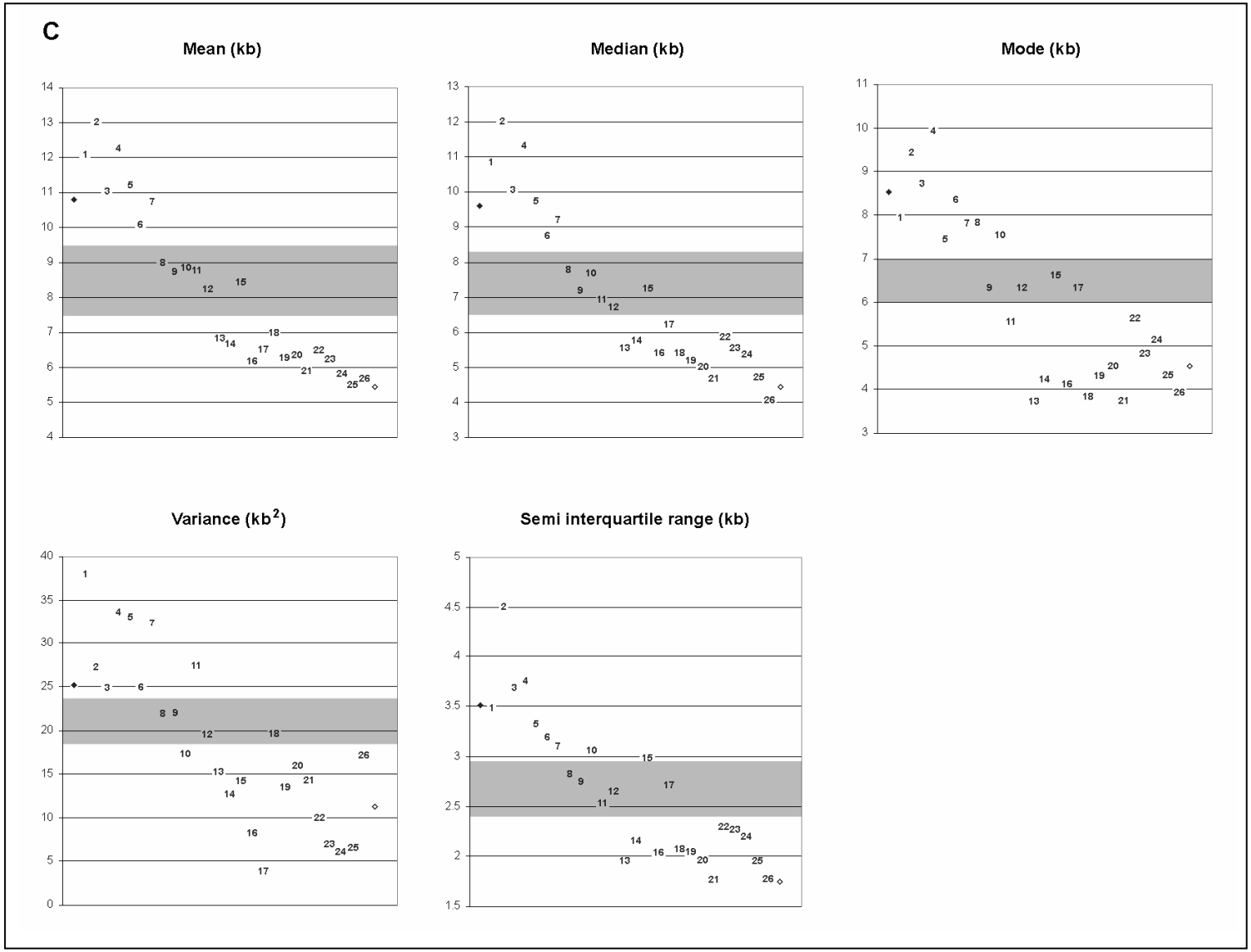
C
Mean (kb)
Median (kb)
Mode (kb)
Variance (kb2)
Semi interquartile range (kb)

D

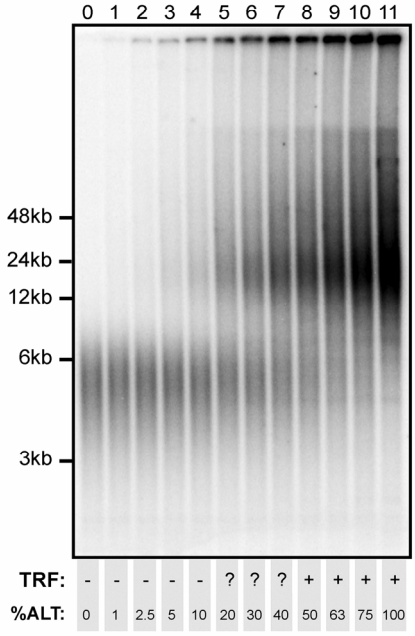

Lane	%ALT	Median	Variance	SIR	TRF
0	0%	4.4	11.4	1.8	-
1	1%	4.5	13.1	1.8	-
2	2.5%	4.6	16.4	1.9	-
3	5%	4.8	19.4	1.9	-
4	10%	5.2	22.1	2.0	-
5	20%	7.1	23.8	2.2	?
6	30%	7.7	23.9	2.3	?
7	40%	8.3	24.5	2.6	?
8	50%	8.6	24.5	2.9	+
9	63%	9.0	24.5	3.2	+
10	75%	9.1	24.7	3.3	+
11	100%	9.6	25.2	3.5	+

E

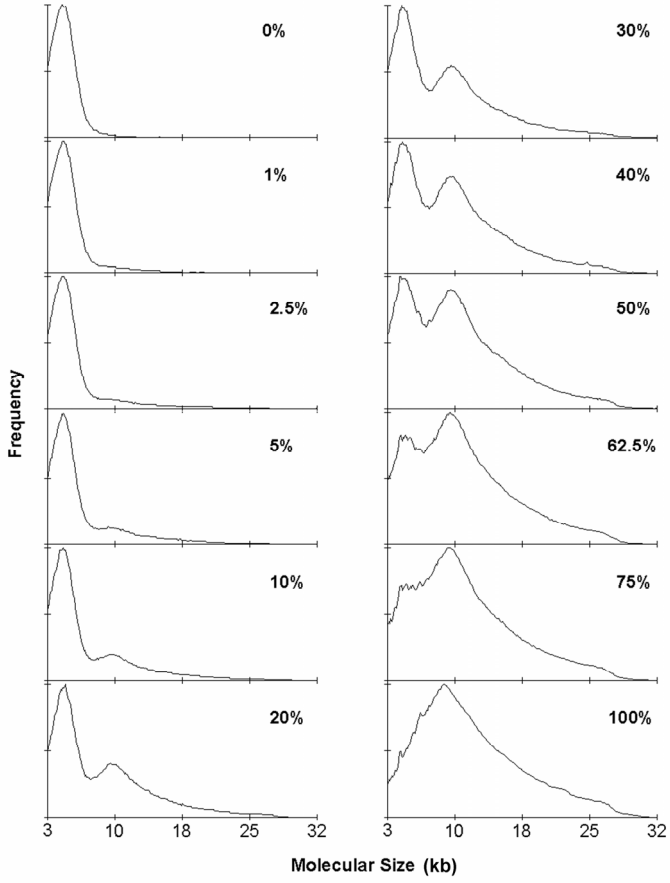

F

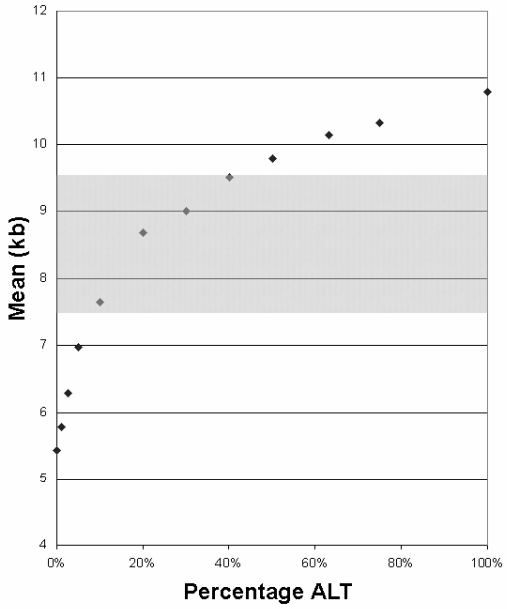
Mean (kb)
12
11
10
9
8
7
6
5
4
0%
20%
40%
60%
80%
100%
Percentage ALT

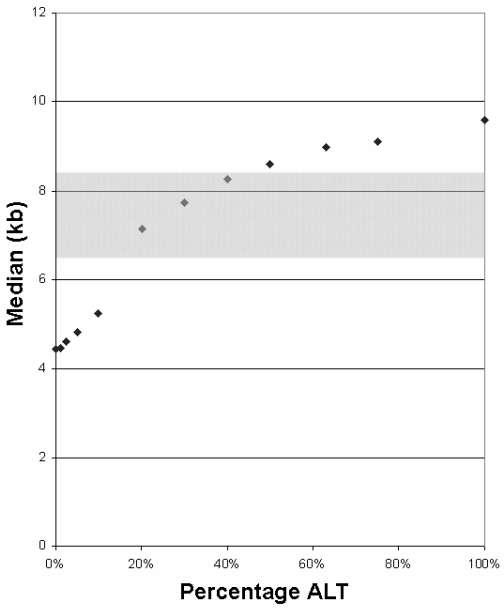
Median (kb)
12
10
8
6
4
2
0
0%
20%
40%
60%
80%
100%
Percentage ALT

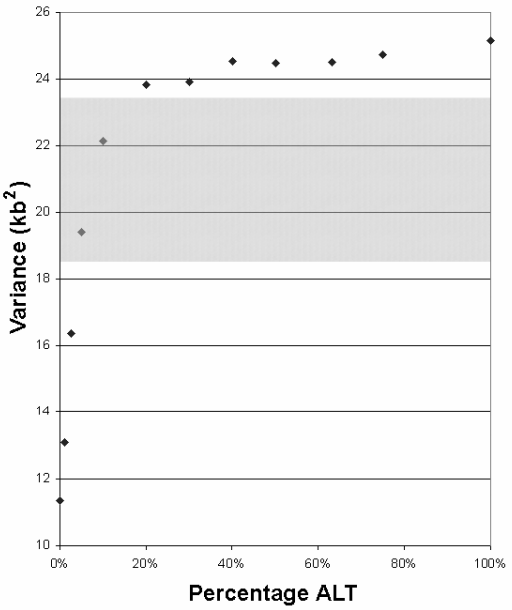
Variance (kb2)
26
24
22
20
18
16
14
12
10
0%
20%
40%
60%
80%
100%
Percentage ALT

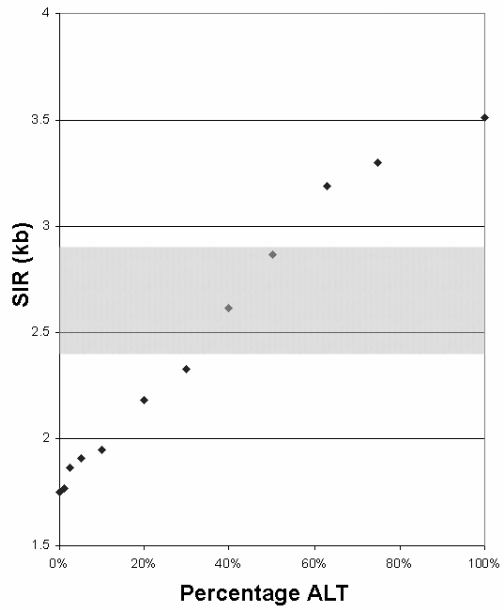
SIR (kb)
4
3.5
3
2.5
2
1.5
0%
20%
40%
60%
80%
100%
Percentage ALT

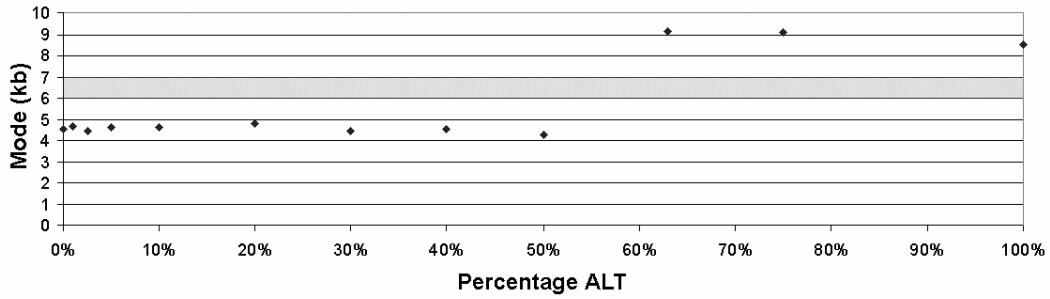
Mode (kb)
10
9
8
7
6
5
4
3
2
1
0
0%
10%
20%
30%
40%
50%
60%
70%
80%
90%
100%
Percentage ALT

been classified as ALT[+] if they have TRF distributions with abnormally high mean and heterogeneity. Based on cell line observations the threshold mean telomere length for determining ALT[+] was originally set at 15 kb[73,344]. Threshold values for ALT[+] have also been determined by using 120% of the mean telomere length in the normal tissue from which the tumour originated[345] or by plotting the mean values for a group of tumours and noticing a distinct group of tumours with a high mean telomere length[270]. Instead of the mean value, the presence of a significant telomere smear above 17-23 kb has also been used[271,346], although this may not add to using heterogeneity as the only determinant. The method for determining ALT[+] heterogeneity is generally not stated but the presence of a TRF smear from 3kb to the wells has been used[73,344].

The telomere length distributions of the 26 STS and ALT[+] and telomerase[+] controls in Fig 3.8B were analysed with the Telometric program[341] to determine the centre of mass statistics, mean, median and mode, as well as statistics indicating heterogeneity, namely variance and semi interquartile range (SIR) (Fig 3.8C). It should be noted that for reasons described in methods, the telomeres below 3kb were omitted and this will affect the absolute values of these statistics. Because ALT-positivity is based on both a higher centre of mass and a larger spread for its telomere length distribution, for each telomere length distribution statistic the 26 STS were grouped into three distinct groups: high, intermediate and low indicating ALT[+], ALT[?] and ALT[-], respectively (Fig 3.8C and summarised in Fig 3.8A).

Since there are no established criteria for determining the presence of ALT activity from analysis of the telomere length distributions of tumour specimens, two approaches were considered. Firstly, and most simply, ALT status could be determined solely from a measure of the centre of mass of the distribution. For the

centre of mass statistic, median was chosen as it appeared to be more stringent in determining ALT[+] than the mode (Fig 3.8C). The mean was not used because telomere lengths were not normally distributed (Fig 3.8B), but it is noted that the mean gave identical results to the median for ALT status. It may be more robust to base the determination of ALT status on a combination of a centre of mass statistic as well as measures of the variance and the range of the distribution. Thus a second set of criteria were investigated that use a centre of mass statistic with the variance and range.

Below are the two sets of criteria used to determine ALT status from the telomere length distribution, both of which gave identical results for the 26 STS here (Fig 3.8A). The cut off values were determined as the mid point between the extremes of the high and intermediate or intermediate and low STS clusters for that particular statistic (Fig 3.8C).

1. Median only criterion:

   ALT[+] if median > 8.3 kb

   ALT[?] if median 6.5-8.3 kb

   ALT[-] if median < 6.5 kb

2. Criterion based on median, variance and SIR

   ALT[+] if median, variance and SIR all high or two high and one intermediate

   ALT[-] if median, variance and SIR all low or two low and one intermediate

   ALT[?] otherwise

   The intermediate ranges were:

Median: 6.5 kb - 8.3 kb

Variance: 18.5 kb^2 - 23.5 kb^2

SIR: 2.4 kb - 2.9 kb

As shown in Fig 3A, both these criteria classify STS 1-7 as ALT[+], STS 8-12 and 15 as ALT[?] and STS 13,14 and STS16-26 as ALT[-].

Because TRF analysis rarely provides equivocal results for ALT status in cell lines[69,73,344], it seems likely that the difficulty in determining ALT status of some tumours arises from admixture of tumour and stromal cells. Also, tumours may have spatial heterogeneity in either telomere length of tumour cells[323] or in the presence of ALT (Section 3.5). In order to assess how a mixed population of ALT[+] and ALT[-] cells affected the determination of ALT status by TRF analysis, we analysed different mixtures of DNA from ALT[+] (GM847) and telomerase[+] (HeLa) cell lines (Fig 3.8D, E and F). The ALT status of the mixture was equivocal (ALT[?]) by our criteria when 20%-40% of the genomic DNA was from the ALT[+] cell line (Fig 3.8D, lanes 5 - 7). Thus the heterogeneity of tumours may account for the equivocal results for ALT status sometimes obtained by TRF analysis.

As can be seen from Figure 3.8D and 3.8F, the variance is the most sensitive to small amounts of ALT[+] genomic DNA being present and the SIR appears to have the most linear response to the varying proportion of ALT[+] DNA and to be least affected by relatively small amounts of ALT[+] DNA. Thus the SIR may be the most sensitive to ALT[-] genomic DNA being present. Comparing the telomere length distribution diagrams Fig 3.8E and 3.8B we can see that STS 3, 4, 7, 13 and 16 may have two populations, but seem to have either two ALT[+] or two ALT[-] populations. STS 8 may have an ALT[+] and an ALT[-] population, with similar

distribution ratios to the mix of 20% ALT[+] that was also judged ALT[?]. The high variance relative to median and SIR of STS 18 and 26 is likely to be due to sensitivity of variance to artefactual signal higher up in the lane and not due to small amounts of ALT[+] cells being present. The intermediate results for STS 9 and 12 (Fig 3.8A) could be due to a small ALT[+] population of less than 5% (Fig 3.8B compared with Fig 3.8E), but it is not possible to distinguish this from background signal.

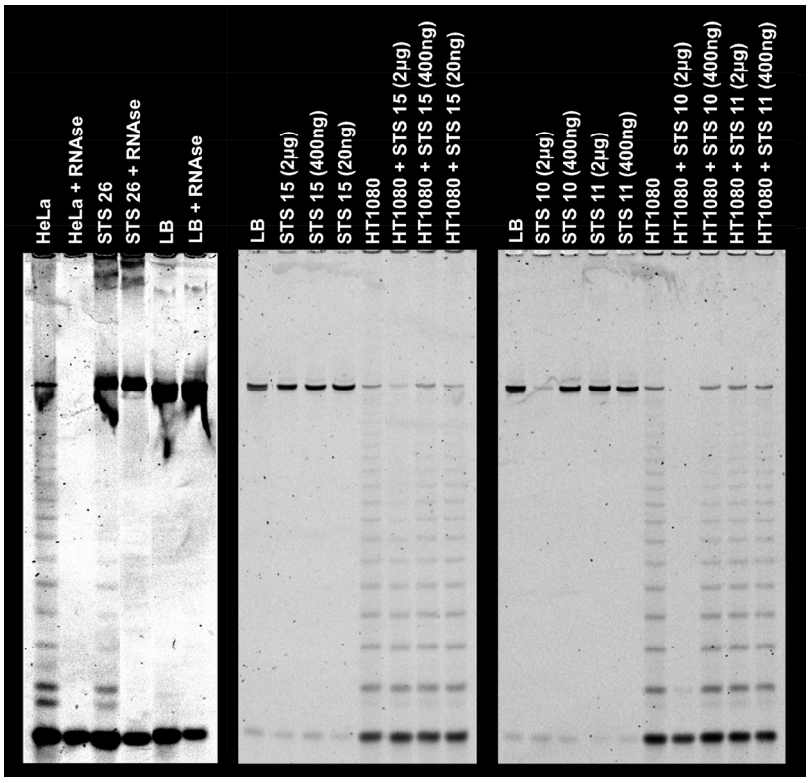

Figure 3.9: TRAP analysis of STS. Example of TRAP assay results for *STS* specimens numbered *10, 11, 15* and *26*. Positive control, *HeLa*, gave a six base pair ladder indicating products from telomerase activity that was not present in the lysis buffer, *LB* (negative control). All positive samples were treated with RNAse to inactivate telomerase and thus distinguish telomerase activity from PCR contamination. All negative samples were diluted to overcome any possible Taq polymerase inhibitors and this was confirmed by mixing 1:1 with the positive control HT1080. For example, a Taq inhibitor in *STS 10* was overcome by a 20 fold dilution. The intense upper band corresponds to the internal PCR control and the lowest band is primer dimer.

Telomerase activity was determined by the TRAP assay for all 26 STS (examples in Fig 3.9), and 4/26 (15%) were telomerase[+] (STS 14, 18, 19 and 26). The telomerase[+] STS were all unequivocally ALT[-] by TRF analysis (Fig 3.8A).

Combined PML immunostaining and telomere FISH on the same frozen sections identified 11/26 STS as APB[+] , and the remaining 15 as APB[-] (Fig 3.10). The comparison between the APB assay and TRF assay results is summarised in Fig 3.8A. All seven of the STS determined to be ALT[+] by TRF Southern analysis were APB[+] (e.g. STS 1,2 and 5 in Fig 3.10), and all 13 of the STS found to be ALT[-] by TRF Southern analysis were APB[-] (e.g. STS 18 and 21 in Fig 3.10). APB analysis allowed all of the STS to be objectively classified as ALT[+] or ALT[-], in contrast to the TRF analysis which was equivocal for 6/26 STS (e.g. STS 8 and 10 in Fig 3.10). Since the APB assay assesses individual cells instead of distributions over the entire population, it may be a more appropriate technique than TRF Southern analysis for tumours that can have mixed populations of normal and tumour cells as well as spatial heterogeneity for telomere length within the tumour.

3.4.2 APBs in paraffin sections of astrocytomas

We also compared the APB assay in paraffin sections with the TRF assay for ALT in 40 grades II - IV astrocytomas (33 GBMs (WHO grade IV astrocytomas) and seven grades II – III astrocytomas; Fig 3.11). For this tumour set the sections were taken from a different part of each tumour than the portions used for TRF analysis[270]. TRF assay and TRAP assay for these tumours only were performed by Hakin-Smith *et al*.[270]. Both assays (TRF and APB) found 13/40 astrocytomas to be ALT[+] (7/33 GBMs and 6/7 grade II – III astrocytomas). There was exact concordance between the two assays for all 40 astrocytomas (Fig 3.11). TRAP assay showed 13/40

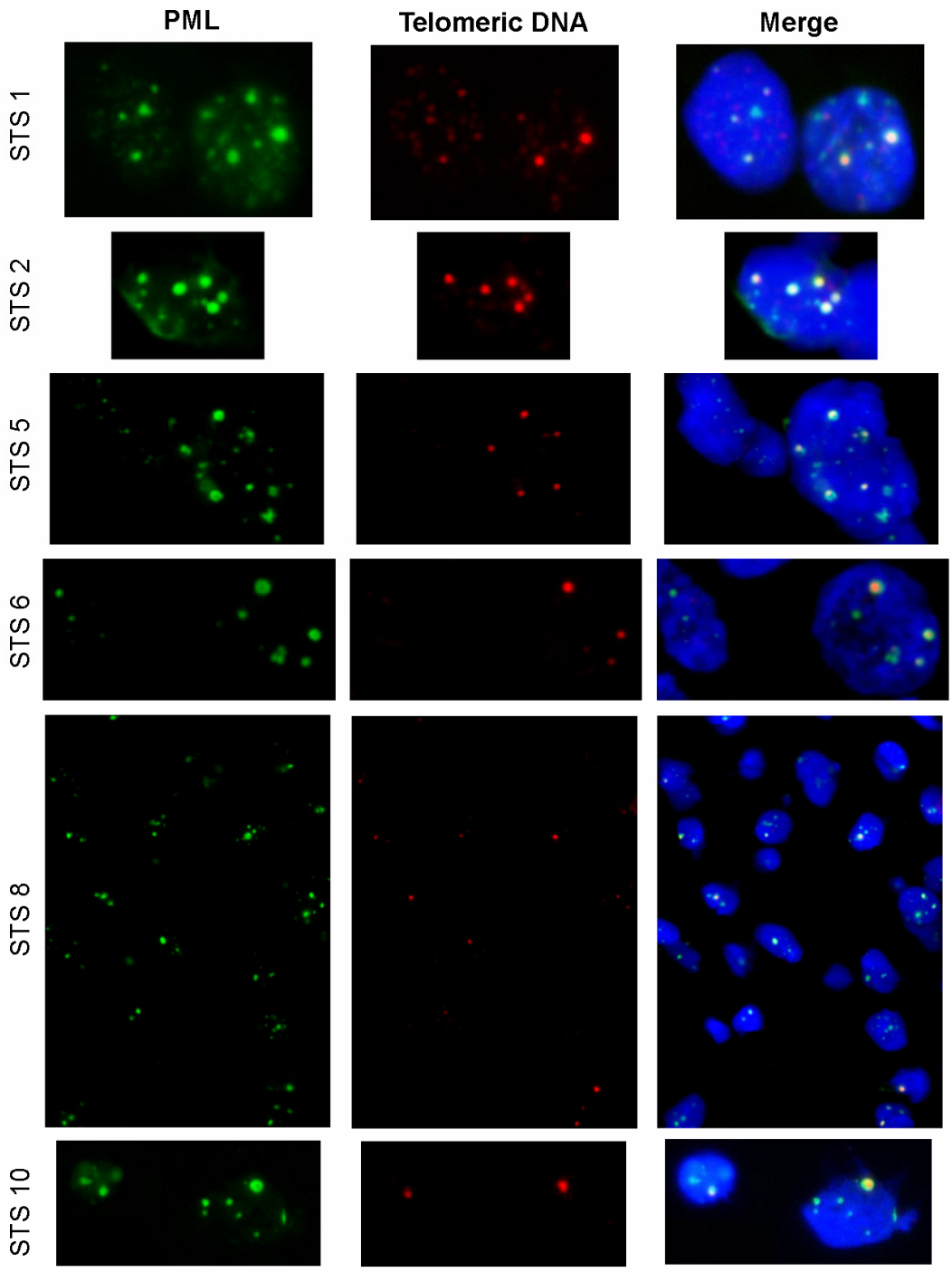

Figure 3.10: APB assay in STS frozen sections. Examples of combined PML immunofluorescence and telomere FISH in frozen sections are shown for eight of the STS specimens that were used to compare the APB and TRF assays for ALT in tumours. Indirect immunofluorescence (FITC label) was used for the *PML* protein and Telomere FISH was performed using a Cy3-conjugated telomeric peptide nucleic acid probe (***A***). In sections of *STS* numbered *1*, *2*, *5*, *6*, *8* and *10*, APBs are visible as bright foci of *telomeric DNA* that colocalise with *PML* (***B***). In the sections of *STS 18* and *21* there are no bright telomeric foci and no colocalisation of telomeric foci with PML bodies – thus these STS are APB[-].

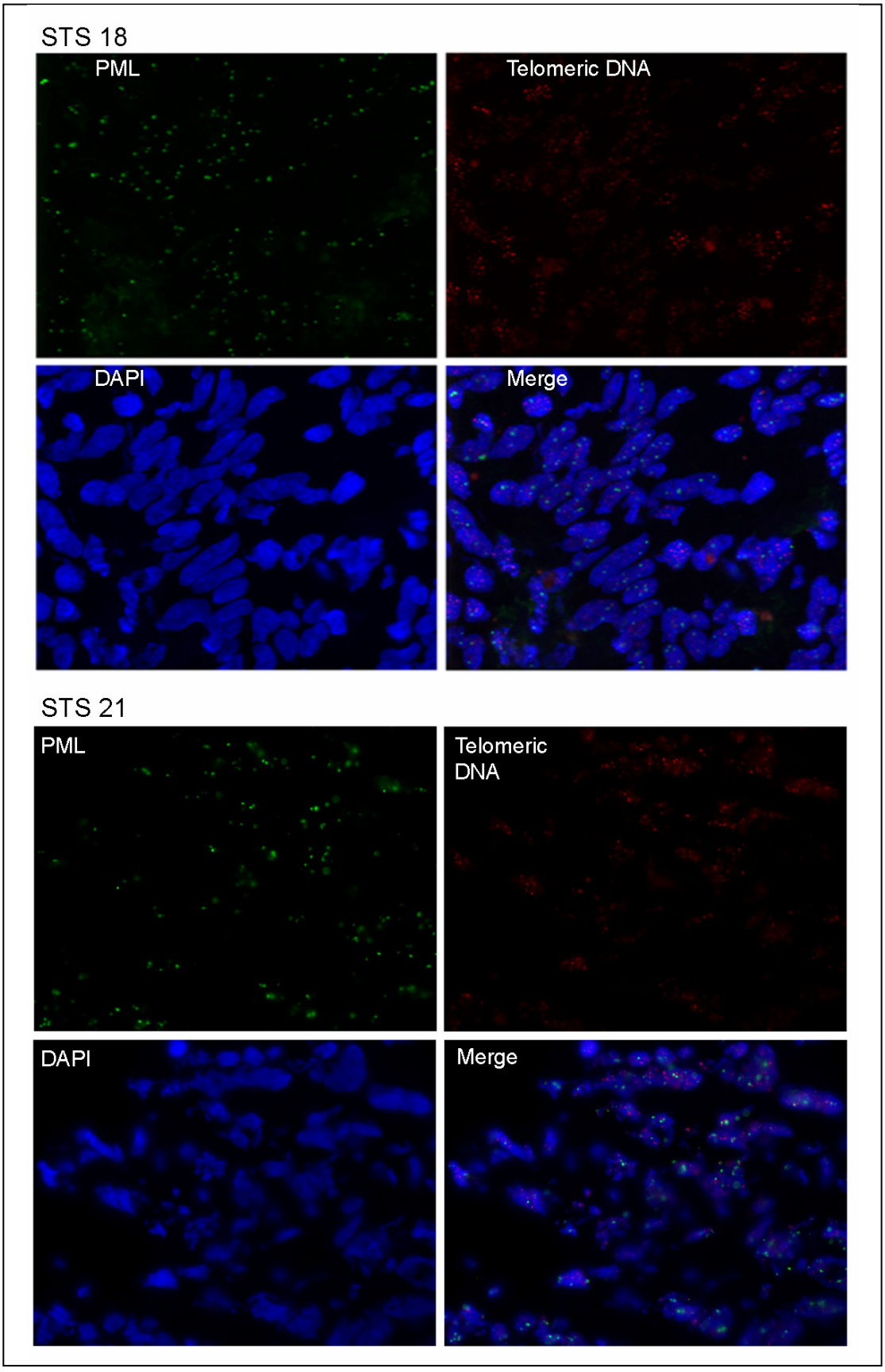
STS 18
PML
Telomeric DNA
DAPI
Merge
STS 21
PML
Telomeric
DNA
DAPI
Merge

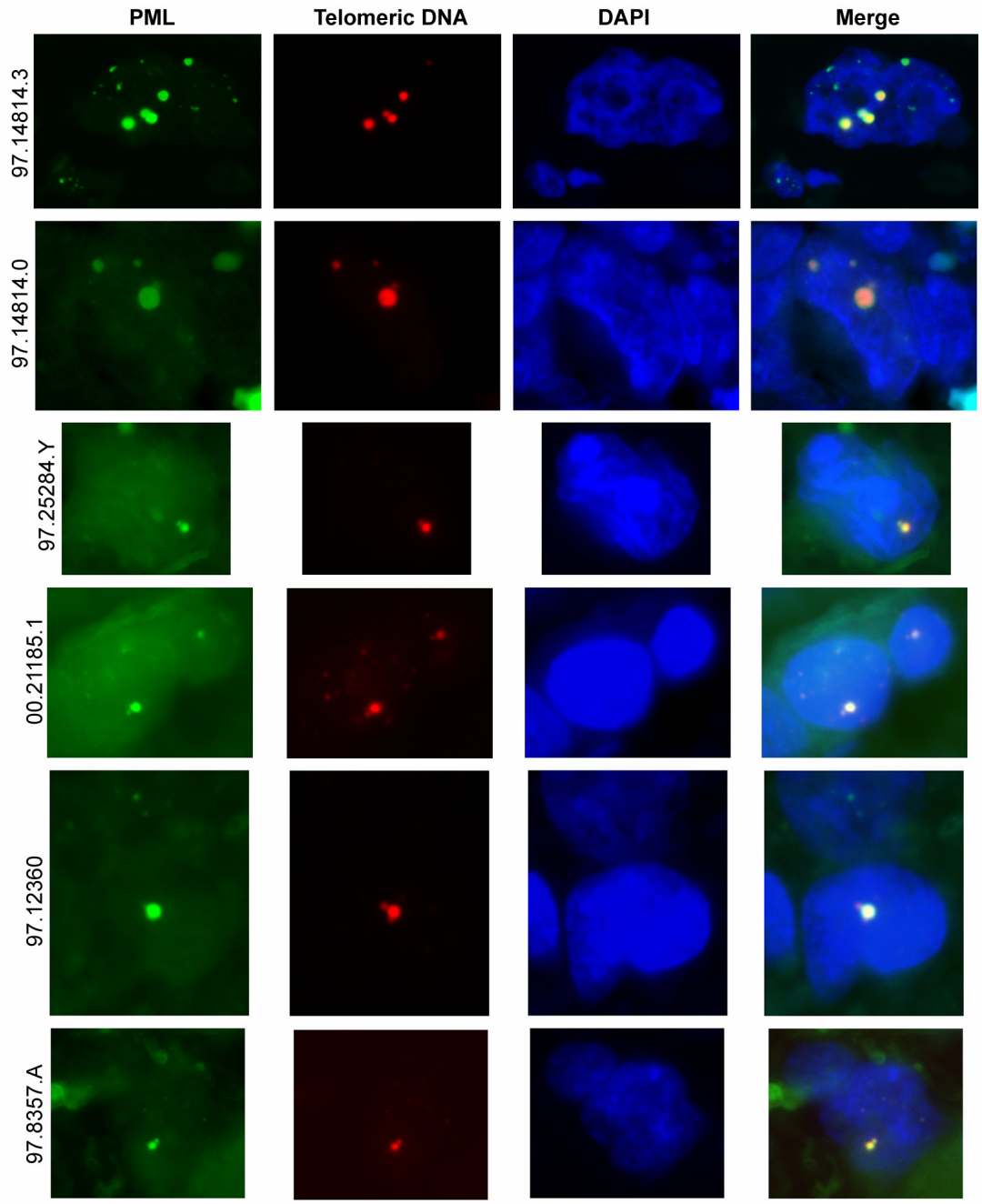

Figure 3.11: APB assay in paraffin sections of astrocytomas. Examples of combined PML immunofluorescence (indirect FITC label) and telomere FISH (Cy3 conjugated peptide nucleic acid probe) in paraffin sections of astrocytomas that were used to compare the APB and TRF assays for ALT in tumours. All astrocytomas illustrated here were glioblastoma multiforme (grade IV astrocytomas), except *97.12360* and *97.8357.A* which were grade III and II/III astrocytomas, respectively (J Royds, personal communication). In all sections except *98.12336.C2*, APBs are visible as bright foci of *telomeric DNA* that colocalise with *PML*. In *98.12336.C2* there were no bright telomeric foci and no colocalisation of telomeric foci with PML bodies, indicating *98.12336.C2* is APB[-] and hence ALT[-]. In the APB[+] specimens shown here the APBs appear to be fusing or dividing - as seen in cell lines (Fig 3.1).

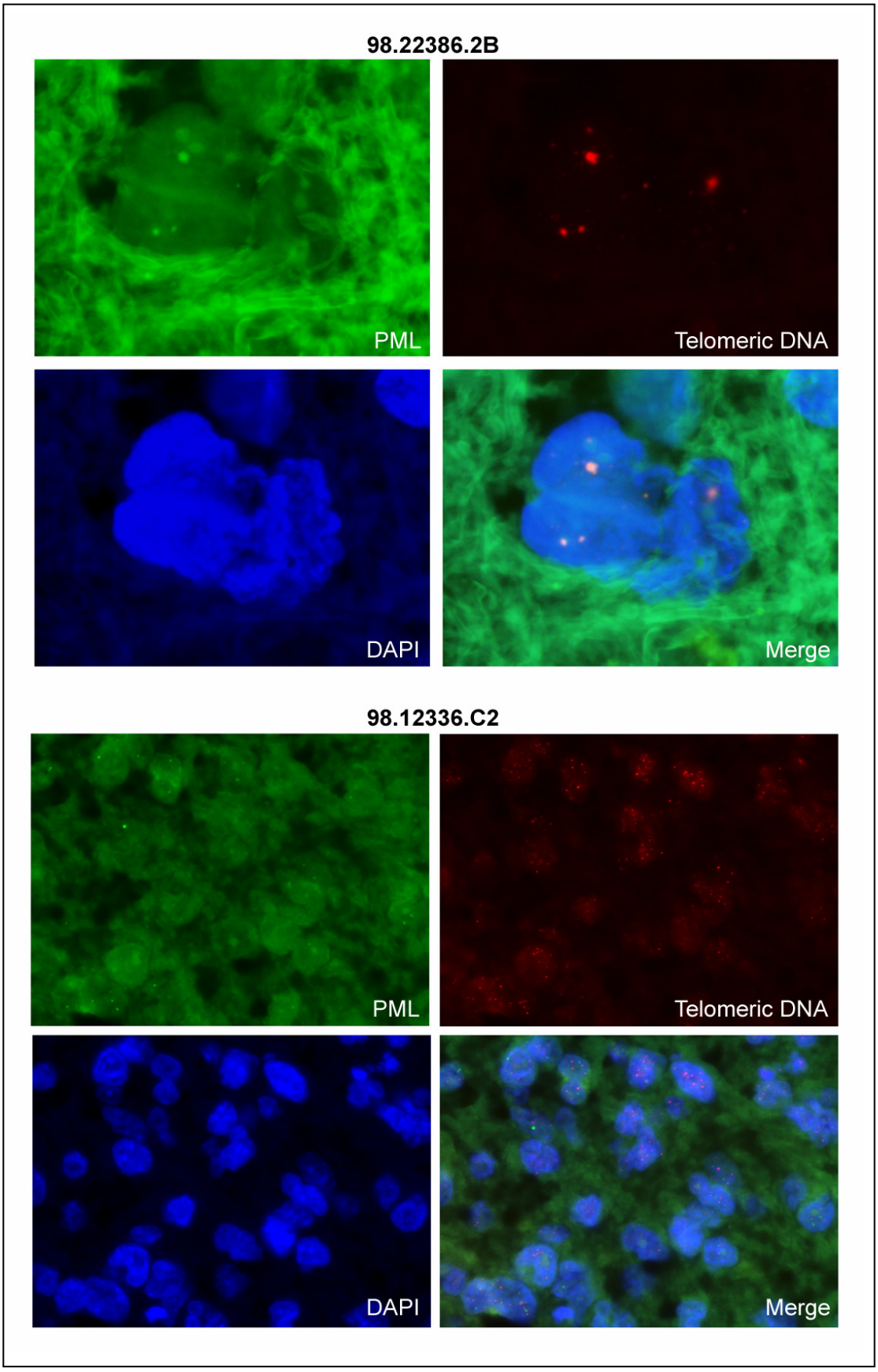
98.22386.2B
PML
Telomeric DNA
DAPI
Merge
98.12336.C2
PML
Telomeric DNA
DAPI
Merge

astrocytomas to be telomerase[+][270]. All 13 telomerase[+] astrocytomas were GBMs and of these 12 were ALT[-] and one was ALT[+]. GBMs testing positive for both telomerase activity and ALT have been reported[270,347].

3.5 Comparison of APB frequency and MS32 minisatellite instability

Instability at the MS32 minisatellite locus is a characteristic of ALT cell lines but was only found in a subset of ALT[+] STS[121]. In collaboration with Jeyapalan *et al.*[121], this was investigated further by comparing the frequency of APB[+] nuclei determined for Section 3.4.1 with the presence of MS32 instability[121]. Table 3.2 shows that the three STS with MS32 instability had the highest frequency of APB[+] nuclei. No MS32 instability was reported[121] for 10 of the ALT[-] STS from Section 3.4.1 that were tested.

Table 3.2: Frequency of APB[+] nuclei and MS32 instability[a]

STS	MS32 instability[a]	Frequency of APB[+] nuclei
1	High	50%
5	High	20%
7	High	20%
3	Normal	10%
6	Normal	8%
10	Normal	5%
2	Normal	<0.1%

[a]MS32 instability was assayed by Jeyapalan *et al.*[121]

3.6 Heterogeneity

Since tumours are not genetically homogeneous[348], it is possible that intratumoral spatial heterogeneity for ALT may occur. One study[271] tested 15 osteosarcomas by TRF analysis at two separate sites, but found no evidence of intratumoral spatial

heterogeneity for ALT. For telomerase activity, however, intratumoral spatial heterogeneity has been reported in 7 - 38% of osteosarcomas, STS and prostate carcinomas tested at 2-3 different sites[271,323,325] and 9/11 GBMs tested at 3-7 different sites showed heterogeneity[324]. Because spatial heterogeneity for ALT could affect interpretation of assays for ALT status, we tested for this in osteosarcomas and GBMs.

For ten osteosarcomas, paraffin-embedded tissue from two separate sites was examined for APBs. The two samples from each tumour were taken from the primary site at the same time point. We found that 2/10 (20%) osteosarcomas had one site that was ALT[+] and the other ALT[-] (example in Fig 3.12). Of the remaining osteosarcomas, five were APB[-] at both sites and three were APB[+] at both sites. Thus there is a comparable frequency of intratumoral spatial heterogeneity for ALT in osteosarcomas as reported for telomerase activity in other tumours[271,323,325].

We also tested for intratumoral spatial heterogeneity for ALT in 13 different GBM tumours (six ALT[-] and seven ALT[+], including the ALT[+]/telomerase[+] GBM described in Section 3.4.2). Two separate paraffin blocks of each tumour were examined for APBs, but no spatial heterogeneity for ALT was found (Fig 3.12; including the GBM that was both ALT[+] and telomerase[+]). However, this sample size (n = 13) was not big enough to significantly exclude heterogeneity levels of 20% or less (using the binomial distribution and requiring $p \leq 0.05$).

3.7 APB assay in fine needle aspiration biopsies

The existence of ALT activity may be a used as a marker for malignancy (see Chapter 4). We investigated if APBs could be seen in fine needle aspiration biopsies of

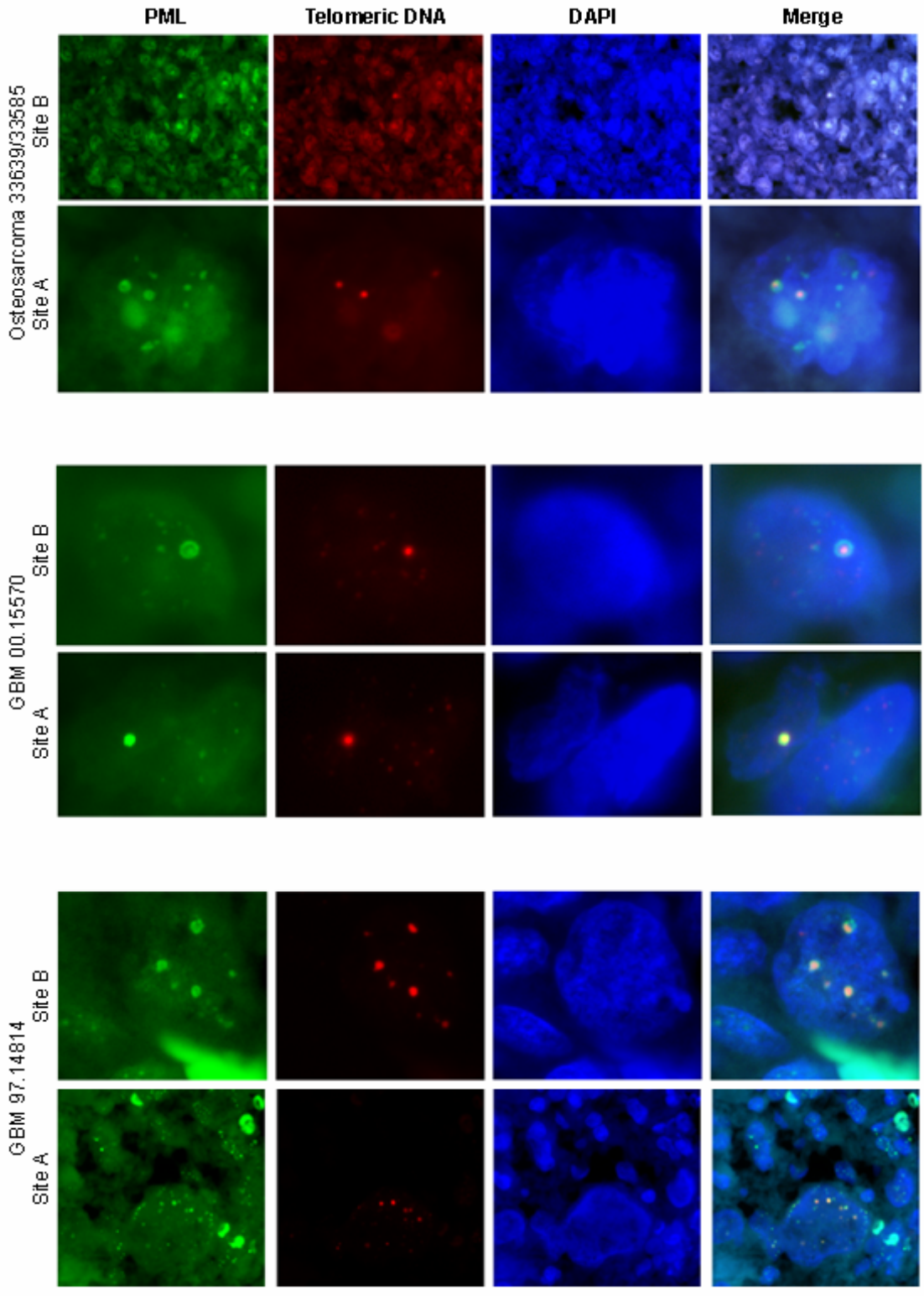

Figure 3.12: Intratumoral heterogeneity for ALT. APB assay performed on paraffin sections taken from two different sites in an osteosarcoma and two GBMs. The osteosarcoma shown here was APB[+] at *site A* and APB[-] at *site B*. Both examples of GBMs shown here were APB[+] at both sites.

ALT[+] tumours from nude mice. The process of fine needle aspiration and application to slides was compatible with APB detection (Fig 3.13).

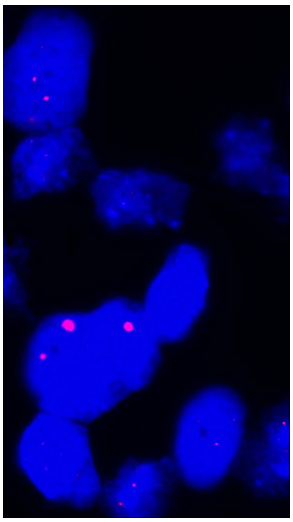

Figure 3.13: APB assay in a fine needle aspiration biopsy (FNAB). Demonstration that the APB assay is compatible with the FNAB technique performed on an ALT[+] tumour from a human cell line (IIICF/c) grown in a nude mouse. This figure shows the signal from telomere FISH using Cy3 conjugated peptide nucleic acid probe merged with the signal from counterstaining the nuclei with DAPI. The bright telomeric foci represent APBs. The telomeres have lower intensity and can barely be seen at this exposure.

3.8 An alternative way to assay APBs

Currently the exact nature of the telomeric repeats in APBs is unknown. There is some evidence that APB telomeric repeats are predominantly extra-chromosomal DNA (C Fasching and A Muntoni, unpublished), however the presence of telomeres (chromosomal) is also possible. Whether the telomeric repeats in APBs are used in the ALT mechanism or simply the by products of the ALT mechanism, characterisation of this DNA may still improve our understanding of the ALT mechanism and provide new ways to assay for APBs and ALT.

Telomere FISH was performed under non-denaturing conditions with single stranded oligonucleotide probes (native telomere FISH) to test for single stranded telomeric repeats in APBs. Fig 3.14A shows that strong signal was found for both single stranded $(5'\text{-TTAGGG-}3')_n$ and single stranded $(5'\text{-CCCTAA-}3')_n$ in the APBs of the ALT[+] cell line SUSM-1. No foci were seen in the telomerase[+] cell line HT1080

(Fig 3.14). Combining native telomere FISH with PML immunostaining showed all the single stranded (5′-CCCTAA-3′)$_n$ foci colocalised with PML bodies and hence were APBs (Fig 3.14). Native FISH with both the C-rich and G-rich telomeric probes showed that the single stranded (5′-TTAGGG-3′)$_n$ and single stranded (5′-CCCTAA-3′)$_n$ colocalised in SUSM-1. Similarly, single stranded (5′-TTAGGG-3′)$_n$ foci and single stranded (5′-CCCTAA-3′)$_n$ foci were seen in the ALT[+] cell lines U-2 OS, GM847 and MRC5-V2 and were still present after treatment with RNase (data not shown).

Single stranded (5′-TTAGGG-3′)$_n$ is known to be present as a 3′ overhang at the end of telomeres in mortal, telomerase[+] and ALT cell lines[349-352]. However, the presence of single stranded (5′-CCCTAA-3′)$_n$ detectable by native TRF analysis has not been reported. The presence of single stranded (5′-CCCTAA-3′)$_n$ was tested for in five ALT[+], two telomerase[+] cell lines and one primary cell strain by native TRF analysis (Fig 3.14B). Presence of single stranded (5′-TTAGGG-3′)$_n$ was found in all cell lines as would be expected from the presence of the 3′-telomere overhang. The presence of single stranded (5′-CCCTAA-3′)$_n$ was detected in all five ALT[+] cell lines and in none of the ALT[-] cell lines or cell strain. Both the single stranded (5′-TTAGGG-3′)$_n$ and single stranded (5′-CCCTAA-3′)$_n$ signal was destroyed by digestion with Mung Bean Nuclease (MBN) treatment, although in two of the ALT cell lines digestion was incomplete for both single stranded (5′-TTAGGG-3′)$_n$ and single stranded (5′-CCCTAA-3′)$_n$. In at least two of the ALT cell lines, IIICF/c and SUSM-1 the single stranded (5′-CCCTAA-3′)$_n$ signal appeared to peak at a higher molecular weight than the single stranded (5′-TTAGGG-3′)$_n$ signal.

Figure 3.14: Single strand (5′-CCCTAA-3′)$_n$ in APBs. ***A*:** Native telomere FISH with oligonucleotide probes indicates the presence of single stranded G-rich and C-rich telomeric repeat foci in the ALT[+] cell line, *SUSM-1*, but not in the telomerase[+] cell line, *HT1080*. The (5′-TTAGGG-3′)$_8$ oligonucleotide probe hybridised to single stranded (5′-CCCTAA-3′)$_n$ and colocalised with anti-PML antibody indicating the single stranded (5′-CCCTAA-3′)$_n$ is in APBs. No signal was seen on telomere ends with either probe (native telomere FISH). ***B*:** Presence of single stranded (5′-CCCTAA-3′)$_n$ in ALT was further characterised by native TRF analysis. TRF analysis, under usual denaturing conditions, of the mortal cell strain, *HFF5*; telomerase[+] cell lines, *HT1080* and *HeLa*; and ALT[+] cell lines, *IIICF/c*, *W-V*, *SUSM-1*, *GM847* and *KMST-6* are shown in the *right* panel, with the gel denatured before probing. This denaturation step was omitted allowing only single stranded *(5′-TTAGGG-3′)$_n$* and *(5′-CCCTAA-3′)$_n$* to hybridise in left and middle panels, respectively. Mung Bean Nuclease (*MBN*), a single strand endonuclease was incubated with the genomic DNA in lanes marked with a "+" to confirm that the probes are not binding duplex telomeric repeats in the native TRF analyses. ***C*:** Creation of 5′ (C-Rich) overhang in the telomerase[+] cell line HT1080. Genomic DNA was treated as usual for TRF analysis, *no nuclease*, or pre-incubated with only Exonuclease I (*ExoI*), a 3′-5′ single strand exonuclease that does not act on double stranded DNA, or *ExoI* followed by Exonuclease III (*ExoIII*); a 5′-3′ single strand exonuclease that will act on double stranded DNA. TRF were then analysed as usual on a *denatured* gel and also on native gels (*left* and *middle* panels). The *left* panel was probed with *(5′-CCCTAA-3′)$_8$* to identify single stranded (5′-TTAGGG-3′)$_n$ and the middle panel was probed with *(5′-TTAGGG-3′)$_8$* to identify single stranded *(5′-CCCTAA-3′)$_n$*.

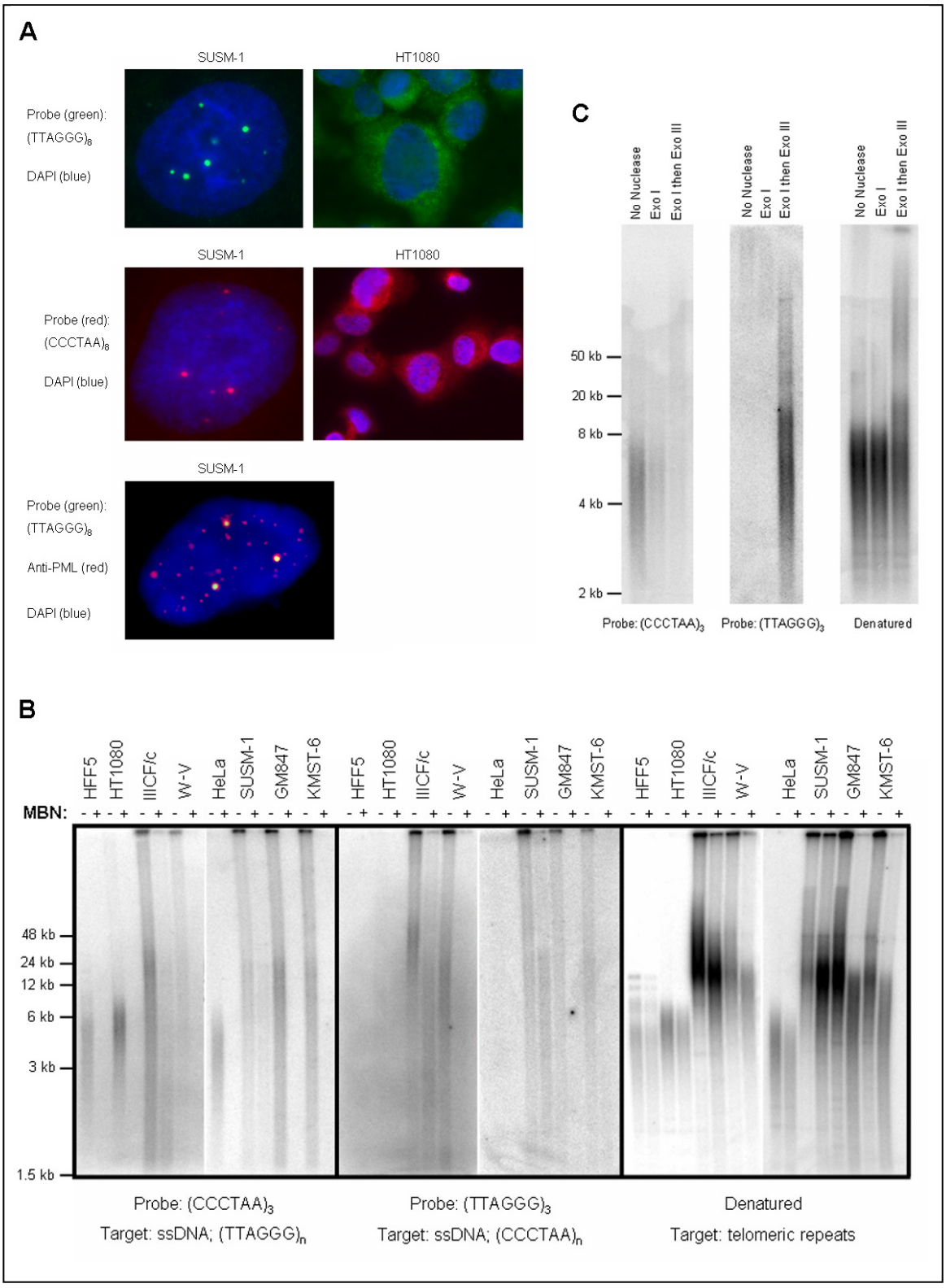
A
SUSM-1
HT1080
Probe (green):
(TTAGGG)8
DAPI (blue)
SUSM-1
HT1080
Probe (red):
(CCCTAA)8
DAPI (blue)
SUSM-1
Probe (green):
(TTAGGG)8
Anti-PML (red)
DAPI (blue)
C
No Nuclease
Exo I
Exo I then Exo III
50 kb
20 kb
8 kb
4 kb
2 kb
Probe: (CCCTAA)3
Probe: (TTAGGG)3
Denatured
B
HFF5
HT1080
IIICF/c
W-V
HeLa
SUSM-1
GM847
KMST-6
MBN:
48 kb
24 kb
12 kb
6 kb
3 kb
1.5 kb
Probe: (CCCTAA)3
Target: ssDNA; (TTAGGG)n
Probe: (TTAGGG)3
Target: ssDNA; (CCCTAA)n
Denatured
Target: telomeric repeats

Another interesting feature of Figure 3.14B is that destruction of single stranded DNA by MBN also destroyed the presence of telomeric DNA migrating above the 20 kb to 25 kb molecular weight marker in the (standard) denatured gel. Thus, much of this slow migrating telomeric DNA may not be long telomeres but a result of secondary structure of telomeric DNA with single stranded $(5'\text{-CCCTAA-}3')_n$ or a result of structures formed between telomeric DNA with single stranded $(5'\text{-CCCTAA-}3')_n$ and telomeric DNA with single stranded $(5'\text{-TTAGGG-}3')_n$. To investigate this, genomic DNA from HT1080 had its 3′-telomeric overhangs mostly removed by digestion with Exonuclease I and then was treated with Exonuclease III to create 5′-telomeric overhangs (Fig 3.14C). This created the presence of slow migrating telomeric DNA above the 50 kb marker.

The presence of single stranded $(5'\text{-CCCTAA-}3')_n$ as another hallmark of ALT opens up new ways to assay for ALT. The creation of an antibody against single stranded $(5'\text{-CCCTAA-}3')_n$ may allow an APB assay that is more appropriate as a routine pathology test, because it would be a one step immunostaining procedure not requiring FISH. It may also be possible to use a PCR based test for single stranded $(5'\text{-CCCTAA-}3')_n$ in patients serum as a cancer marker.

3.9 Summary of results (see Chapter 6 for discussion)

This chapter firstly consolidated APBs as a hallmark of ALT in cell lines. The correlation between APB[+] and ALT[+] cell lines was extended by demonstrating 14/14 ALT[+], 3/23 telomerase[+] and 0/5 mortal cell lines/strains were APB[+]. Combining these results with published data shows 29/31 ALT[+], 3/31 telomerase[+] and 0/10 mortal cell lines/strains are APB[+]. The three APB[+]/telomerase[+] cell lines only had a low frequency of APB[+] nuclei (< 0.5%). Also, loss of ALT activity was shown to coincide with the disruption of APBs in collaboration with Jiang *et al*.[2].

This collaboration showed using TRF analysis that clones from an ALT[+] population with APBs disrupted by SP100 overexpression lost all telomere length fluctuations except a gradual shortening consistent with the "end replication problem" erosion usually seen in telomerase[-] cells.

Detection of APBs was then developed into an assay for ALT in tumour specimens. The method of detecting APBs with combined immunofluorescence and telomere FISH was optimised for paraffin sections and scoring criteria for tumours were established. The APB assay was found to be compatible with fine needle aspiration biopsy. This chapter also compared different criteria for scoring ALT in tumours by the standard ALT assay, TRF analysis.

Importantly, the APB assay was verified as a test for ALT in tumours, and in this study, was superior to the standard assay for ALT in tumours. It was demonstrated that the APB assay concurred exactly with the standard assay for ALT (TRF analysis) in the 60 tumours for which TRF analysis gave unequivocal results (20 of which were ALT[+]). In the 6/26 STS for which the TRF analysis gave equivocal results, the APB assay gave definitive results. This may be due to the APB assay being a more appropriate technique for non-homogeneous samples. 3/6 of the STS with equivocal ALT status from TRF analysis had TRF length distributions consistent with a small ALT[+] subpopulation (5-20%). This study showed for the first time that intratumoral heterogeneity for ALT exists; using the APB assay 2/20 osteosarcomas were found to have intratumoral heterogeneity for ALT. It was shown that TRF analysis gave equivocal results in a simulation of intratumoral heterogeneity for ALT when a mixture of genomic DNA had an ALT[+] component of 20% to 40%. In collaboration with Jeyapalan *et al*.[121], it was shown that the STS with MS32 minisatellite instability had a higher frequency of APBs (≥ 20% nuclei APB[+]).

Finally single stranded G- and C-strand telomeric repeats were discovered in APBs and it was shown that single stranded C-strand telomeric repeats detectable by native TRF analysis was ALT specific. Digestion of single stranded telomeric repeats in ALT[+] cells eliminated the migration of telomeres above the 25 kb marker. Creation of a 5′-overhang in a telomerase[+] cell line (after digestion of the 3′-overhang) showed migration of telomeres above 50 kb. Thus the presence of single stranded C-strand telomeric repeats in ALT[+] cells may make their telomeres appear longer when TRF analysis is used, but potentially also provides new opportunities for clinical detection of ALT cancers.